Robust Feature Extraction Algorithm for analysis of Radar Targets using Multi-Object Tracking on Range Velocity Space

by

Saravanan Nagesh

to obtain the degree of Master of Science

at the Delft University of Technology (faculty EEMCS),

to be defended publicly on 23rd October , 2019 at 13:30 PM.

Student number:	4744160
Project duration:	January 20, 2018 – October 23, 2019
Thesis committee:	Prof. dr. A. Yarovoy, TU Delft, Professor, Chairman Microwave Sensing, Signals and Systems
	Dr. ir. R.F. Remis , TU Delft, Associate professor, Circuits and Systems
	Dr. O.Krasnov , TU Delft, Assistant Professor Microwave Sensing, Signals and Systems

TUDelft

Abstract

In this thesis, we propose, a Robust data extraction algorithm capable of extracting reliable target features of multiple moving targets of different classes over all channels of a S Band Doppler Polarimetric Radar PARSAX. The proposed algorithm is capable of generating a time series data by tracking, clusters of detections - representing extended targets using a multi target tracker modified to track on sequential frames of Range Doppler Maps .The targets considered in this study are Automobiles of different classes (4 wheel drive and above). A performance analysis of the algorithm, for data extraction possibility with respect to target density has been presented. In addition the possibility to use the extracted features for Radar Classification has been investigated.

Keywords - Extended Target, Kalman Filter, Data Association, Multi target tracking.

Acknowledgements

Contents

List of Figures

List of Tables

Nomenclature

BSA	Back Scattering Alignment
BSM	Back-Scattering Matrix
BT product	Time-bandwidth product
CA-CFAR	Cell Averaging Constant False Alarm Rate
CFAR	Constant False Alarm Rate
CUT	Cell Under Test
DBSCAN	Density Based Spatial Clustering of applications with noise
EM	Electromagnetic
FFT	Fast fourier transform
FMCW	Frequency Modulated Continues Wave
GNN	Global Nearest Neighbours
LFM	Linear frequency modulation
LRT	Likelihood Ratio Test
MCDA	Multi-Channel Data Extraction Algorithm
MMSE	Minimum Mean Square Error
MTDF	Multi-Target Data Association Filter
MTI	Moving target indicator
PCM	Polarisation Covariance matrix
PRF	Pulse repetition frequency
PRI	Pulse repetition interval
PRT	Pulse repetition time
PSM	Polarisation Scattering Matrix
RADAR	Radio Detection And Ranging
RCS	Radar cross section
RF	Radio frequency
Symbols	
SINR	Signal to Interference and Noise Ratio
SNR	Signal-to-noise ratio

1

Introduction

1.1. Motivation

The area of research which focuses on the possibilities of a radar to access and predict the outcome of events is termed as Cognitive Radar, where the term cognition stands for "knowing, perceiving or conceiving as an act" [2]

One of the major use cases of Cognitive radar is, in the area of Automatic Target Classification(ATC), where a target detected by a radar is recognised based on its features, identified as a specific class and finally classified as a target of the identified class.

The primary requirement for an ATC to classify a target, is a feature database, which contains information to recognise the targets, belonging to a specific class. Thus if a new class of targets have to be identified, it would require a feature analysis to be conducted on that specific class of targets. Hence it is safe to say, features play a vital role in ATC systems and the analysis of new features to recognise new targets is mandate for such systems.

In general , features that are used to recognise a target can vary based on the type of targets and type of system used to extract features from a target.

With the advent of high resolution radar systems, targets whose dimensions are larger when compared to the resolution of the radar, occupy multiple resolution cells by reporting multiple detections from a single measurement[3][11][12], this makes it possible to acquire additional features that could provide better results when compared to conventional systems. The approach is fairly straight forward, when dealing with static targets. However when considering the case of moving targets having fluctuating measurements, the process of feature extraction is rather complicated. In addition when considering real world scenarios with varying number of extended moving targets, consisting of various data-association bottlenecks, the task at hand is challenging.

As ATCs are real time systems working under such complicated environments, it only seems fair, to analyse and acquire features from targets in real world scenarios, thus improving the performance of ATCs, which would eventually make Cognitive radars a reality.

1.2. Goals

The following can be described as the goals / objects of this study:

- To propose an approach to extract real radar data from moving extended targets.

- To identify features of an extended target, that can be used to differentiate between two or more moving extended targets.

- To investigate the possibilities of categorising the target into different class based on the identified features.

1.3. Literature Review

To identify a suitable approach to classify extended moving targets, a wide range of literature has been investigated. The various approaches followed by academics and industries can be broadly classified as follows:

1. Imaging Based Approaches[21][32][33]

2. Model based Approaches[3][4][11][12]

3. Micro- Doppler Approaches [68][69]

Imaging approaches mainly focus on extracting high resolution 2 dimensional images capturing the extent of a target in range and cross range or single dimension High Resolution Range profile (HRRP), which measures the RCS of a vehicle along the range dimension using a Synthetic aperture radar. The obtained image based features are used with template matching techniques to differentiate between targets or different structures.

Model Based approaches consider estimating the RCS of a moving target by using mathematical model to predict the distribution of the extended moving targets, the obtained distributions are investigated based on the KullbackLeibler divergence for possible variations from known distribution. In case of industries, the use of sophisticated test benches inside expensive anechoic chambers are used to obtain precise measurements of ground vehicle from different aspect angles [71][72].

For studies related to micro doppler patterns are widely carried out considering humans and animals as targets, where movement of the parts of the body constitute the micro-doppler pattern, however, very little studies related to micro doppler patterns from extended ground targets is known. This may be primarily due to the unavailability of systems with high doppler sensitivity.

It is also interesting to note that very little literature is available which focus on the extraction of polarimetric data for feature analysis. In most cases Doppler Polarimetric radars are incapable of extracting a full polarimetric scattering matrix for a target (to be explained in following sections 3).

However the considered "PARSAX: S-band polarimetric Doppler radar" is capable of measuring all elements of the Polarisation scattering matrix [10], thus an opportunity to explore the possibilities for Polarimetric feature analysis.

1.4. **Novelties and Contributions**

In this study the following topics/concepts have been investigated, analysed and demonstrated:

- We investigate the possibilities of mitigating the various data-association problems,when dealing with closely spaced moving extended targets over multiple frames of data, using radar polarimetry .

- A Novel, Multi Channel Data extraction Algorithm (MCDA) based on the "Flood Fill algorithm" and "Polarimetric Data Fusion concepts", is proposed for the mitigation of Level 1 data-association bottlenecks, concerning measurements of closely space extended targets from channels of differing nature.

  The approach is demonstrated by extracting the full polarimetric data, simultaneously from 4 different channels of a Doppler Polarimetric Radar -Parsax, for every target over multiple frames of measurement. The extracted data is stored as a "Target Detection Database".

- We investigate the possibilities of creating a time series data of raw measurements for moving extended targets, by solving level 2 data associating problem concerning varying number of moving targets over multiple frames of measurement.

- A Multi Target Data association Filter (MTDF), based on Nearest Neighbour Kalman tracker is proposed, for associating the extended targets, detected over multiple frames of measurement.

  The approach is demonstrated by tracking and associating multiple measurements for multiple targets over multiple frames of data to create the required time series data. The time series data created for every target is stored as a "Target Track Database".

- An performance metric for assessing the various radar data association concerns when creating the proposed time series data has been formulated and the same has been used for evaluating/identifying level 3 data association cases, concerning successive merging and splitting measurements of extended targets (a typical phenomenon encountered when measuring data from dense target locations).

  The proposed metrics are validated using synthesised cases and utilised in accessing the quality of the created time series data based on real radar data for every target.

- An analysis based on concepts from literature [5],[22],[23],[27],[29],[31],[62] is conducted over the extracted time series data, to identify possible features to characterise moving extended targets. The identified features are extracted for every target and stored as a "Target Feature Database"

- A proof of concept to investigate the possibility, to use the extracted features for future studies related to target classification/ clustering have been presented.

Throughout this study the term target(s) applies to different classes of moving automobiles captured using the S band Doppler Polarimetric FMCW Radar PARSAX.

1.5. Thesis Structure

The thesis has been structured to explain and validate each individual segment of the proposed algorithm:

Chapter 2: Characterisation of Extended Moving Targets using FMCW Radars

In this section fundamentals of range doppler processing in case of FMCW radar have been discussed and how the same has been adapted for creation of the measurement and tracking space called "Range Velocity Cube" has been illustrated. The section includes the design of a MTI stage, 2D Cell Averaging CFAR detector and the mathematical model for an extended target characterised on the range velocity space.

Chapter 3: Multi Channel Polarimetric Data Extraction using Fusion Cluster based on Flood Fill Algorithm

In this section the concepts related to polarimetric data have been discussed and the doppler processing stage from the previous chapter has been extended to the range velocity maps created across 4 different polarimetric channels.

A study on related algorithms for unifying detections of an extended target has been carried out, and the use of the "Flood Fill" algorithm for the same and characterising the extended target as objects on the range velocity image have been presented.

Possible data fusion strategies for combining detections across the polarimetric channels for extracting full polarimetric data simultaneously across all channels has been investigated and presented.

Chapter 4: Inter-frame Data Association mitigation using Multi Object Tracking

In this section, possible data association concerns with measurements from different channels over multiple frames has been discussed and steps to mitigate the same using the science Multi Target Tracking has been presented. A performance metric evaluating data association concerns discussed, has been proposed and evaluated on synthesised cases.

Chapter 5: Feature Analysis for Extended Moving Targets using time series data

In this section, the fundamentals related to target feature analysis have been discussed and possible candidates as "features" of an extended target have been identified. The fundamentals of label-less classification - Clustering has been discussed and a sample example of the same has been presented.

Chapter 6: Experimental Results

In this section we present data collected from a highly dense traffic location -A13 highway, and use the same to create 3 databases specific to detections, tracks and features.

Each section of the report discussed is demonstrated on the real radar data situations and a quality metric for the database extracted is provided.

A proof of concept to use the extracted features for categorising the targets into sub-classes has also been presented.

Chapter 7:Conclusion and Future Work

In this section, the final conclusions of this study are summarised along with possible limitations, open topics and extension of the study as a future scope.

2

Characterisation of Extended Moving Targets using FMCW Radars

In this Chapter the basics of range doppler processing chain for the FMCW radars, Design of a Cell Averaging Constant False Alarm Rate Detector and mathematical model for characterising extended targets as cluster of detections have been discussed, in addition the measurement space 'Range Velocity Cube' used for tracking and data extracting is introduced.

2.1. Range Doppler Processing for FMCW radars

Frequency modulated continuous wave radar are preferred in both military and civilian applications due the ability to determine the range and radial velocity of target simultaneously[22]. The basic block diagram of a FMCW radar is as shown in figure2.1.
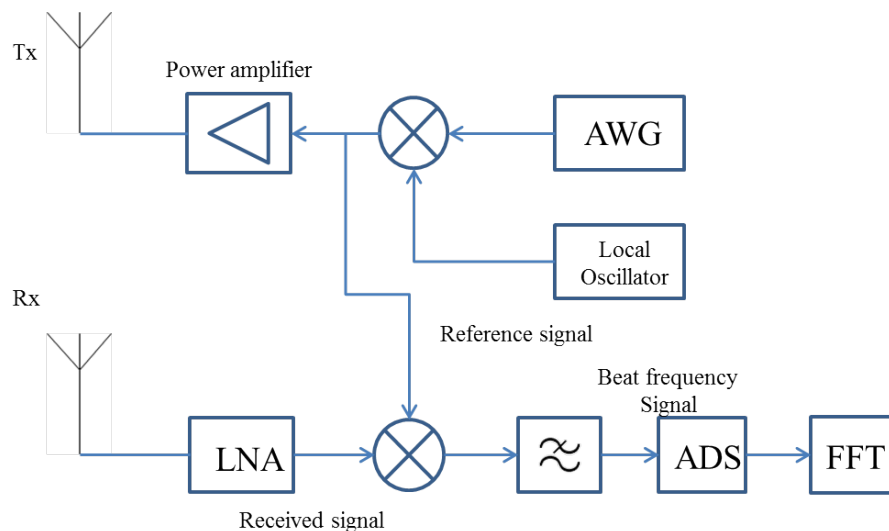
Figure 2.1: FMCW Radar monostatic

The transmitted signal is given by:

$$s_T(t) = A_T exp(j2\pi f_c t + j\pi\alpha t^2) \tag{2.1}$$

where, t is the instantaneous time for the chirp of duration T such that $-T/2 < t < T/2$, A_T is amplitude of transmitted signal, $\alpha = \frac{B}{T}$ is the ratio of Bandwidth B and chirp duration T, f_c is the centre carrier frequency.

The transmitted signal when encounters a target is scattered back to the radar , the received signal at the receiver is given:

$$s_R(t) = A_R exp(j2\pi f_c(t - \tau) + j\pi\alpha(t - \tau)^2) \tag{2.2}$$

where, τ represents the delay due to the presence of a target and is given by $\frac{2R_0}{c}$.

Thus we see from equation 2.1 and 2.2, the transmitted and received signal consists of a phase and amplitude components for from a single pulse for a single target. The following subsections the relation/ effect of the amplitude and phase component due to a presence of a target are discussed:

2.1.1. Phase

Consider the phase of the transmitted wave and received wave with delay τ in equation 2.3 and 2.4.

$$\phi(t) = 2\pi(f_c t + 0.5\alpha t^2); \ t \in (\frac{-T}{2}, \frac{T}{2}) \tag{2.3}$$

$$\phi(t - \tau) = 2\pi\left(f_c(t - \tau) + 0.5\alpha(t - \tau)^2\right) \tag{2.4}$$

hence the phase post demodulation and dechirping is given by:

$$\begin{aligned}\Delta\phi(t) &= \phi(t) - \phi(t - \tau) \\ &= 2\pi(f_c\tau + \alpha\tau t - 0.5\alpha\tau^2)\end{aligned} \tag{2.5}$$

consider the case for a moving target with a velocity v at a distance R which is incident by a burst of n chirps, the delay wrt to the target is given by: (Assuming an approaching target has a positive delay).

$$\tau(t) = \frac{2R + 2vTn + 2vt}{c} \ t \in vTn + (\frac{-T}{2} + \tau, \frac{T}{2} + \tau) \tag{2.6}$$

where, c is the speed of light, T is chirp duration, t is the fast time and n is slow time index.

Substituting equation 2.6 in equation 2.5 we arrive:

$$\begin{aligned}\Delta\phi(t, n) &= 2\pi(f_c\frac{2R + 2vTn + 2vt}{c} + \alpha\frac{2R + 2vtn + 2vt}{c}t) - \pi\alpha(\frac{2R + 2vTn + 2vt}{c})^2 \\ &= 2\pi(\frac{2rf_c}{c} + (\frac{2R\alpha}{c} + \frac{2vf_c}{c})t + \frac{2\alpha v}{c}t^2 + (f_c\frac{2v}{c} + \alpha t\frac{2v}{c})Tn)\end{aligned} \tag{2.7}$$

consider the shift in frequency f_d due to target velocity given and delay due target at range R as below :

$$f_d = \frac{2vf_c}{c}$$
$$\tau = \frac{2R}{c}$$

(2.8)

considering equation 2.8 in equation 2.7 :

$$\Delta\phi(t,n) = 2\pi(f_c\tau + \alpha\tau t + f_d t + \frac{2\alpha v t^2}{c} + f_d T n + \frac{\alpha t 2v}{c} T n)$$

(2.9)

as the ratio of $\frac{v}{c} < 1$ and under the assumption $\alpha\tau + f_d \approx \alpha\tau$ the above equation is approximated as

$$\Delta\phi(t,n) \approx 2\pi(f_c\tau + \alpha\tau t + f_d T n)$$

(2.10)

2.1.2. Amplitude

Consider the received signal from a target located range R.

$$P_R = \frac{P_T G_T G_R \sigma \lambda^2}{(4\pi)^3 R^4}$$

(2.11)

where, P_T is the peak transmitted power in watts, G_T is the gain of the transmit antenna, G_R is the gain of the receive antenna, λ is the carrier wavelength in meters, σ is the RCS of the target in square meters, R is the range from the radar to the target in meters.

Considering the case of simple target the received amplitude before dechirping is given by:

$$A_R = A_T e^{j\psi} \sqrt{\frac{G^2 \lambda^2 \sigma}{(4\pi)^3 R^4}}$$

(2.12)

Assuming unit amplitude transmitted we can consider $A = A_T e^{j\psi}$ the complex reflectively and parameters wrt to the target as constant given by:

$$\mu(R,\lambda) = \sqrt{\frac{G^2 \lambda^2 \sigma}{(4\pi)^3 R^4}}$$

(2.13)

Considering the above assumptions the received signal for a burst of n chirps with phase information derived from equation 2.10 can be considered as :

$$s_R(n,t) = A_R e^{j\Delta\phi} A_T \mu(R,\lambda) e^{-j\psi} e^{2\pi(f_c\tau=\alpha t+f_d Tn)}$$
$$= \hat{A} e^{-j\psi+j2\pi f_c\tau} e^{2\pi(\alpha\tau t+f_d Tn)} \tag{2.14}$$

where, $\hat{A}$ represents the estimated amplitude received from a target at a range R, τ is delay by which the FMCW waveform is shifted, f_d Doppler Shift in frequency due to motion of the target, α is slope of FMCW waveform, f_c is carrier frequency, n is slow time index, t is fast time.

When considering the case of more than one target present the equation 2.14 is considered as:

$$s_R(n,t) = \sum_{i=1}^{N} \hat{A}_i e^{-j\psi+j2\pi f_c\tau_i} e^{2\pi(\alpha\tau_i t+f_{d_i} Tn)} \tag{2.15}$$

where, i is the index of target and N is total number of point like targets.

2.1.3. Fast Fourier Transform

In order to estimate the range and doppler shifts of every N target, a two stage FFT processing is applied on the fast time and slow time of the dechirped received signal as given below:

Consider equation 2.14:

$$
\begin{aligned}
FFT\left[s_R(n,t)\right] &= \frac{1}{\sqrt{2\pi}} \int \int \hat{A} e^{-j\psi+j2\pi f_c\tau} e^{j2\pi(\alpha\tau t+f_d Tn)} e^{-2\pi f_t t} e^{-2\pi f_n n} dt\, dn \\
&= \frac{1}{\sqrt{2\pi}} \hat{A} e^{-j\psi+j2\pi f_c\tau} \int \int e^{j2\pi(\alpha\tau t-f_t t)} e^{j2\pi(f_d Tn-f_n n)} dt\, dn \\
&= \frac{1}{\sqrt{2\pi}} \hat{A} e^{-j\psi+j2\pi f_c\tau} \int \int e^{j2\pi(\alpha\tau-f_t)t} dt\, e^{j2\pi(f_d T-f_n)n} dn \\
&= \frac{1}{\sqrt{2\pi}} \hat{A} e^{-j\psi+j2\pi f_c\tau} \partial(\alpha\tau-f_t) \partial(f_d T-f_n)
\end{aligned}
\tag{2.16}
$$

where, f_t and f_n are the frequency components on fast time and slow time respectively.

The presence of a target can be identified as a peak appearing in the $\alpha\tau$ in range domain, $f_d T$ in the frequency domain, with an amplitude as per equation 2.17 and phase 2.18 as:

$$\hat{A} = \frac{A_r}{\sqrt{2\pi}} \sqrt{\frac{G^2\lambda^2\sigma}{(4\pi)^3 R^4}} \tag{2.17}$$

$$\hat{\phi} = -\psi + 2\pi f_c\tau \tag{2.18}$$

The same extended for a multiple target case can be given by:

$$S_R(R, f_d) = \sum_{i=1}^{N} \frac{1}{\sqrt{2\pi}} \hat{A}_i e^{-j\psi + j2\pi f_c \tau_i} (R_i, f_{d_i}) \tag{2.19}$$

where; $S_R(R, f_d)$ is your received target return in range and doppler

(R_i, f_{d_i}) corresponds to index of ith target at ith Range bin and ith Doppler bin.

$\hat{A}$ is the amplitude corresponding to the target at coordinates(R_i, f_{d_i})

Figure 2.2 illustrates the output of the two stage doppler processing for a noiseless case.
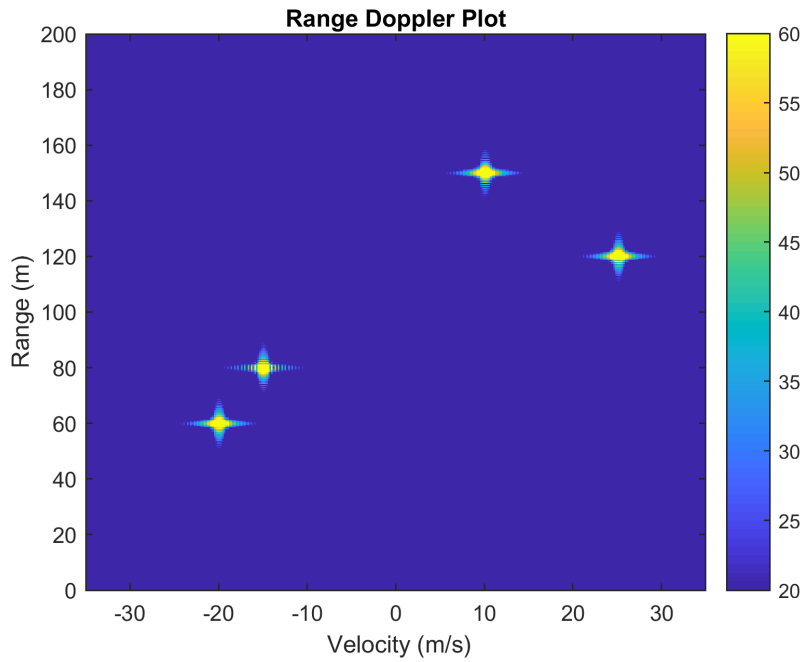
Figure 2.2: Range Doppler plot obtained after the two stage doppler processing for returns from targets for a noiseless case.

2.1.4. Moving Target Indicator

When considering the case of real radar measurements, the influence of noise and clutter have to be taken into account. The noise can be considered as a Gaussian random process with samples statistically independent to each other and those of clutter measurements centred at zero.Clutter generally arises due to the presence of unwanted objects within the Radar beam, such as trees, birds, wind, etc.. as the returns from unwanted objects may be not have the same statistics for every instant of the measurement, it gives rise to an effective additive amplitude to the clutter returns[23]. In addition as the clutter is not stationary , for example moving trees due to wind, it gives rise to a clutter spectral spread, although this effect is relatively small, it still results in a Doppler shift for returns from the clutter. This results in a clutter spectrum concentrated at zero doppler and at period intervals of the radar PRF, as a result information related to slow moving targets are lost, hence it is necessary to filter out zero doppler spectrum, which can be done using a single linear high pass filter called Moving Target Indicator (MTI) filter applied on slow time data to suppress the clutter components.

Consider the received returns from the radar consisting of noise and clutter given by equation 2.20:

$$S_R(f) = \sum_{i=1}^{N} S_R(fn_i, ft_i) + N(f) + C(f)$$

$$= \sum_{i=1}^{N} \frac{1}{\sqrt{2\pi}} \hat{A}_i e^{-j\psi + j2\pi f_c \tau_i} \partial(\alpha\tau_i - f_t) \partial(f d_i T - f_n) + \frac{P_c}{T\sigma_f \sqrt{2\pi}} \sum_{k=-\infty}^{\infty} \exp\left(-\frac{(f - k/T)^2}{2\sigma_f^2}\right)$$

$$(2.20)$$

where; T is 1/PRF, Pc is the clutter power and k is index of samples.

The spectral information for the returns from a radar, consists of noise and clutter, as the clutter comprises of stationary unwanted ground reflections with a minimal relative motion wrt to the radar, its power spectrum is concentrated at zero doppler[23].

σ_f represents the over all clutter spread consisting of summation of standard deviations of clutter fluctuations within the radar beam and root mean square velocity of the clutter due to wind is give by equation 2.21:

$$\sigma_f = \frac{2 * vrms_{(wind)}}{\lambda} \tag{2.21}$$

As the clutter spectral spreading is « compared to PRF, as shown in equation 2.20, the mean square value of clutter power can be calculated from:

$$Pc = \frac{1}{PRF} \int_{-PRF/2}^{PRF/2} Sc_o(f)df \tag{2.22}$$

where; $Sc_o(f)$ denotes the central portion of clutter power spectrum.

hence the clutter is expressed as a Gaussian shape function given by:

$$Sc_o(f) = \frac{Pc}{T\sigma_f\sqrt{2\pi}}exp\left(-\frac{f^2}{2\sigma_f{}^2}\right) \tag{2.23}$$

The presence target, clutter and noise for the returns from radar is as shown in figure 2.3 below:
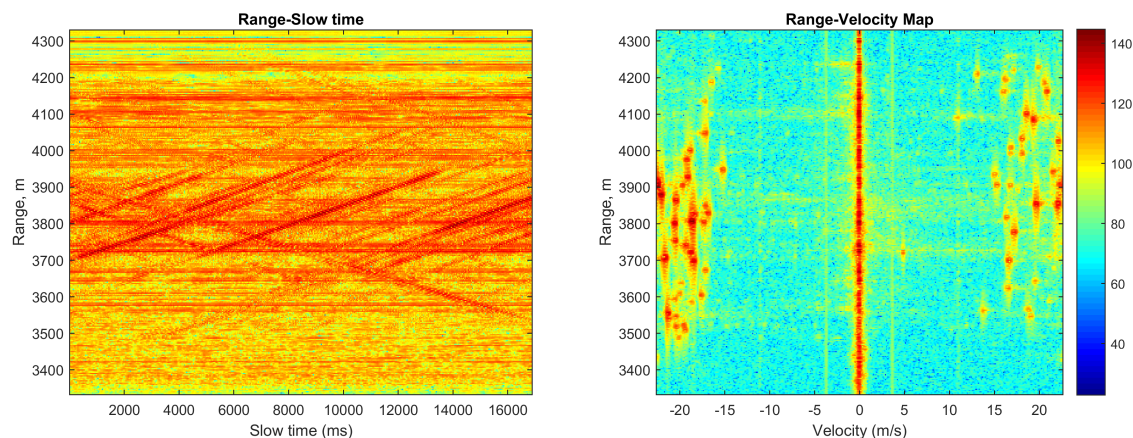
(a) Range Slow time plot   (b) Range Doppler Plot

Figure 2.3: (a) Horizontal lines represent zero doppler information corresponding to stationary clutter, the lines with positive and negative slopes indicate moving targets with a constant velocity equal to slope of the line; (b) Range Doppler plot showing target occupying co-ordinates $[\alpha\tau, f_dT]$ as per equation 2.19
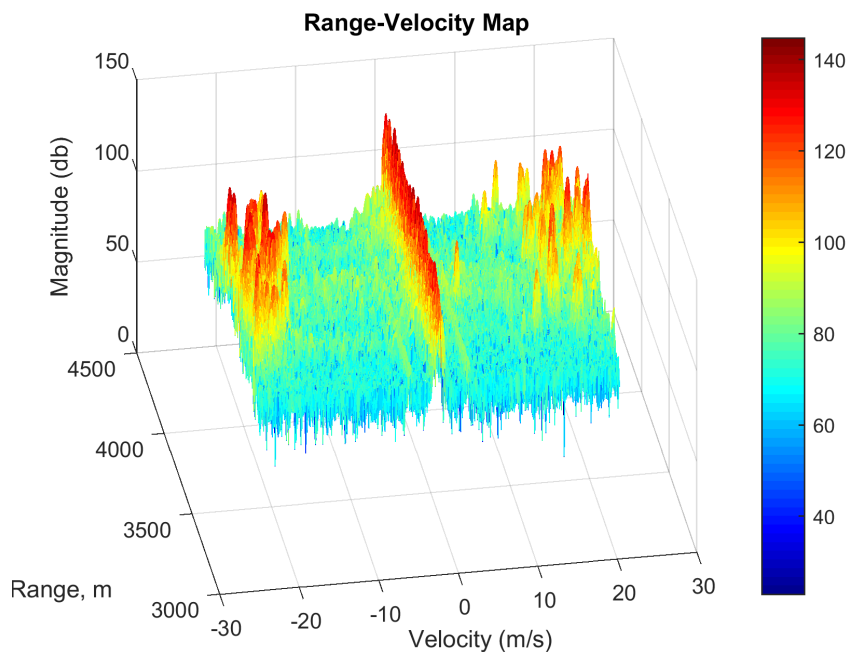
Figure 2.4: 3D representation of Range Doppler plot showing Gaussian shape clutter spread around zero doppler with a magnitude as result of summation of clutter amplitude for a collection n slow-time samples

In order to suppress the target like reflections from clutter spread at zero doppler and allows returns from target only with little or no degradation, a high pass filter allowing only doppler spectrum above the cut off frequency greater than maximum clutter spread is designed[24]. The MTI stage designed for this study consists of a 2nd order High pass Butter-worth filter , with transfer function given by:

$$H(j\omega) = \frac{1}{\sqrt{1 + (\frac{f_c}{f_d})^2}} = \begin{cases} 0 & f_d < f_c \\ 1/\sqrt{2} & f_d = f_c \\ 1 & f_d = \infty \end{cases} \tag{2.24}$$

where; f_d are the doppler frequencies of both target and clutter,
f_c is cut off frequencies greater than clutter doppler spread.

The magnitude and phase response of the designed filter is as shown in figure2.5
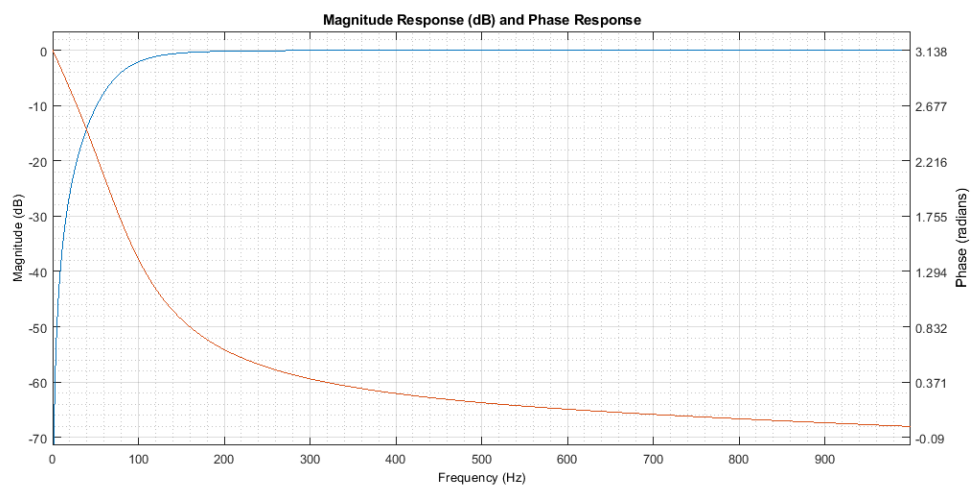
Figure 2.5: The blue line shows the magnitude response for considered range of frequencies and similarly the red line shows the effect of phase response

The filter applied along the slow time axis of the measured radar data and than FFT is performed to generate the clutter free range doppler map, the related performance and improvement due to the MTI stage can be visualised from figure 2.6 and 2.7 as seen below:
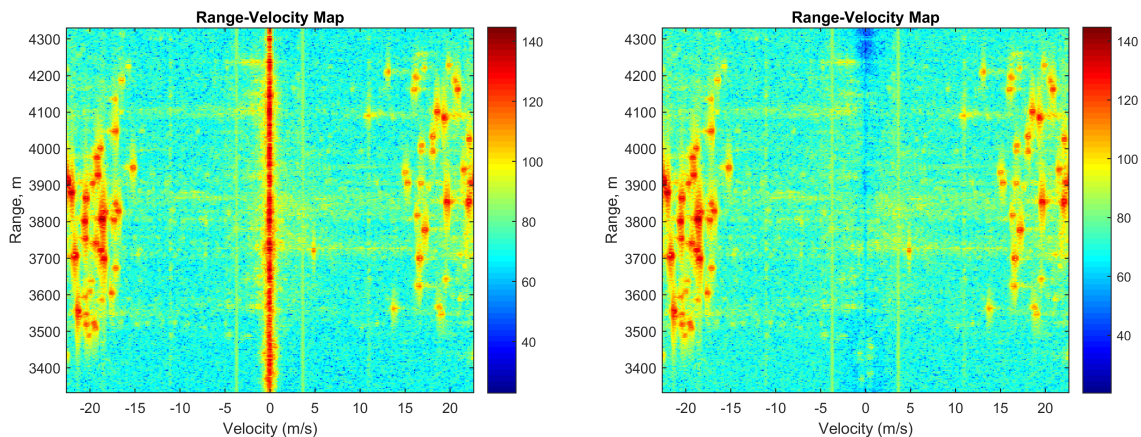
Figure 2.6: (a) The 2D view of range doppler plot with clutter present (b) The 2D view of Clutter free range doppler plot
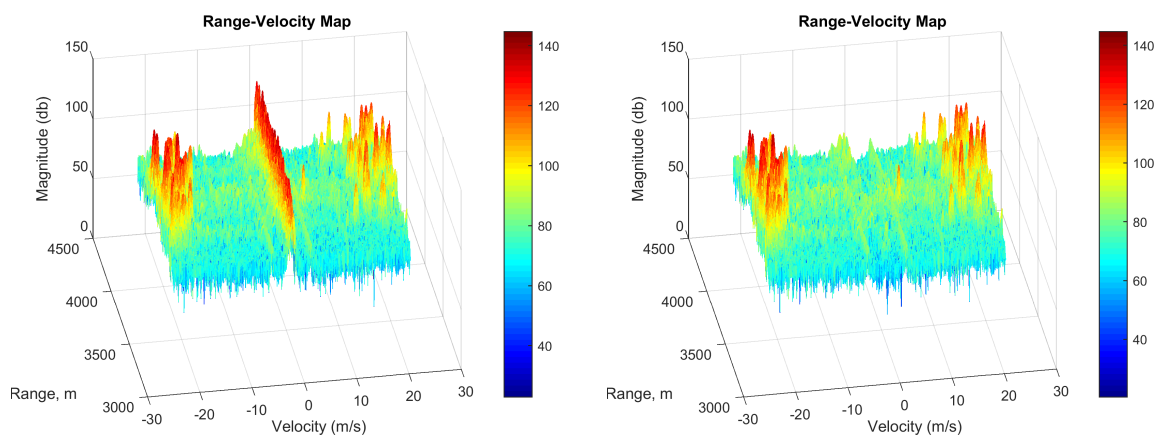
Figure 2.7: (a) shows the presence of a strong clutter and spread around zero doppler region, (b) shows the effect of MTI stage on the data set in eliminating clutter

2.2. CFAR Detector

For any Radar system, a detection is based on the received reflections at the radar and the ambient thermal noise present in the receiver. In general, measurements from a target are collected in range, angle, cross range and Doppler, individually or combined. The received Radar measurements are sampled as per resolution of the dimension in which they were collected. Once collected, the Radar detection works on the principle of threshold comparison using a Likelihood Ratio Test (LRT). In most situations strong variations in the interference power, mostly due to thermal noise or variations in terrain reflectively give rise to False alarms, which cause the radar to invoke actions that consume finite Radar resource.[5].

Hence most Radars are designed to accommodate a specific false alarm rate. In this section the design of a 2D Cell Averaging Constant False Alarm Rate (CA-CFAR) Detector for the scope of this thesis will be discussed.

2.2.1. Basic CFAR Design

The Basic architecture and elements for a CFAR algorithm are as shown in figure 2.8 below:
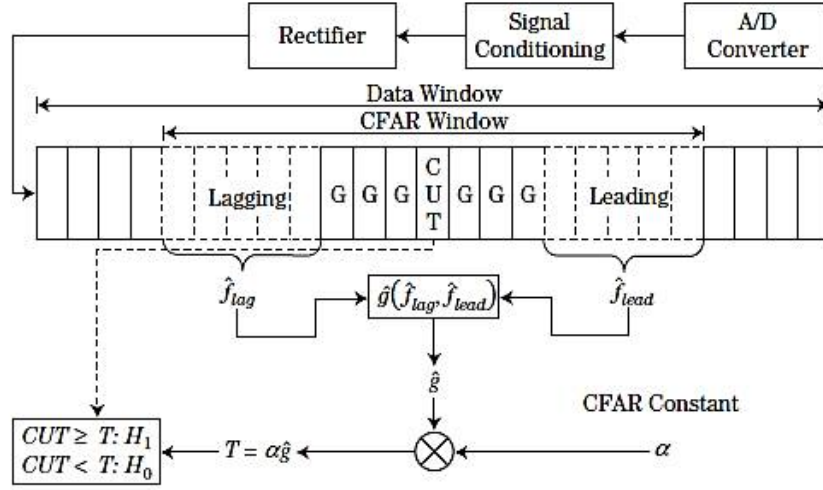
Figure 2.8: CFAR architecture [5]

The CFAR detector works on the principle of LRT, a target is detected when the return at a resolution cell of a measurement space is greater a determined threshold. In most real world scenarios the noise and clutter characteristics are unknown and thus the threshold has to be estimated. To estimate the threshold a CFAR window is considered within the measurement space also know as the data window, this consists of leading and lagging reference window N_T, a Guard window and the cell which is tested for a target called Cell under test (CUT). The characteristics of the noise and clutter are estimated by considering the measurements in the reference window, a threshold for determining the presence of the target in CUT cell called the CFAR threshold given by 'T' is calculated, by considering a CFAR constant α which is calculated for a desired P_{FA}. The Guard window as the name suggests is placed around the CUT cell to avoid measurements from target which may be present in nearby cell, from biasing the estimated threshold[5]. The calculation of the CFAR constant is given by the relation in equation 2.25:

$$\alpha = N_T(P_{FA}^{\frac{-1}{N_T}} - 1) \tag{2.25}$$

where, α is the CA-CFAR constant, N_T is the reference window, P_{FA} is probability of false alarm.

2.2.2. 2D Cell Averaging CFAR

The most widely used CFAR detector is the Cell Averaging CFAR, as the name suggests the noise power is calculated by averaging over the training cells around the reference window, the estimated noise power is computed as:

$$P_n = \frac{1}{N_T} \sum_{m=1}^{N_T} x_m \tag{2.26}$$

where, x_m is the measurement at m^{th} Training cell.

Based on the dimension of data, the dimension of the CFAR window is chosen, an example of 1D CFAR and 2D CFAR are as shown in figure 2.9 below:
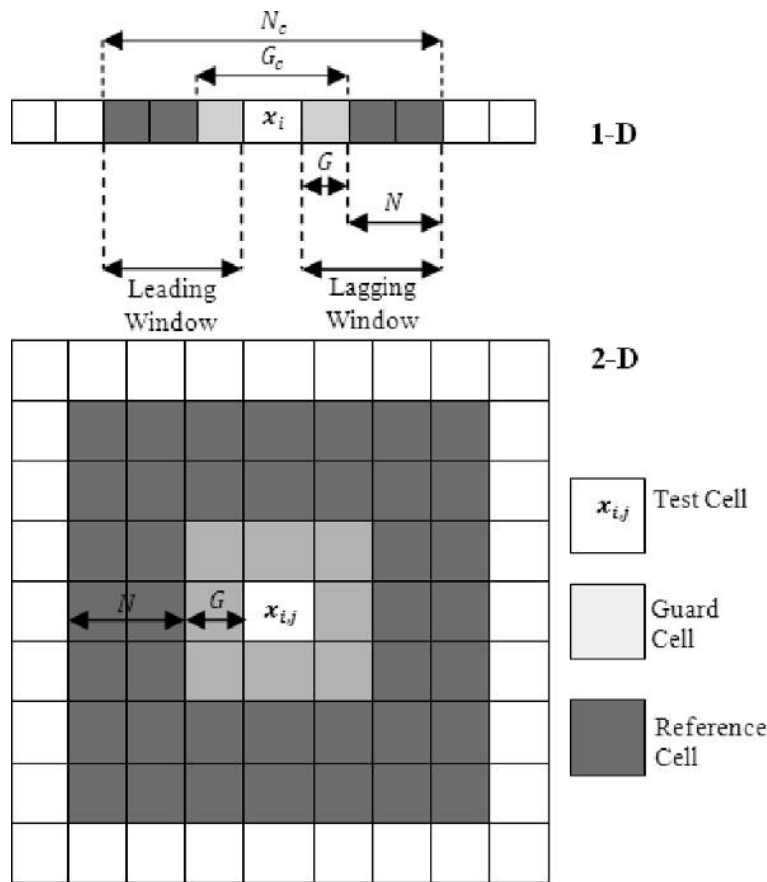
Figure 2.9: 1D and 2D CFAR[6], In both cases x_{ij} represents the cell under test (CUT) surrounded by either a square or rectangular shaped guard window, given by G, which is flanked by the reference window, as mentioned the difference between signal to noise is calculated based on the difference between signal strengths between reference cell and CUT section.

In case of this study as the measurement space is a 2 dimensional range velocity map is considered, hence a 2D CFAR detector has to be designed. In order to accommodate both point targets and extended targets (to be introduced) the Guard Band is chosen relatively large compared to the reference cells to avoid target miss as a result of wrong noise power estimations due to large targets occupying both reference window and guard window which would result in the same intensity levels leading to result of no target detection even when targets are present. The values of Guard window and Reference/training window are determined based on trial and error.

2.2.3. Performance 2D CA-CFAR

The performance of a CA-CFAR is evaluated based on CFAR loss, target masking and clutter boundaries in comparison to a NP detector for a given Probability of Detection P_D. In general the CFAR threshold must be equal or close to the threshold defined by an NP detector, this is not possible in the cases of real data measurements as the variance in the CFAR statistic pushes the CFAR threshold to be greater than that of an NP detector for the given same P_{FA}, therefore indicating a loss in SINR to achieve the same P_D as a NP detector, the "CFAR loss" is thus defined as the ratio in SINR required by the CA-CFAR to that required by a NP detector for a given P_D [5]. The mathematical derivation of the same is as shown below:

The expression of P_D and P_{FA} derived for a NP detector are as shown below:

$$P_{FA} = \exp\left(\frac{-T}{\sigma_i^2}\right) \tag{2.27}$$

where σ_i^2 is variance of measurement. P_D is defined by

$$P_D = \exp\left(\frac{-T}{\sigma_i^2(1 + SINR)}\right). \tag{2.28}$$

SINR as function of P_{FA} and P_D for a NP detector is given by :

$$SINR_{NP} = \frac{\ln\left(\frac{P_{FA}}{P_D}\right)}{\ln(P_D)} \tag{2.29}$$

SINR as function of P_{FA} and P_D for a CA-CFAR detector is given by :

$$SINR_{CA} = \frac{\left(\frac{P_{FA}}{P_D}\right)^{1/N} - 1}{1 - (P_D)^{1/N}} \tag{2.30}$$

The CA-CFAR loss is thus given by:

$$L_{CA-CFAR} = \frac{SINR_{CA}}{SINR_{NP}} \tag{2.31}$$

The 2D CA-CFAR designed in the case of this study has the following parameters, a square training window of size 4×4, a square guard window of 6×6 and a $P_{FA} = 10^{-6}$.

The Performance comparison of the designed CFAR with the NP detector is as shown below:
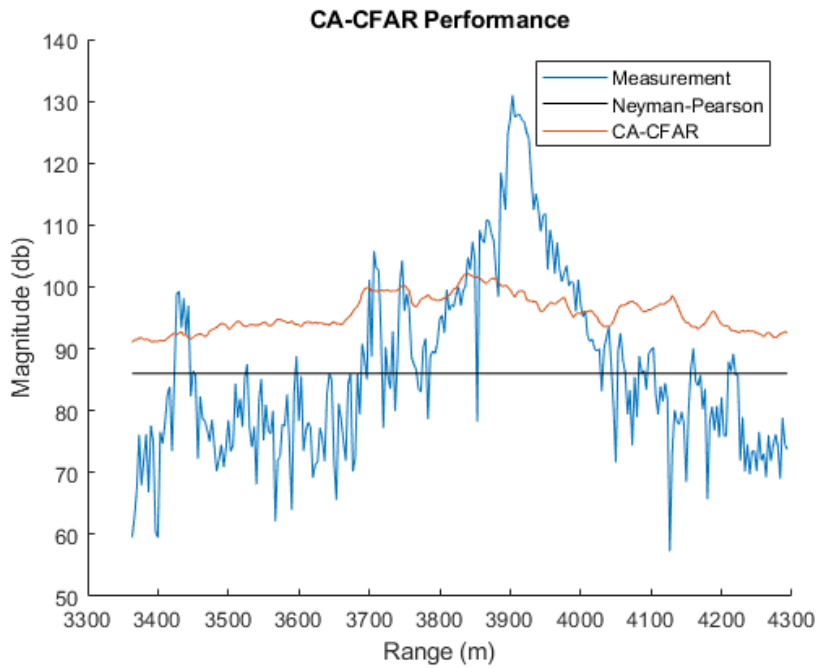
Figure 2.10: Threshold Comparison CA-CFAR vs NP for a specific doppler bin, it is clearly seen that the CA-CFAR out-performances the NP detector for the considered data-set.

The CA-CFAR performance is also evaluated using receiver operating characteristics (ROC), which evaluates the probability of detection of targets above the CA-CFAR threshold can be determined by the SNR roc curves and the performance for different values of Pfa can be determined by the Pfa roc curves as shown in figures 2.11 and 2.12. As the measurement consists of extended targets[25][26] (to be explained in detail in next section), the ROC curves are considered for Swerling 1 model.
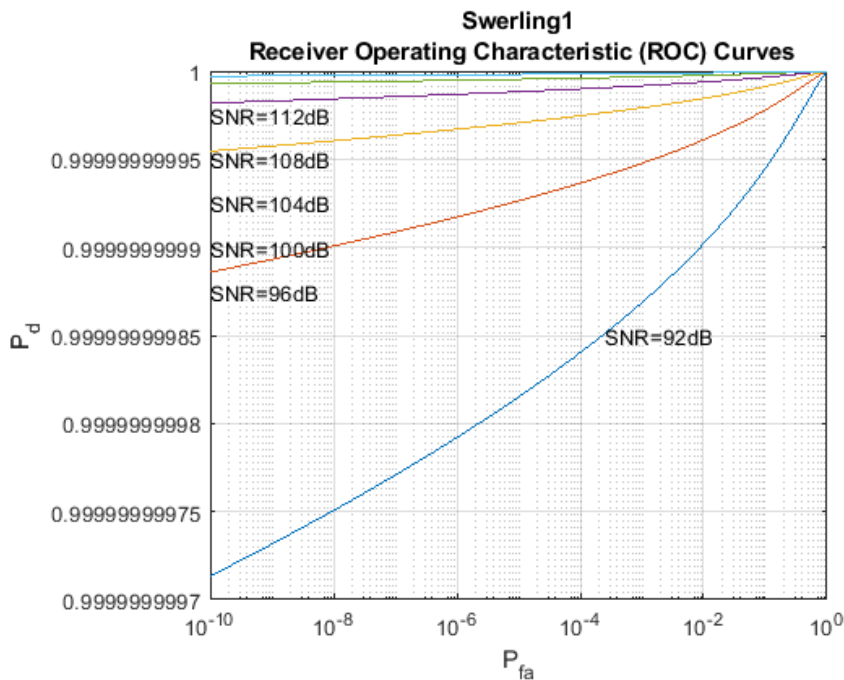
Figure 2.11: SNR ROC for designed CA CFAR

ROC curves are plotted for values $PFa = 10^{-4} 10^{-6} 10^{-9} 10^{-11}$
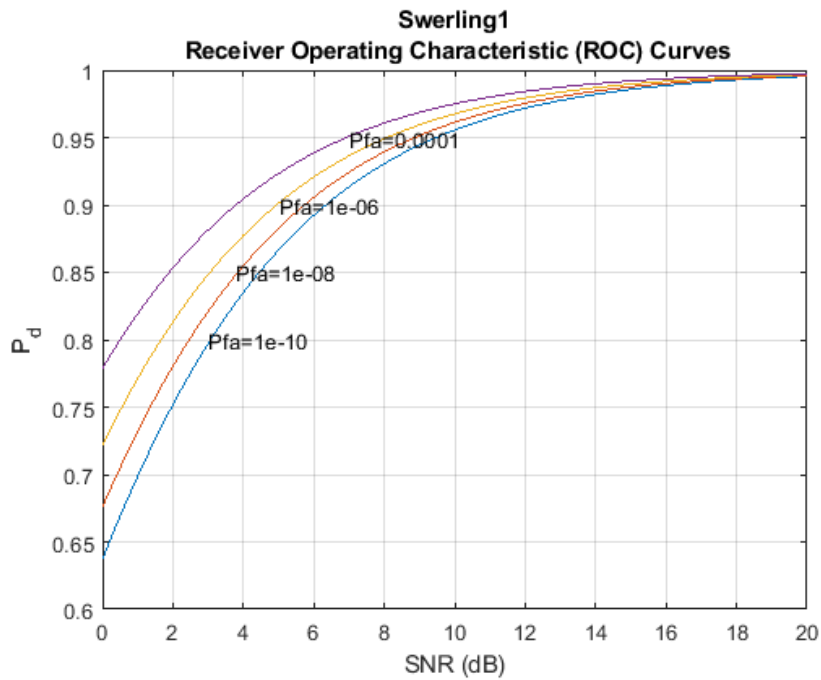
Figure 2.12: Pfa ROC for designed CA CFAR

2.2.4. Detection Map

The Detection Map is a binary image with consisting of logical high value for every pixel for the considered range doppler image occupied by a target. The logical high status is awarded based on CA CFAR threshold calculated for every pixel of the range doppler plot with respect to the determined reference window.

The output of the CA CFAR is as shown in figure2.13 and is compared against the actual range doppler plot.
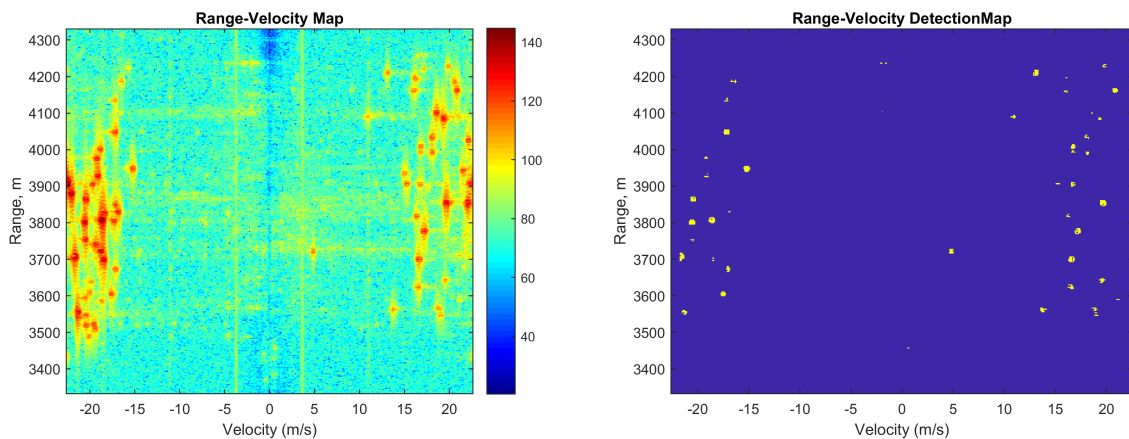
Figure 2.13: (a) The 2D view of range doppler plot and (b) shows the generated Detection map consisting of yellow objects relating to targets against the blue background indicating the noise floor, it is observed that the detection map is in agreement with the range doppler plot

2.3. Extended Target Characterisation

When considering data received from high resolution radars, objects of interest appear extended in multiple resolution cells of the Radar, hence identified as "extended targets" [3].

Extended targets can be represented as back-scattered signal reflections from multiple closely space point like scatters which can be grouped together to characterise one larger object. In order to understand the possibilities of extended targets, fundamentals related to range and doppler resolution for a FMCW radar in general and the same for the considered measurement setup are investigated.

2.3.1. Range Resolution

Range Resolution of a radar can be defined as the minimum distinguishable distance between two closely space targets at a -3dB criterion from the peak of the main lobe.

It is calculated by the expression:

$$\delta R = c/(2B) \tag{2.32}$$

2.3.2. Doppler Resolution

Doppler resolution can be defined smallest detectable difference in doppler shift for a moving target detected by the FMCW radar system, in general the doppler estimation depends on the number of slow time samples and duration of the FMCW chirp, the doppler resolution can be calculated as:

$$\delta f_d = 1/2N \tag{2.33}$$

where N is number of slow time samples;

2.3.3. Extended target as per range doppler resolution

Considering equations 2.19 for multiple targets and considering resolutions in range and doppler discussed in 2.32 and 2.33, it can be inferred that if 2 point targets , have a difference in range smaller than or equal to δR and the difference in doppler frequencies between the same same pair of detections is less or equal to δf_d for the considered radar system, than the pair of detections belong to the same target, holding the previous statement true, all 'k' nearest detections that satisfy the discussed conditions, can be grouped together as one larger, extended target. The mathematical proof for the same can be as seen in equation 2.35

Consider equation 2.19

$$S_r(R, f_d) = \sum_{i=1}^{M} \frac{1}{\sqrt{2\pi}} \hat{A}_i e^{-j\psi + j2\pi f_c \tau_i}(R_i, f_{d_i}) \tag{2.34}$$

where i is index for every detection such that $i = [1, 2, ..., M]$ with 'M' as total number of detections for one range doppler map.

Let 'k' represent a group of closely spaced detections, and for every group let there be 'o' detections, where $o \subset i$, there fore we can say that two detections belong to the same group, if the absolute value of the difference between their coordinates is $\leq$ resolution of the radar $(\partial R, \partial f_d)$.

Considering a target is extended in range (and/or) doppler, by occupying multiple resolution cell above CA-CFAR threshold designed, the equation for one extended target 'i' is given by[28]:

$$S_{ri} = \int I(R, f_d)\hat{A}_i(R, f_d)\partial R \partial f_d \tag{2.35}$$

where; $\hat{A}$ is the estimated amplitude of the target scatter appearing at range R and doppler f_d. The integral indicates the cumulative effect from all range and doppler cells $(\partial R, \partial f_d)$ occupied by the extended target.

As extended targets have multiple scattering centres and every scattering centres may have equal or different amplitudes, the total estimated amplitude based equation2.17 is given by equation 2.36,

$$\hat{A}_i = \frac{1}{\sqrt{2\pi}}\sqrt{\frac{G^2\lambda^2}{(4\pi)^3}}\sum_{j=1}^{o} A_{rj}\sqrt{\frac{\sigma_j}{R_j^4}} \tag{2.36}$$

where, $\hat{A}_i$ is the estimated amplitude of the ith target,

The phases of each scatterer of an extended target might be either random or correlated [27], hence the resulting RCS will be a random variable following a distribution, depending on the nature of scatters. Thus the RCS of an extended target as per various literature [3][27][23] is given by:

$$p(\sigma) = \frac{k}{(k-1)!\,\sigma_{av}}\frac{k\sigma}{\sigma_{av}}^{k-1} exp[-\frac{k\sigma}{\sigma_{av}}]; \sigma \geq 0 \tag{2.37}$$

2.3.4. Measurement Set up

In this study, measurements collected from an in house experimental radar -"PARSAX: High-resolution Doppler-polarimetric FMCW radar" operating at a range resolution of 3.3m[10], target of interest are chosen as automobiles of different types from different locations. As physical dimensions of the considered targets are larger than or equal to range resolution of the radar[4], the discussed, characterisation of detections in closely spaced resolution cell, as a unified extended target is supported. Figure 2.14 shows the detected target on range doppler space as a cluster of detections.
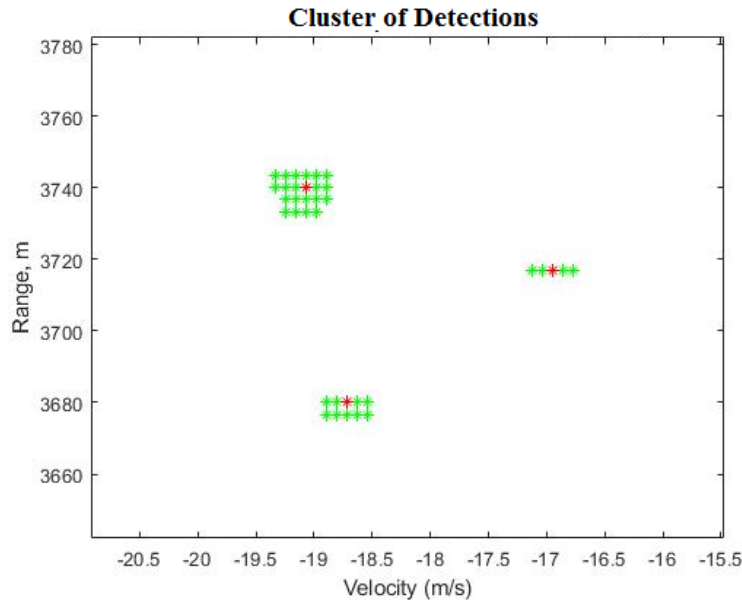
Figure 2.14: The figure shows three extended target characterised as a cluster of detections, the green points indicate all detections spread occupying multiple resolution cells in range and doppler or in doppler only . The red point indicates calculated centre of gravity

2.4. Range Velocity Cube

In general the term Radar data cube is used in context of MIMO radars [5], where the dimensions of the cube are fast-time, slow time and number of receive channels, in the context of this study a modified version of the Radar data cube, termed "Range Velocity Cube" is considered where the dimensions are range, velocity and multiples of CPI.

Consider a parent data matrix (NxM) consisting of (N)Slow time and Fast time (M) , the (NxM) matrix is sampled along its slow time axis considering a smaller collection (k) slow time samples where,$k << N$, thus creating child data matrix (k x M) , following which a windowing and a 2D-FFT is performed, this generates a single range doppler map/image , the doppler information is than converted to velocity using the relation in equation 2.38 , therefore have a range velocity (RV) image.

$$V_r = f_d\lambda \tag{2.38}$$

where, V_r is radial velocity, f_d is doppler shift wrt target and λ is wavelength of transmitted waveform.

Considering k' as the coherent processing interval, every RV image created is stacked one behind the other. This when viewed continuously shows the evolution of the target signatures as a function of CPI, which is non other than the slow-time.[30]. The stacked collection of images, hence forms a movie which represents the movement of a target in range and velocity. A visual explanation of the processing implementation steps to obtain the Range Velocity Movie on Matlab is as shown in figure 2.15.

The Range Velocity movie thus created acts as the measurement space containing moving targets from which data needs to be extracted. To extract data the object is to be tracked on the subsequent frames of the Range Velocity movie, hence the Range Velocity Movie
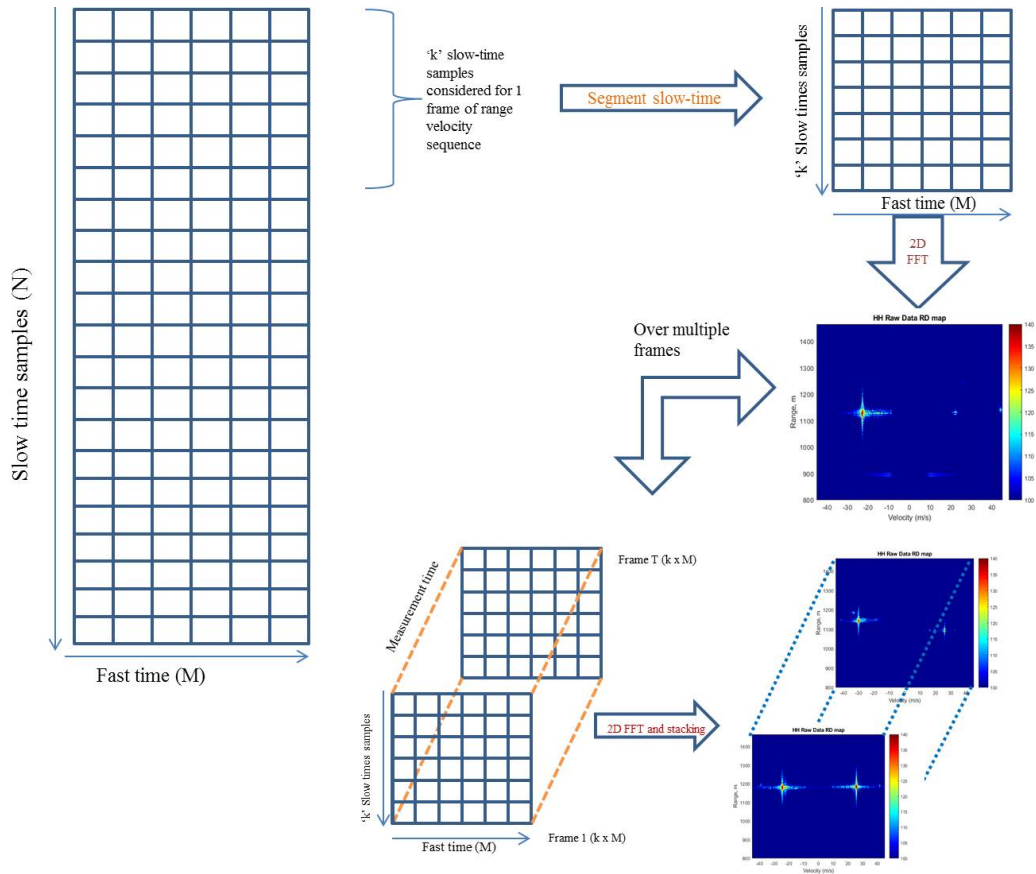
Figure 2.15: Range Velocity Video Algorithm

is also used to present the trajectory for the automobile from which data is extracted. A detailed explanation of the tracking module is discussed in Chapter 4.

2.5. Conclusion

In this chapter, the basics for range doppler processing for an FMCW radar was discussed, the characterisation of an extended moving target as an cluster of detections was presented, the mathematical proof supporting the same was derived. Finally, the measurement space for tracking the evolution of features of a target on slow time called the "Range Velocity Cube" is presented. The following chapter, the Characterisation of the Extended target Cluster using information from all 4 polarimetric channels will be discussed.

3

Multi Channel Polarimetric Data Extraction using Fusion Cluster based on Flood Fill Algorithm

Polarised EM waves, provide more information about a target compared to plain EM waves, hence studies related to returns from Polarised EM waves is of great interest. There have been various studies in the past, related to classifying targets using polarimetric information, for stationary targets [32] and moving target[33] both using imaging systems such as Synthetic Aperture Radars (SAR), in both cases only information related co-polar channels (HH and VV) and imaging configurations related to angular dependencies of incident and scattering directions are studied . Alternatively, very little study in using parameters related to the target itself[31] such as object geometry or its dielectric properties, which can be investigated using various EM vector scattering operations/ operators on the Polarimetric Scattering Matrix.

In this chapter, the fundamentals of radar polarimetry are discussed and the same considered in the case of measurement setup using the Parsax radar is explained. For simultaneous data extraction from all 4 polarimetric channels, a novel multi channel fusion cluster, based on the Flood Fill Algorithm, is presented, its performance in clustering detections related to a specific target to form an extended object is evaluated against standard 'K nearest neighbours' technique. The output of this stage of the algorithm forms the "Detection database" which consists of full polarimetric information of target collected over different multiple frames of the range doppler maps. The detection database will be used in the next stage to solve inter-frame data association.

3.1. Radar Polarimetry

When an Electromagnetic (EM) wave encounters a target, a portion of the incident wave is absorbed by the target and the rest is reflected or in better words re-radiated, the EM wave received by the Radar is thus augmented by the target's properties. Thus, the properties of this re-radiated waves are used to identify some features of a target such a Radar Cross sectional area (RCS). However, when considering Polarised EM waves, the response is different, which provides additional information, such as the target's shape

orientation and material composition that can be used in the case of better identification and classification of the targets, this information is contained in the Polarisation Scattering Matrix (PSM) in the form of complex back-scattering coefficients.

In order to determine the PSM, it is necessary to understand the type of radar configuration and type of target considered for the study, as this would determine how the targets are characterised by the polarised EM wave, in this study we focus on a monostatic configuration of the radar meaning, both transmitter and receiver are on the same co-located platform as shown in figure 3.1
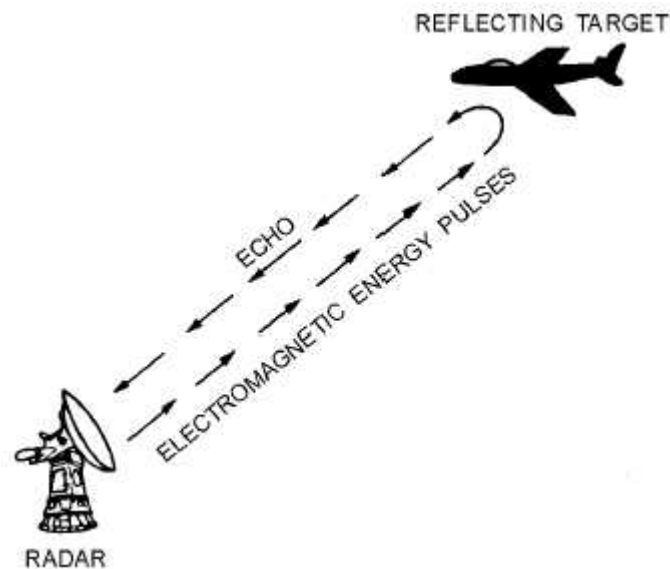
Figure 3.1: Basic monostatic radar configuration[43]

Another important aspect needed to be considered is size of the target compared to the foot print of the radar system, if the size of the target is smaller than the foot print it is treated as an isolated scatterer from the perspective of power exchange, hence this target can be characterised by the radar cross section. In cases where the target is larger than the footprint of the radar system, the target is characterised independent of its extent, in this cases it is considered as a scattering co-efficient. As the scope of this study is limited to cars on a highway, the size of the target is smaller than the footprint of the radar system, hence in order to better understand the characterisation of a target the standard radar equation for a monostatic case is considered.

3.1.1. Polarimetry Radar Equation

The radar equation describes the interaction of an EM wave with a given target, by establishing the relation between the power which is incident on a target $\overrightarrow{E_I}$ and the power which is re-radiated by the same target $\overrightarrow{E_S}$ [31]

$$P_R = \frac{P_T G(\theta, \phi)^2 \sigma \lambda^2}{R^4 4\pi^2} \tag{3.1}$$

where,
P_R is received power and P_T is transmitted power
$G(\phi, \theta)$ antenna gain as a function of elevation and azimuth

R is radial distance between Radar and target
λ is the wavelength
σ is RCS

For targets smaller than the foot print of the radar system as shown in figure 3.2
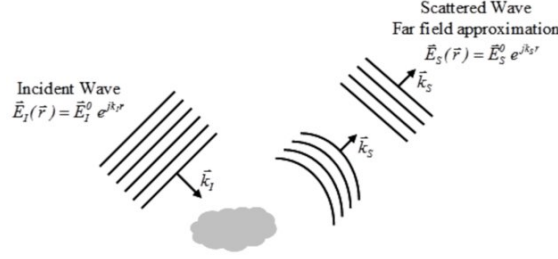
Figure 3.2: Interaction of EM wave and target smaller than radar foot print[32]

With all parameters of the Radar equation fixed, the RCS expresses the ratio reflected EM strength from a target to that which was incident on it is given by equation 3.2:

$$\sigma = \lim_{R \to \infty} 4\pi R^2 \frac{\left|\overrightarrow{E_s}\right|^2}{\left|\overrightarrow{E_I}\right|^2} \tag{3.2}$$

where,
$\overrightarrow{E_s}$ is reflected or back-scattered energy received at the Radar
$\overrightarrow{E_I}$ is incident energy on the target
R is radial distance between target and Radar.

The RCS of a target as per equation 3.2 is a function of the following parameters

- Wave frequency
- Elevation and Azimuth angles of incident and scattering directions - (θ_I, ϕ_I), (θ_S, ϕ_S)
- Object Geometrical structure
- Object dielectric properties

In addition when considering the case of a moving target the parameters are now a function of slow time, hence the mathematical formulation of the same is given by equation 3.3

$$\sigma(t) = \lim_{R \to \infty} 4\pi R(t)^2 \frac{\left|\overrightarrow{E_s(t)}\right|^2}{\left|\overrightarrow{E_I}\right|^2} \tag{3.3}$$

where, the notation (t) indicates a function of slow time.

As extended moving targets fall under the class of fluctuating target [34], the RCS is expected to change wrt time . Depending on the type of target and the behaviour of its scatters the RCS of a fluctuating target will either change from one slow time burst to another (in case of slow fluctuating targets) else will change from each PRI (in the case of fast fluctuating targets)[23][34].

But when considering RCS as a function of polarisation, the signature of a target cannot be described using a single value, hence the Polarisation scattering matrix is considered to describe the interaction of a target with illuminated polarisation component. In the following section the Polarisation Scattering Matrix (PSM) is introduced.

3.1.2. Polarisation Scattering Matrix

General Literature

When considering polarised EM waves , the RCS of a target depends polarisation of the incident field $\vec{E_I}$ denoted by p and the polarisation of the scattered field $\vec{E_S}$ denoted by q, hence the RCS dependent on polarisation is given by equation 3.4.

$$\sigma_{qp} = 4\pi R^2 \frac{\left|\vec{E_{Sq}}\right|^2}{\left|\vec{E_{Ip}}\right|^2} \tag{3.4}$$

In order to exploit the vector nature of the polarised EM field, the scattering process at a target is considered as a function of the EM fields, hence we consider the studies related to polarisation of a plane monochromatic electric field, which can be represented by the so called Jones vector [31] [35] [36] [37] [38] [39]. In addition when considering the case of a pair of orthogonal Jones vectors to form a polarisation basis, in which, any polarisation state of a given EM wave can be expressed. Hence considering the Jones vectors of the incident and scattered waves, the scattering process occurring at a target is expressed by equation 3.5 [31]

$$\vec{E_s} = \frac{e^{-jkR}}{R} \begin{pmatrix} S_{11} & S_{12} \\ S_{21} & S_{22} \end{pmatrix} \vec{E_I} \tag{3.5}$$

where, $\begin{pmatrix} S_{11} & S_{12} \\ S_{21} & S_{22} \end{pmatrix}$ is the Polarisation scattering matrix, elements Sij are called complex scattering coefficients with i for Transmitted and j for Received polarisation.

The diagonal elements of the PSM are termed as co-polar terms referring to the same polarisation states and the off diagonal elements are called cross-polar terms and provide the orthogonal polarisation states in the incident and back-scattered waves.

$\frac{e^{-jkR}}{R}$ represents the effects of wave propagation in amplitude and phase on the receiving wave.

Polarisation Back-Scattering Matrix (BSM) for Parsax System

A common practice by most polarimetric radars, to measure/ estimate non-/simultaneously all elements of the PSM, (discussed in previous section) adopt a pulse to pulse switching, either at the receiver or transmitter sides, this in general causes frequency and phase ambiguities in polarimetric measurements[40]. To mitigate this bottleneck, the use of "sounding signals that present a dual orthogonality property" [41][42].

"A pair of opposite (up and down) linearly frequency modulated (LFM) signals, which occupy the same bandwidth and time interval, can be used in this case. The two probing signals can then be feed into two differently polarised transmitting channels so leading to the dual-orthogonality characteristics,"[40][10].

"The PARSAX radar is a fully polarimetric S-band radar which uses dual-orthogonal digitally generated sounding signals. It is characterised by a high dynamic range at reception and the advanced digital processing at intermediate frequency allows simultaneous measurements of all the elements of the polarisation BSM during one sounding sweep."[40]. The block diagram in figure 3.3 describes the processing stages of the Parsax system.
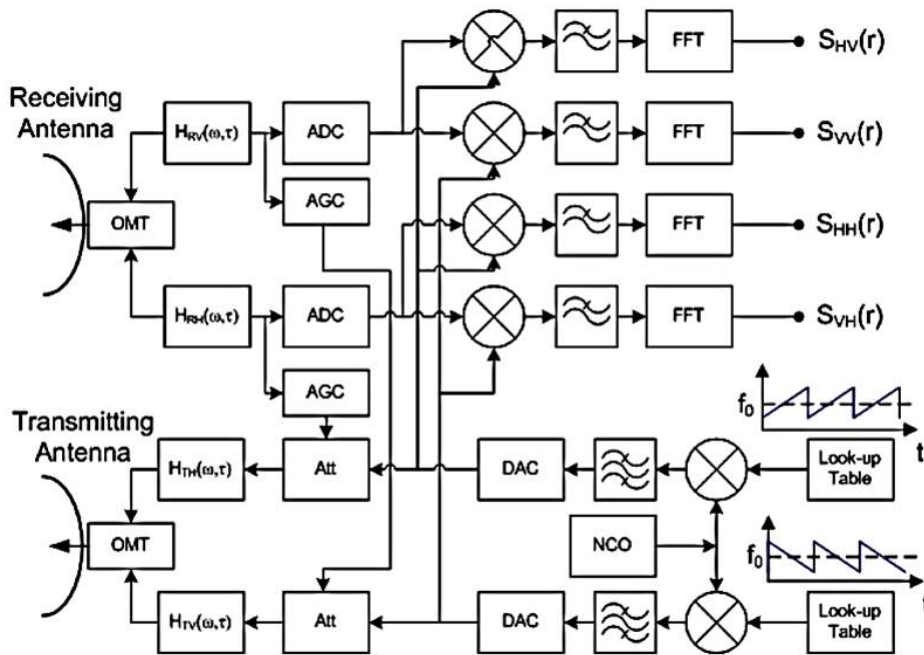
Figure 3.3: Block-diagram of the PARSAX full polarimetric CW radar with dual-orthogonal sounding signals[10]

As the scope of this study does not involve the design of the system, but merely, the use the of the estimated elements of the BSM from experimental data sets acquired by the Parsax system pointed over different locations, to emphasise the reflections of the sounding signal echoes captured from moving cars as targets. The considered scattering coordinate framework for this study is fixed as a monostatic "Back Scattering Alignment" (BSA), coordinate system is as shown in figure 3.4

where, $(\hat{x}_T, \hat{y}_T, \hat{z}_T), (\hat{x}_R, \hat{y}_R, \hat{z}_R), (\hat{x}_S, \hat{y}_S, \hat{z}_S)$ is the right handed coordinate system of the transmitter, receiver and scatterer respectively, with the $\hat{z}_T$ pointed towards the target and , $\hat{z}_S$ pointing away from the target, as the radar is in monostatic configuration , the
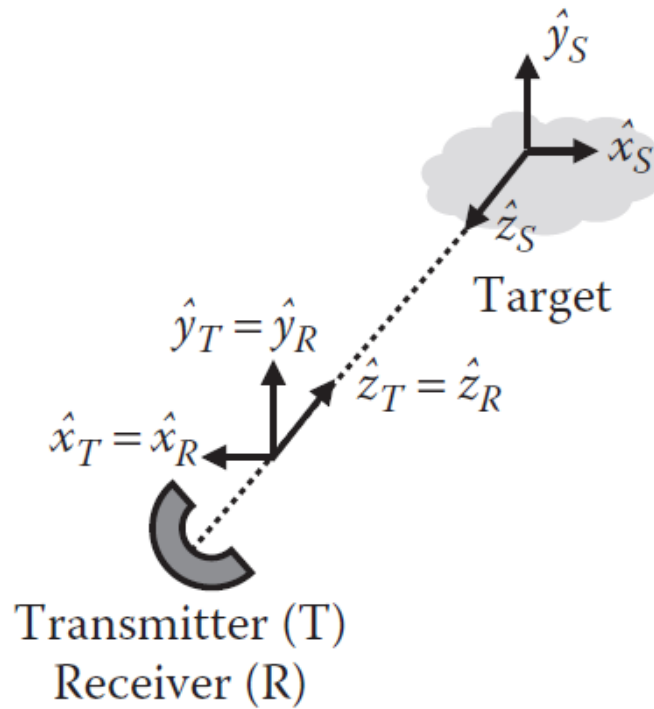
Figure 3.4: BSA monostatic coordinate system[31]

coordinate system for the two antennas coincide.

Hence the estimated polarisation back scattering matrix S for the considered system is given by equation 3.6[40].

$$S = \begin{pmatrix} \dot{S}_{HH}(\tau, f_d) & \dot{S}_{HV}(\tau, f_d) \\ \dot{S}_{VH}(\tau, f_d) & \dot{S}_{VV}(\tau, f_d) \end{pmatrix} \tag{3.6}$$

where, $S_{xx}(\dot{\tau}, f_d)$ represents co-polar components and $S_{xy}(\dot{\tau}, f_d)$ represents cross polar components, with (τ, f_d) representing target range and doppler.

As the radar is considered in a monostatic configuration the cross polar elements have the same value. Where as in the case of a bi-static configuration the cross polar elements will also have different values.

Hence the total back scattered power in case of a polarimetric radar system in monostatic configuration is given by equation 3.7

$$Span = trace(SS^T) = \left|S_{HH}(\tau, f_d)\right|^2 + 2\left|S_{HV}(\tau, f_d)\right|^2 + \left|S_{VV}(\tau, f_d)\right|^2 \tag{3.7}$$

3.1.3. Extended Target Characterisation on Polarimetric Channels

Based on the processing stages discussed in chapter 2 2, the back-scattered returns of polarised EM waves from the extended moving target are received on all 4 channels of the Parsax radar, the following figures 3.5-3.10 describe the different processing stages applied simultaneously on all 4 channels.

Range Doppler Processing all channels
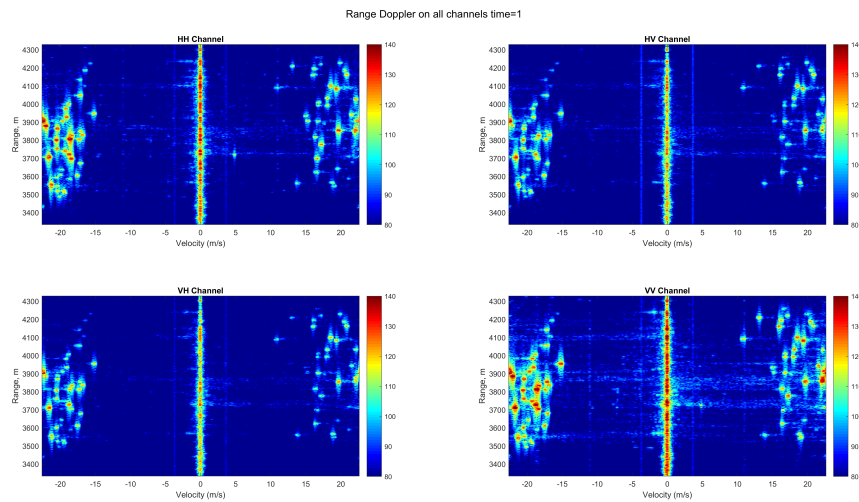
Figure 3.5: Range Doppler processing w/o MTI on all 4 Polarimetric channels

MTI applied to all 4 channels
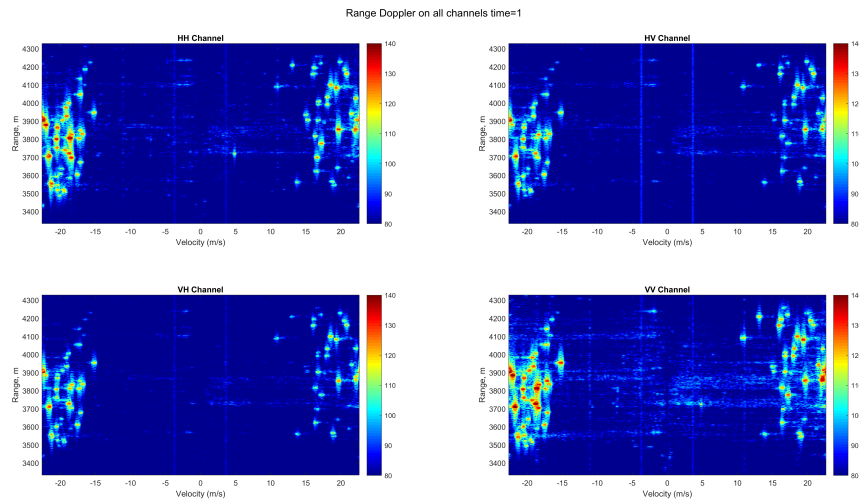
Figure 3.6: Range Doppler processing with MTI on all 4 Polarimetric channels, it can be seen that clutter at zero doppler has been eliminated on all channels

CA-CFAR applied on all channels
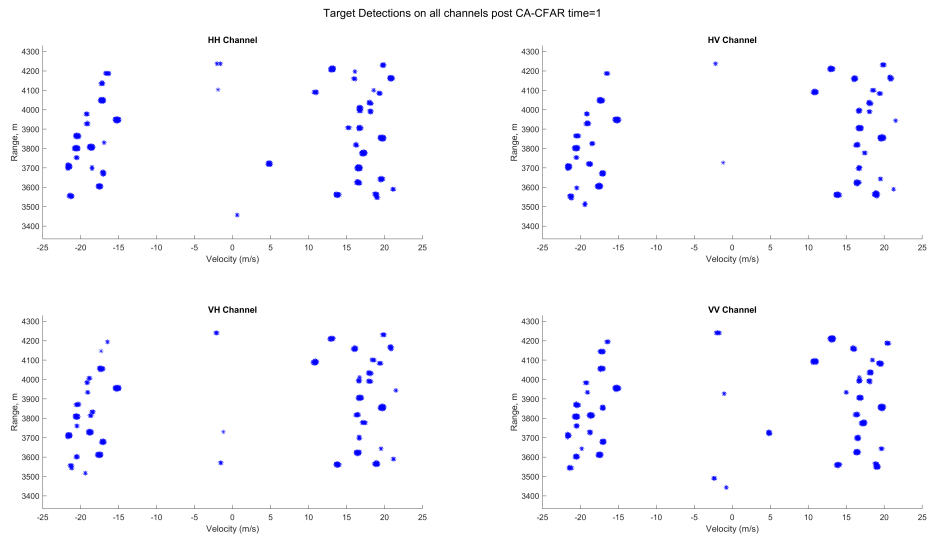
Figure 3.7: Target detections on 4 channels post CA-CFAR with Pfa 10e-6 and 6X6 training window
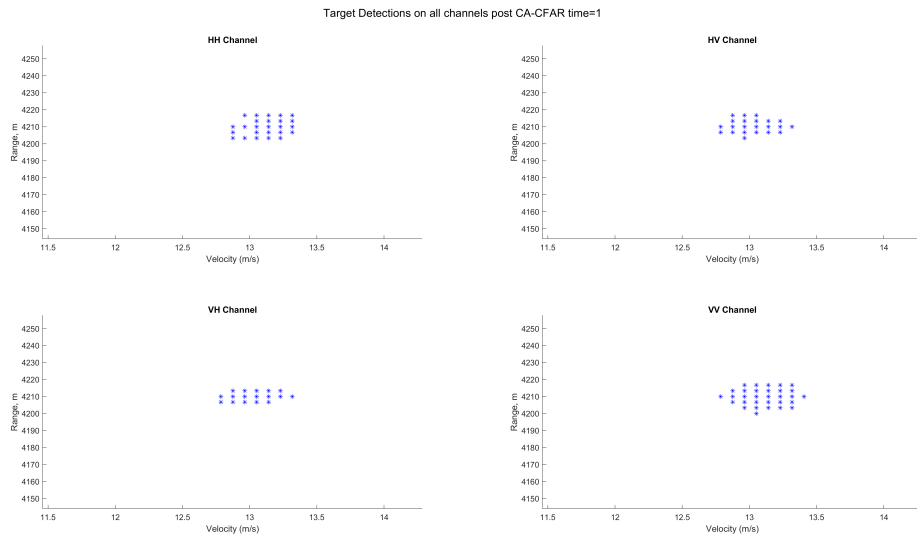
Figure 3.8: Target detections are different on each channel due to effect of polarisation

Extended Target Cluster using 'k' nearest neighbours
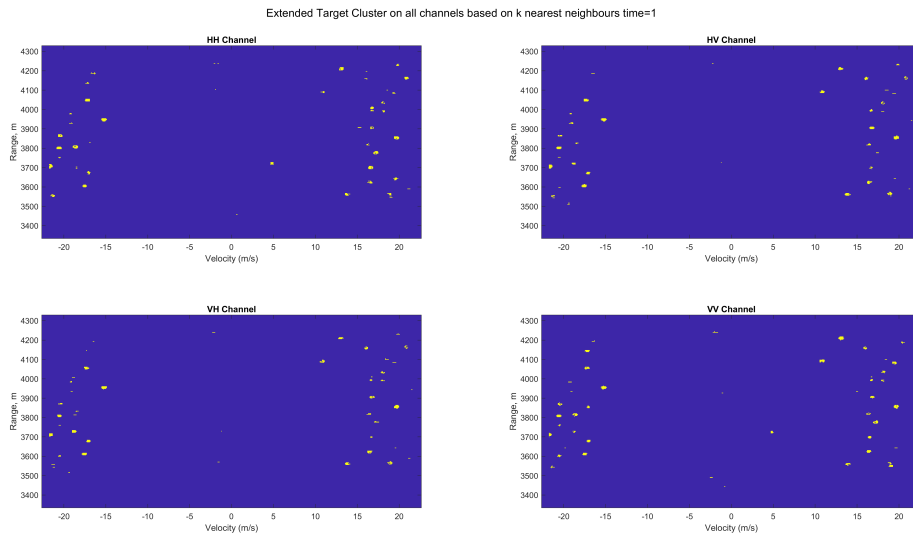
Figure 3.9: Extended Object created by clustering all detections of a target based on k nearest neighbours
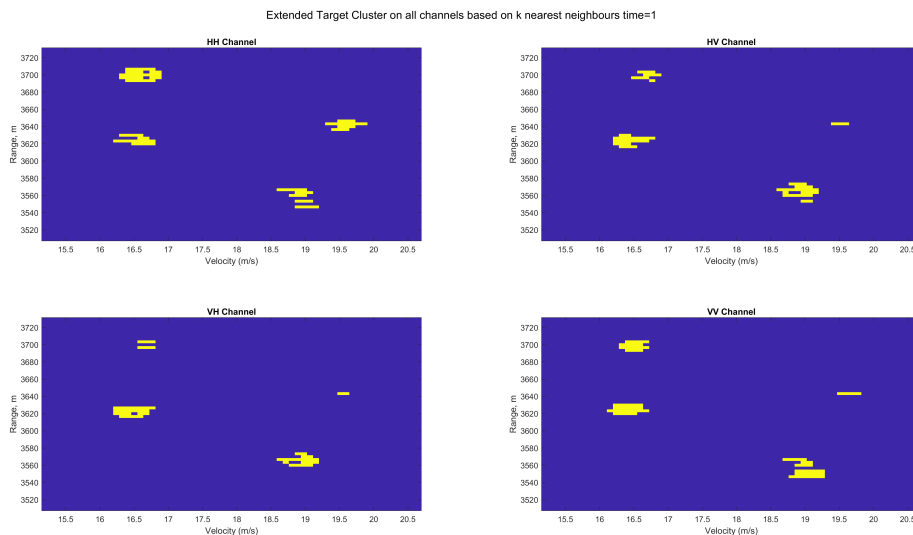
Figure 3.10: Extended Object created by k nearest neighbours is different for different targets on each channel

The physical properties of each target interact differently to the type of polarisation [31], in addition since the detections belong to extended moving targets , there is significant variation observed for the same target across different polarimetric channels and between different frames of measurement. This phenomenon can be observed in figures 3.11-3.15. For each figure, the central plot consists of detections of one target from all channels, the other plots (top left, top right, bottom left and bottom right) show the extended object created for the same target, based on the detections of their respective channels, * is the marker for detections from HH channel, diamond is the marker for HV channel, square is the marker for VH channel and dot is the marker for VV channel detections respectively.

Different Shapes for same target in different channels
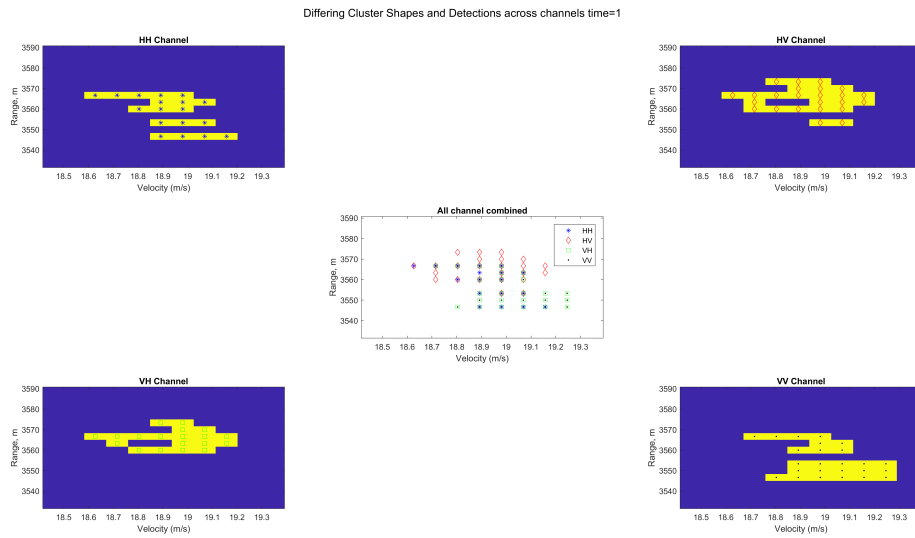
Figure 3.11: Different shapes for same target in different channels

No detections is some channels

As the amplitude of target reflections is stronger in the Co-polar channel compared to cross polar channel, at times a target is not detected in the cross polar channels as seen below:
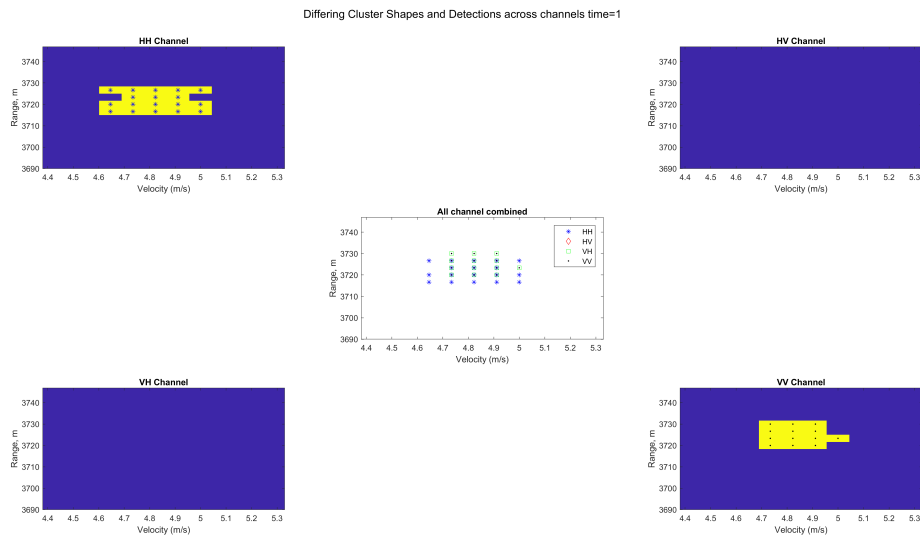
Figure 3.12: Differing detections in different channels

Different number of targets across channels

As the targets are moving there is an expected change in the position of the target considered in simulation shown in figure 3.10 and 3.11 from one scan to another, with
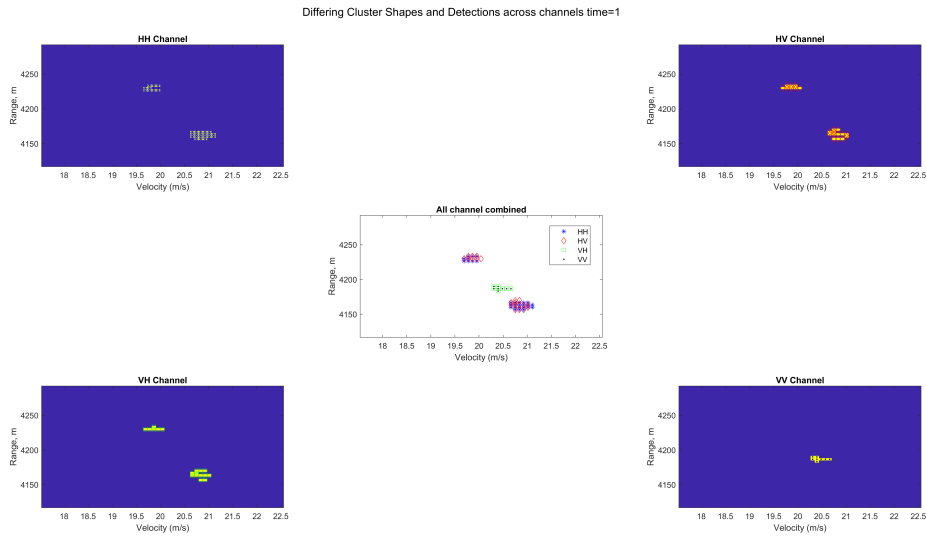
Figure 3.13: Differing objects in different channels

velocity remaining nearly the same, as a result of the shift in the position of the target, the scattered field reflected from the target may be different, hence the shape of extended cluster is different from scan to scan as seen in figures 3.14- 3.15.

Different structure of cluster from scan to scan
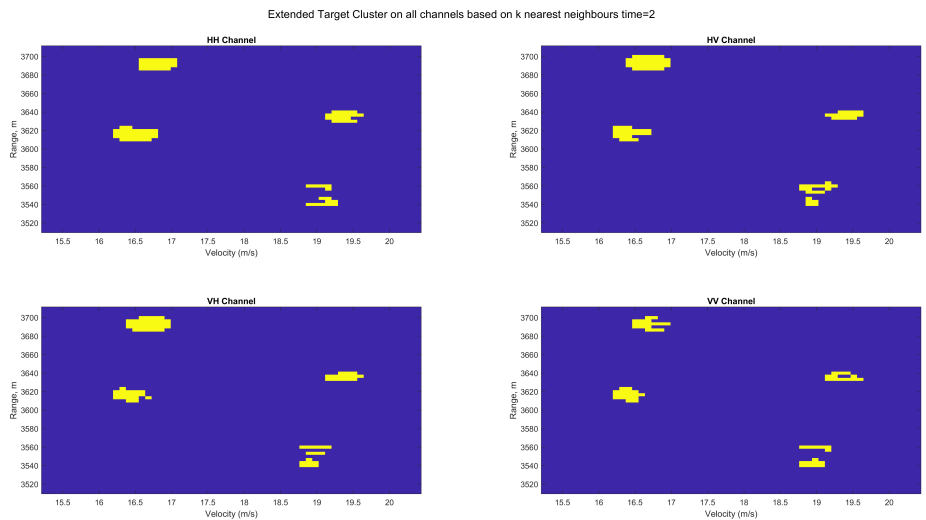
Figure 3.14: Shape of extended objects changed from scan to scan compared to figure 3.10

In order to extract polarimetric information from all 4 channels simultaneously , it requires that all 4 channels must be synchronous. As it was observed in the previous figures 3.10-??, that there is variation among channels and between scans, a possible strategy to combine information across all channels is required, in addition as the k nearest neighbours method proves ineffective in producing a unified image for a single target, further study into different clustering techniques is required.
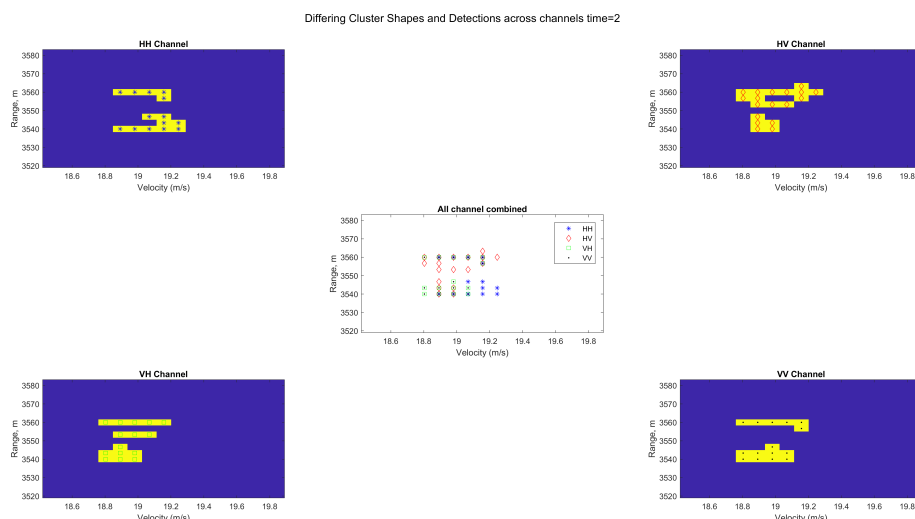
Figure 3.15: Shape of extended objects changed from scan to scan compared to figure 3.11

3.2. Clustering Algorithms

Clustering is defined as the process of grouping individual smaller objects of similar properties into one unified larger object/ group called a cluster. Clustering algorithms are widely used for statistical data analysis in various areas such as, pattern recognition , data compression, image analysis etc.. for applications involving classification and categorisation, based on the type of data and the understanding as to what constitutes a cluster, there are numerous algorithms which can be used for "Clustering data".[44]

In the context of this section data here is referred to as the pixel occupied by a target detections (pixels with intensity greater than that of CA-CFAR noise threshold) and a cluster refers to a collection of closely spaced detections for each "individual" target. In the following subsections 3 general clustering algorithms have been investigated and the best fairing algorithm in terms of consolidated structures and computation time are considered.

3.2.1. K nearest neighbours

For given set N with 'n' number points which contains a subset M with 'm' detections, given a start point, the "k nearest neighbours" algorithm uses a user defined distance function to find the 'k' nearest points belonging to the subset M, to form c groups of clusters 'C'. The mathematical formulation of the same can be as seen in equations 3.8 and 3.9:

$$C_{m_i} = m_j |\, \|m_j - m_i\| \le d \qquad\qquad (3.8)$$

where, $\|\|$ is the user defined distance function, d is the distance threshold, C_{m_i} is the cluster of m_i detections, m_j is the detection under test and m_i is the detection confirmed detection, given $\forall$ m $\in$ M with M $\subset$ N .

$$C = \sum_{l=1}^{c} C_l \qquad (3.9)$$

where, C is the total number of clusters

As it was observed in the previous section in figures 3.10-??, there are various problems in the k nearest neighbours hence an alternative approach is investigated.

3.2.2. Density Based Spatial Clustering of applications with noise DBSCAN

DBSCAN is a clustering algorithm which works best on point clouds to cluster points with a minimum spatial density, given a search radius (Eps) and a prior related to the minimum number of points (minpts) required to define a cluster, the DBSCAN algorithm determines if a point belongs to a cluster or not. The algorithm starts with a arbitrary point and looks for points within a search radius (Eps), all points found with the radius are added to a cluster provided the criteria for min number of points is met, the minimum number points required for cluster formation is considered as the "core points" once a cluster is formed every point within the vicinity of the search radius is assimilated into the cluster to make it more dense, the process continues until the cluster is completely found, when the number of points fall below the minpts condition, but shares points with the connect cluster, it is consider as the border points which ends the completion of a clustered region. Once a cluster is completed, the process continues forming different clusters of different sizes until all bins are exhausted, the end results in a set of connected objects depicting the target, unconnected objects which may residual detections which are unconnected along with noise. In this study since a binary data set is considered , the case is either target or noise, hence what is not labelled as a target is by default considered as noise[45][46]. The mathematical formulation of DBSCAN algorithm given by equation 3.10

$$N(p) = q \in D | dist(p, q) \leq Eps \qquad (3.10)$$

where, N(p) is a point under test, q is a point present in a created cluster, D is domain of the data points in our case the detections, dist(p,q) is the euclidean distance, Eps is the predefined search radius.

The algorithm can be summarised as in figure 3.16

Though the algorithm is promising and has various advantages compared to the k nearest neighbours algorithm, the implementation of this algorithm is limited by the choice of the Eps-minpts (search radius and minimum points) parameters combination, the large fails to cluster data set with considerable difference in sizes as the parameters are not chosen correctly, in addition to the clustering algorithm a parameter search algorithm is required to find the right Eps-minpts combination. In addition as we are dealing with fluctuating targets, the size of cluster is expected to change from scan to scan which would require parameter search stages to be performed from every frame. As the scope of this study does not focus too much on clustering, alternative simple but effective approaches are investigated.
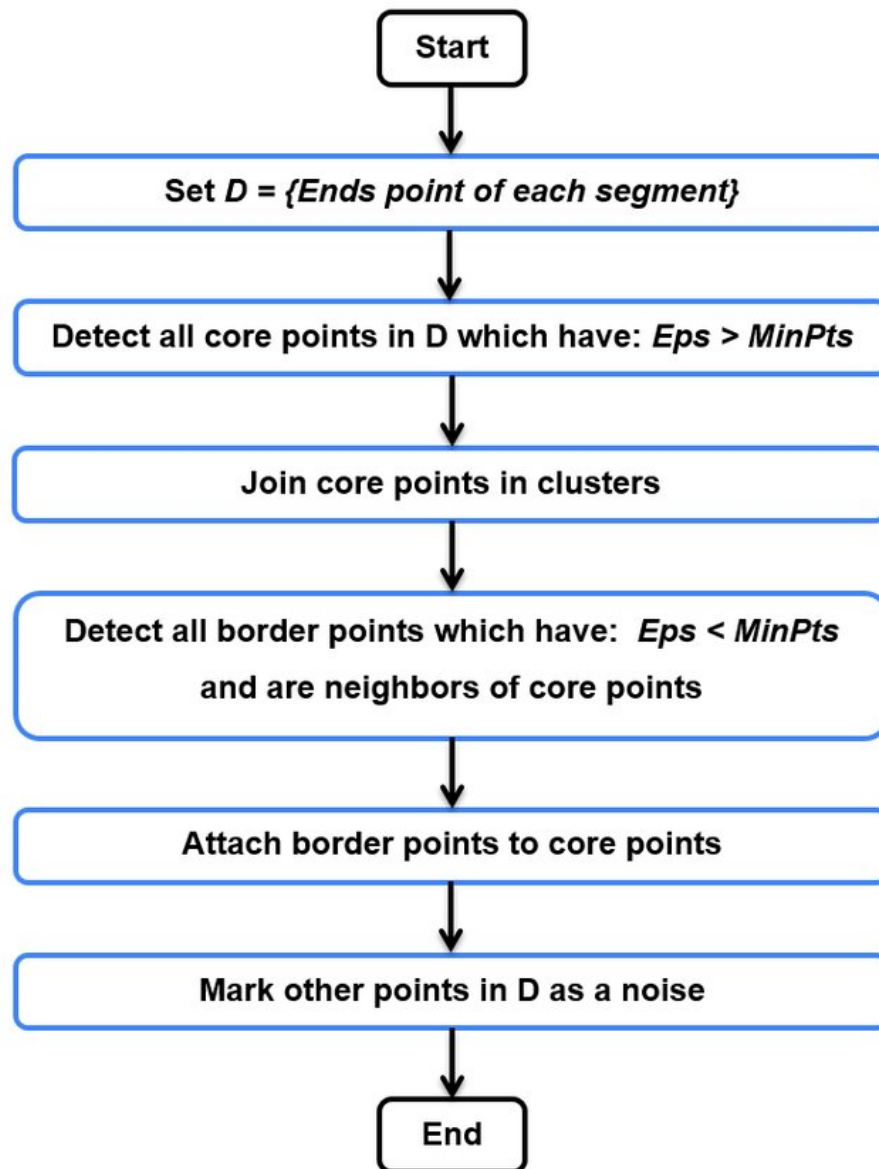
Figure 3.16: Flowchart of the DBSCAN algorithm [46]

3.2.3. Flood fill algorithm

Generic

Flood fill algorithm is a widely used algorithm in image processing in the areas of morphological image processing[48][47], the algorithm connects neighbouring pixels of the same value, when applied to a grayscale image (binary image in our case) or data which has been pixelated or binned into pixels. Based on a specified threshold for any given image, the subsequent connect sub-images are generated. The algorithm does not require any prior knowledge related to location or number of clusters like the kNN algorithm and does not require any search radius or minimum connected points as in the case of the DBSCAN algorithm. The implementation is simple and is capable of automatically connecting nearby pixels and generating labels to every individual cluster. As an added advantage a geometric centre for each cluster can be determined, which is vital in the case of associating clusters between different frames (the details will be

discussed in the following chapter 4). The algorithm follows a queue based approach along either the rows or columns of the considered grayscale image. An interpretation of the algorithm's working can be visualised in figure 3.17.
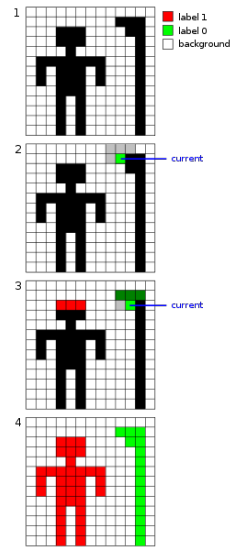
Figure 3.17: Flood fill algorithm on binary image applied row wise[49]

With respect to the scope of this study, the detection map discussed in chapter 2 produced as an output of the CA-CFAR can be used as the pixelated binary image, as discussed the detection map consists of states 1 for pixels with values above the CA-CFAR threshold and state 0 for values below the threshold. Hence the Output of the CA CFAR is directly feed to the Flood Fill algorithm, the scope of improvement with respect to kNN algorithm cluster can be seen as in figure 3.18
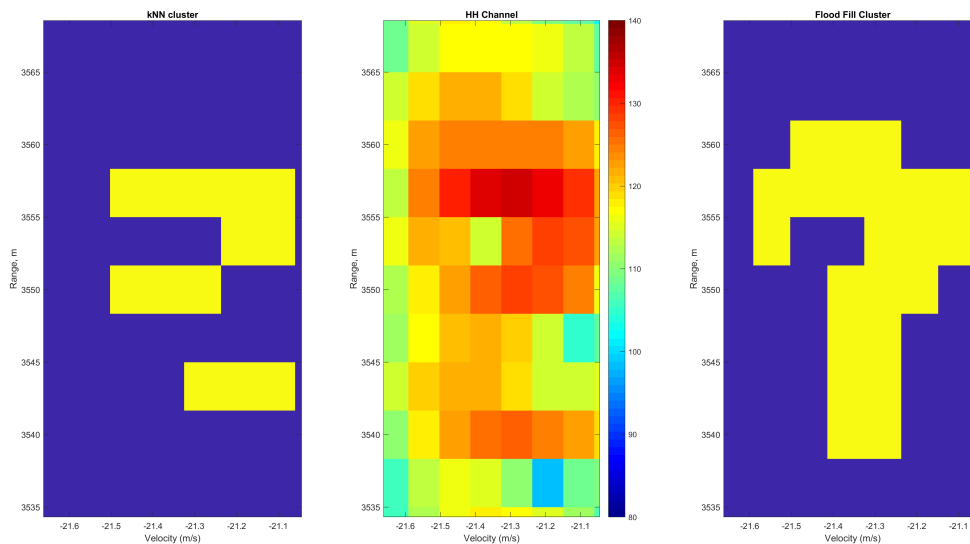
Figure 3.18: Comparing Target in RD map in centre against cluster created by kNN algorithm in left to Flood Fill algorithm in right, it is seen that the Flood fill algorithm out performance the kNN algorithm

The improvement factor can also be seen when applied across all 4 polarimetric channels as seen in figure 3.19.
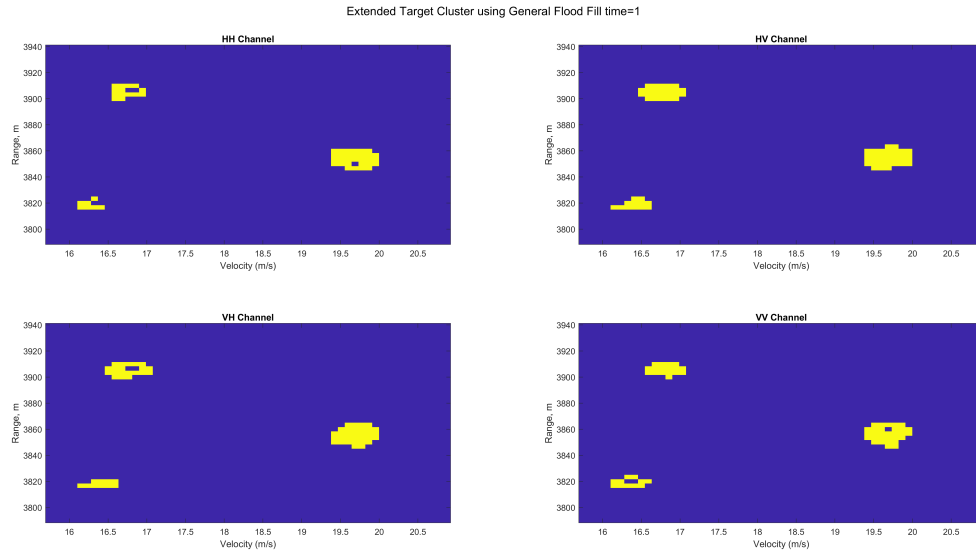
Figure 3.19: General Flood Fill across all 4 channels

It is seen that there is a better improvement in the created clusters compared to the kNN algorithm in figure 3.15.

A drawback that appears trivial is that, the formed clusters in some cases are not completely filled as solid object, instead appear as porous in nature. As we are dealing with objects changing from scan to scan as a result of motion, this may result in two possible draw backs and critical errors when considering interaction of the objects between frames :

- The porous objects are highly likely to vary much more compared to solid objects from one frame to another.

- Determining a reference centre between frames is mandatory for associating objects across frames,hence determining a geometric centre stable from scan to scan becomes erroneous.

Hence additional methods to mitigate the porous objects are investigated[50].

Proposed Flood Fill Algorithm

In order to mitigate the porous objects in addition to the standard flood fill algorithm an additional dilation and erosion stages are performed[48]:

- Dilation:
  Is a standard processing in morphological image reconstruction used to spread out a lower layer image termed a marker using a second layer image called the mask, it is represented by the operator $\oplus$ and applied as equation 3.11:

$$A \oplus B = \bigcup_{b \in B} A_b \tag{3.11}$$

where, A is the primary image (1st layer) and B is marker image resulting in A_b image augmented by B.

The result of a dilation process can visualised as shown in figure 3.20

Figure 3.20: Dilate operation

It is observed that for a given porous image is not filled, but also an additional pixel in the borders are also converted to detections, if the flood fill algorithm is applied post only dilation cluster closely spaced will be wrongly interpreted as larger objects, hence the second step of erosion is performed.

- Erosion:
  The erosion process works similar to dilation step but instead perform the inverse operation only on the foreground area of the image , it is given by the operator $\ominus$, as applied in the equation 3.12.

$$A \ominus B = \bigcap_{b \in B} A_{-b} \tag{3.12}$$

where, A is the primary image (1st layer) and B is marker image resulting in A_{-b} image transition by B.

The result of a erosion post dilation can visualised as shown in figure 3.21

Figure 3.21: Erosion operation

The results of the joint dilation and erosion applied in combination to the flood fill algorithm results can be visualised in figure 3.22 and can be compared against 3.19 with flood fill alone.

Though the secondary problems related to creation of consolidated clusters to represents is solved, the primary object of extracting the polarimetric information from the pixels occupied by a target across all 4 channels simultaneously is still open, hence the further analysis for consolidating multi channel data is investigated.

Figure 3.22: Resulting clusters using proposed variant of flood fill algorithm, it can be seen that solid object across all channels is achieved

3.3. Data Fusion Strategies

Polarimetric information related to a target plays a vital role for analysis regarding targets physical properties as seen in chapter 2, hence the possible extraction of data from all channels is required, as the behaviour of a target with a polarised field depends on the type of target, polarisation field incident and the channel in which the data is received, the scattering and consecutively the formation of clusters depicting detections is not uniform in all 4 channels , as observed in figure 3.22 , different shapes of clusters were created across different channels for the same object as seen in figure 3.11 - ??.

As this study deals with multiple objects closely spaced and moving in slow-time the bottleneck of data association within channels for a same object and between frames is required to be solved. The details of inter frame data-association will be discussed in the chapter 4, hence focus is concentrated on solving inter channel data association.

Though there are various studies related to polarimetric data fusion for terrain obser- vations of efficient target detections [51][52], which itself is an elaborate area of study, there is very little information matching the context of this study. Hence it is safe to say, Polarimetric data fusion for moving land objects, is a possible open research topic identified in through this study.

However with the prior knowledge of the Parsax detections capabilities [40], and from general polarimetric radar literature [31], two possible data fusion strategies have been identified as :

1. Logical Data Fusion :
   Combining Detections across channels by using the detection maps from all 4 chan- nels. with prior information that targets detected on Co-polar channels are more likely to different compared to Cross-polar channels, possible combinations of de- tection maps are analysed.

2. Polarimetric Data Fusion :
   As the study focuses on extraction of target information, the same can be analysed in aspects, an additive combination of received signal amplitudes by combining range doppler maps.

A flowchart depicting the possible strategies is as shown in figure 3.23
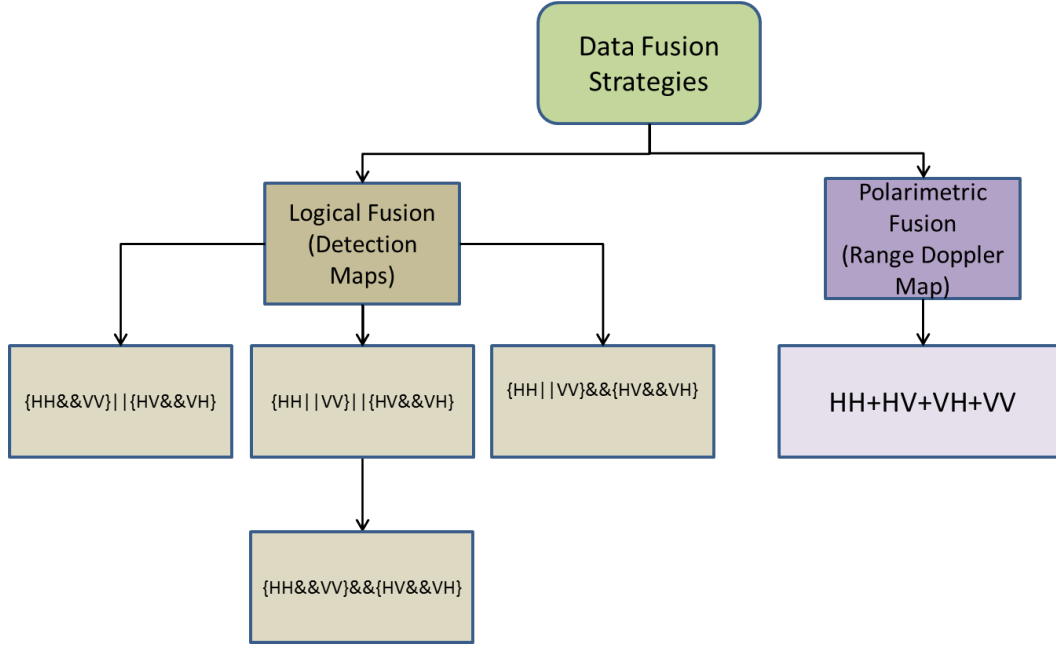
Figure 3.23: Data Fusion Strategies

The proposed fusion strategies are investigated for creation of a fusion cluster which can be used as reference for extracting polarimetric information from all channels and also as a reference between different frames of data, a final fusion algorithm is chosen based on the correlation co-efficient[53] for number of cluster created by the fusion algorithm against clusters in each channel. In addition, a bounding region and geometric centre is defined by the fusion algorithm, this can be used as a reference to mitigate inter-channel data association, therefore making simultaneous extraction over all channels possible. The geometric centre acts as the reference point for a target across frames , which can be used for tracking the object across multiple frames, the details of the same will be discussed in the next chapter 4.

** For the case of simplicity, we shall hence forth considered only positive doppler clusters.

3.3.1. Polarimetric Data Fusion

A simple summation of range doppler maps of polarimetric amplitudes for a monostatic configuration is given by equation3.13.

$$RD_{mapT} = \sum RDHH + 2RDHV + RDVV \tag{3.13}$$

Where;

RD_{xx} is range doppler map containing amplitudes from co-polar channels and RD_{xy} is range doppler map containing amplitudes from cross -polar channels.

The proposed fusion cluster algorithm is as shown in figure 3.24
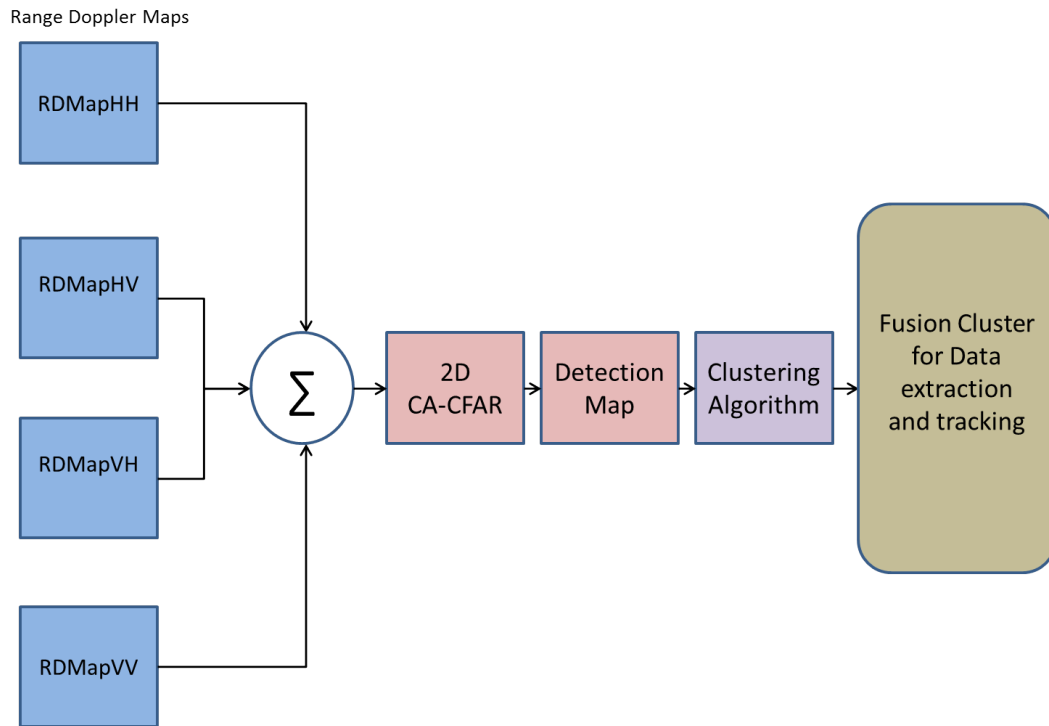
Figure 3.24: Summation over range Doppler maps from all 4 channels, the difference in colour indicates modification/ transition of data over time

For the proposed fusion strategy a Fusion Cluster map is generated, consisting of clusters representing targets detected across all channels, the clusters are compared against the data from range doppler maps and detection map as shown in figure 3.25 - 3.27
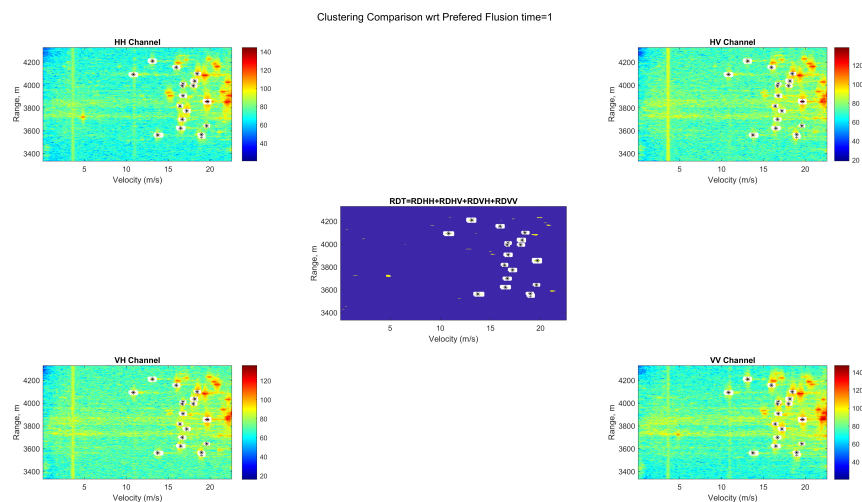
Figure 3.25: Fusion cluster compared against all 4 channels

As the information observed is only over a single frame, the correlation co-efficient for
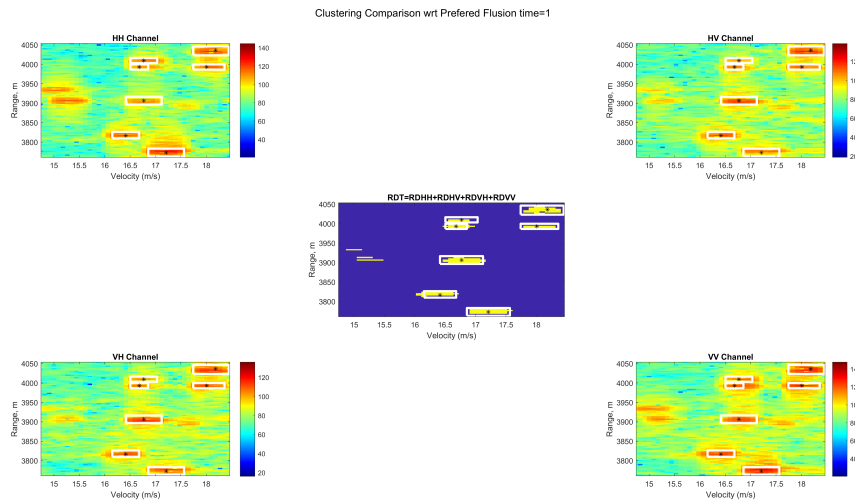
Figure 3.26: Close up view of clustered regions on range doppler maps, it is observed that the bounding region defined by the algorithm is irregular and data across cross-polar channels are missed
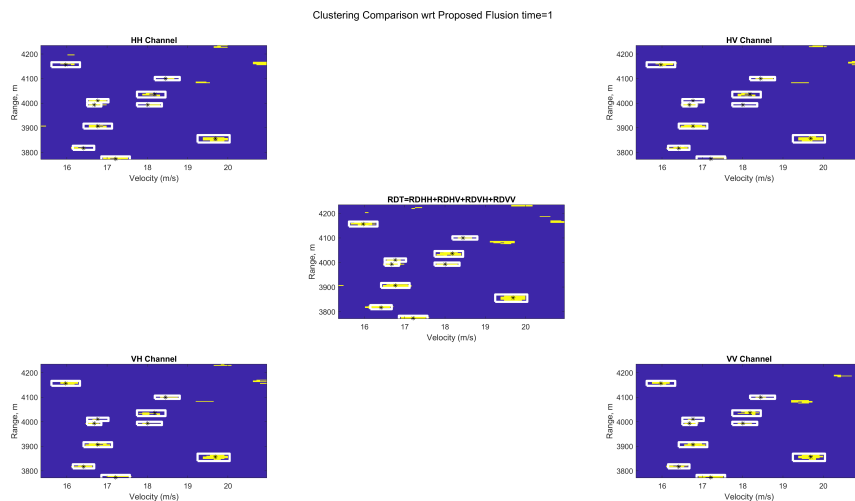
Figure 3.27: Close up view of clustered regions on detection maps, it is observed that there is mismatch between bounding regions and clusters created by the algorithm

number of clusters created by the Fusion algorithm and the targets detected across all channels is calculated as seen in figure 3.28

3.3.2. Logical Detection Map fusion

The detection map created as an output of the 2D CA-CFAR applied on the range doppler maps on all channels is a binary image, consisting of detections and noise. Since the radar is operating in a monostatic configuration, the data from cross polar channels is relatively the same , meaning the resulting binary images are also close related.

Data from co-polar channels however varying strongly based on the interactions with the target, for example a target detected in HH channel may not be detected in the VV channel due to the nature of target and its interaction with the field, hence with this
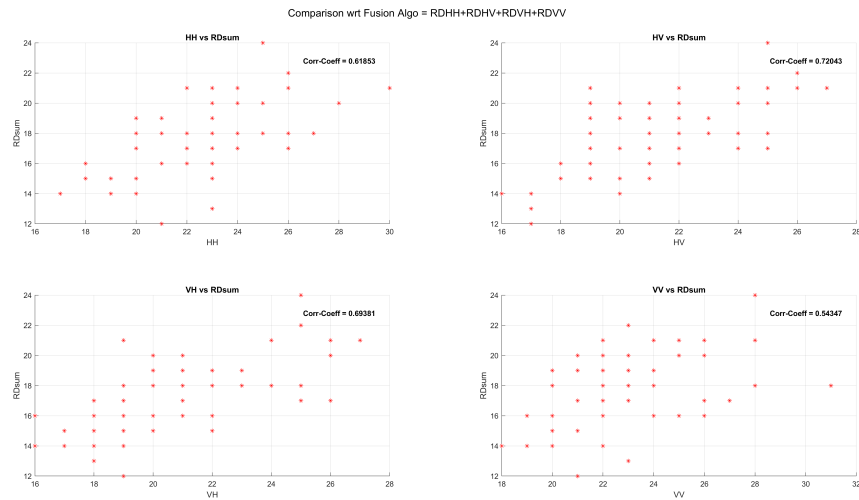
Figure 3.28: Scatter plot with correlation co-efficient for comparing clusters across channels and clusters created by fusion algorithm, it is observed an average 64 percent correlation is observed

prior information, the following 4 Fusion strategies are suggested:

1. Fusion A - or(and(DMapHH,DMapVV),and(DMapHV,DMapVH))

2. Fusion B - or(or(DMapHH,DMapVV),and(DMapHV,DMapVH))

3. Fusion C - and(or(DMapHH,DMapVV),and(DMapHV,DMapVH))

4. Fusion D - and(and(DMapHH,DMapVV),and(DMapHV,DMapVH))

where;
DMapXX - stands for Detection Map in Co-polar channels
DMapXY - stands for Detection Map in Co-polar channels
and - "Logical AND" and or - "Logical OR" operations

Fusion A, B, C, D are names for each fusion combination for reference.

The general fusion algorithm is as shown in figure 3.29

In figures 3.30-3.34 the 4 logical fusion strategies are compared based on resulting logical fusion maps and correlation coefficient o number clusters created in channels to those created by the fusion clusters.

For additional analysis correlation coefficients for detections in all channels and fusion algorithms is performed.

It can be seen that Fusion algorithm A - or(and(DMapHH,DMapVV),and(DMapHV,DMapVH)) has the highest/best correlation with data across all channels. Hence is chosen as the candidate from Logical fusion strategies.

3.3.3. Finalised Result

The results across all strategies are finally compared for total number of targets in each channels across 66 frames of radar data collected from the Parsax radar , to number of fusion target clusters created by the proposed algorithm, as in figures 3.35 and 3.36
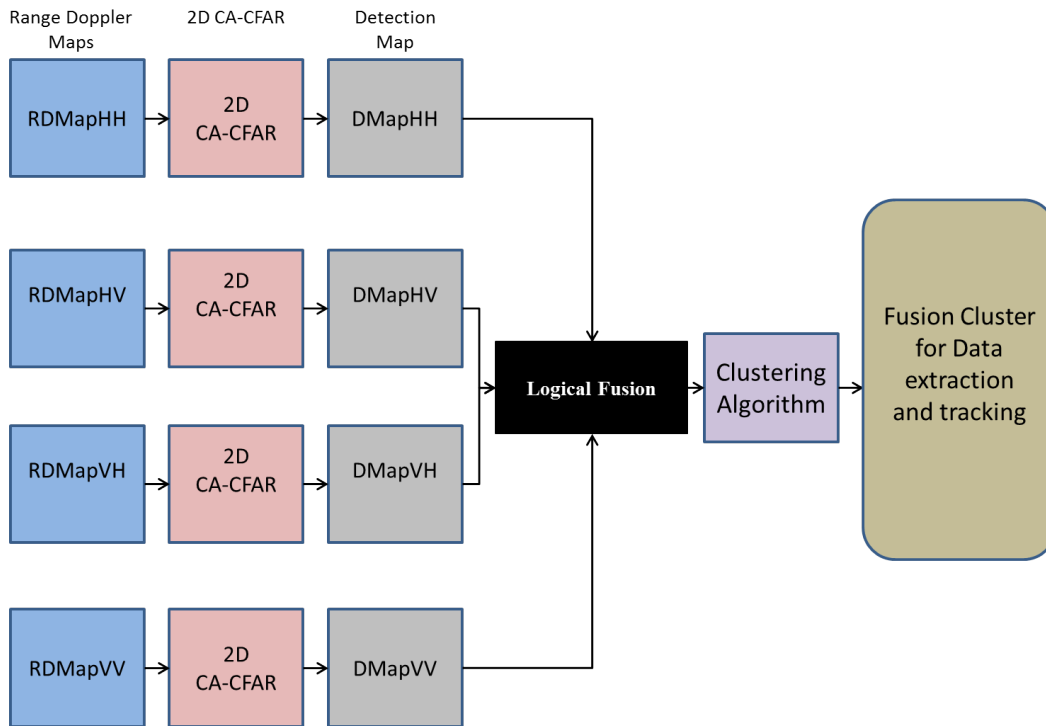
Figure 3.29: Logical Fusion Algorithm, the change in colour indicates change in data
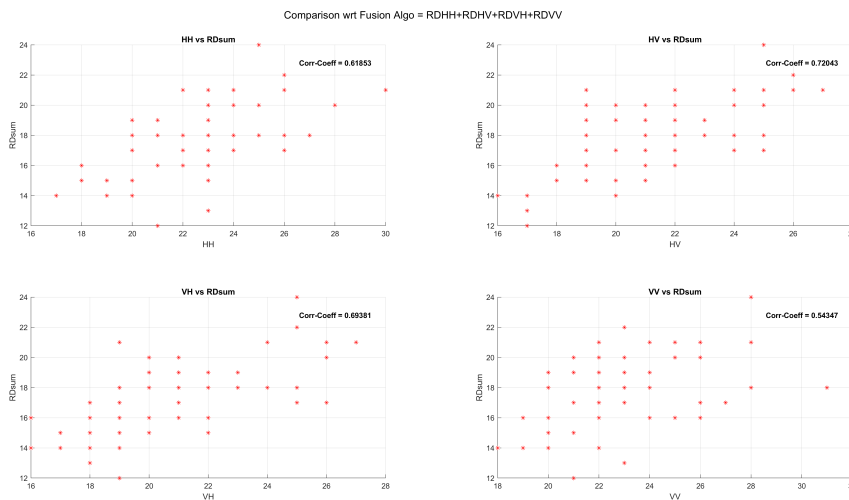
Figure 3.30: Generated Fusion Clusters across channels, it is observed that Fusion algorithm B is relatively friendly in creation of clusters and Fusion algorithm D is the most aggressive with least number of clusters

The Logical Fusion algorithm "Fusion A" result is verified against the Range Doppler maps for all channels and Detections maps, as in figures. 3.37-3.40

As observed, in case of Co-polar channels due to target interaction, the data may not be available in one of the channels but the bounding region is defined in perfect sync with all other channels, the resulting cluster formed from fusion algorithm is a perfect match to depict a unified target across channels.
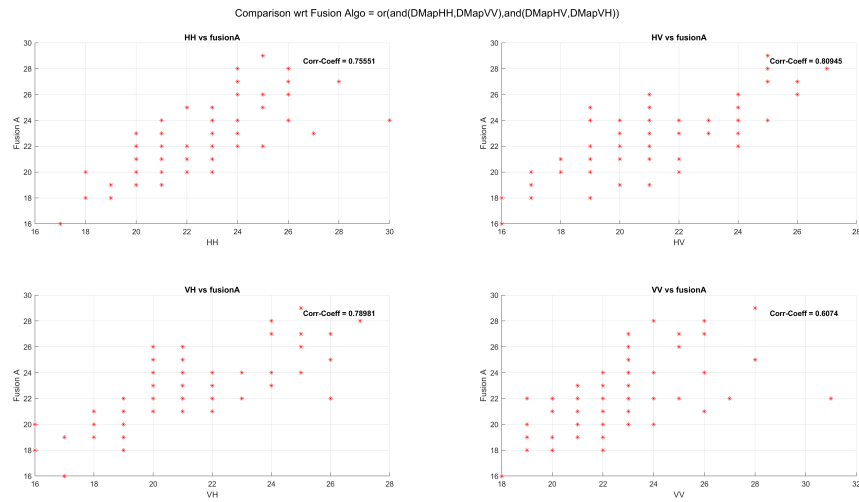
Figure 3.31: Scatter plot for number of clusters created by Algorithm Fusion A vs clusters in all channels, average correlation co-efficient 74.93 percent
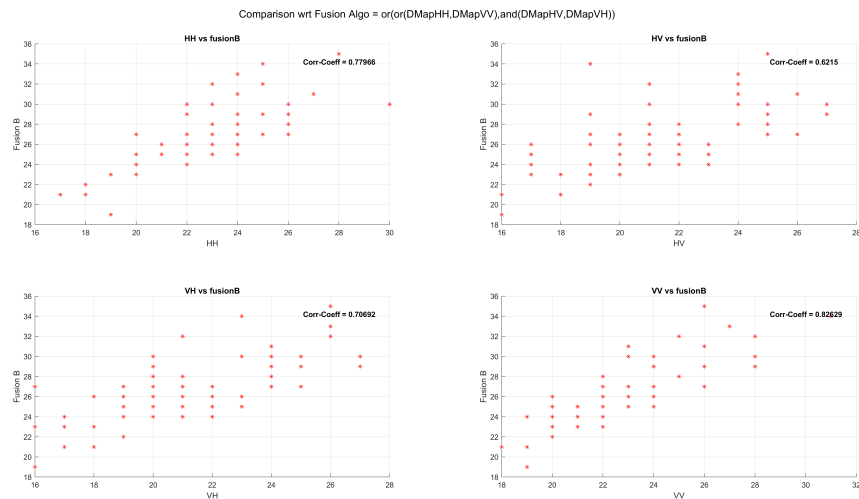
Figure 3.32: Scatter plot for number of clusters created by Algorithm Fusion B vs clusters in all channels, average correlation co-efficient 72.23 percent

3.4. Multi-Channel Data Extraction Algorithm (MCDA)

Based on the discussion , steps and proof discussed in the previous sections, a Data extraction strategy to extract polarimetric data across all 4 channels simultaneously efficiently is formulated. The steps of the finalised approach is summarised as flow chart as shown in figure 3.41.

The advantages and highlights of this algorithm in case of this study are as given below:

1. Consolidated Geometric object created for every target.

2. Geometric centre for every cluster relating with every target detected.

3. Bounding Box around consolidated cluster, for incorporating any residual measurements due migrating target.
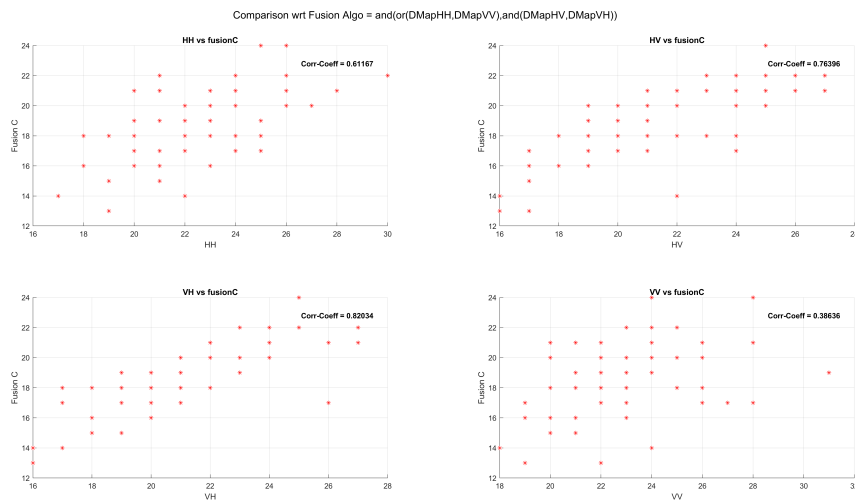
Figure 3.33: Scatter plot for number of clusters created by Algorithm Fusion C vs clusters in all channels, average correlation co-efficient 64.52 percent
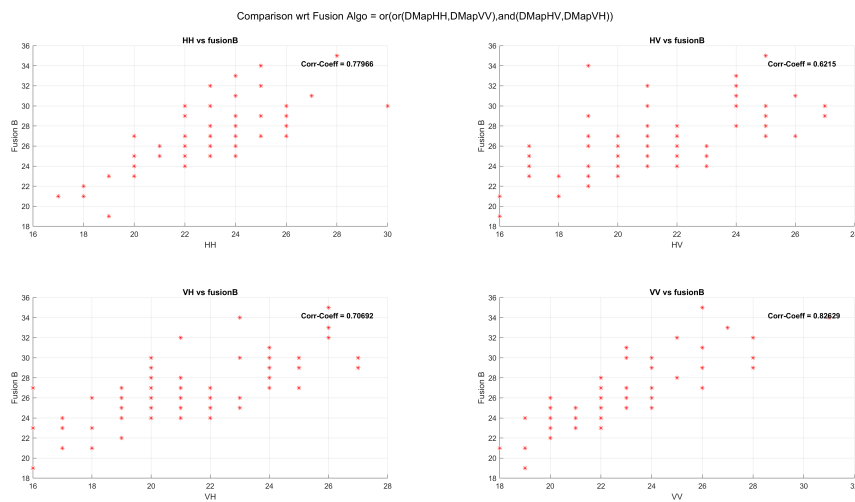
Figure 3.34: Scatter plot for number of clusters created by Algorithm Fusion B vs clusters in all channels, average correlation co-efficient 54.55 percent

4. Frame wise target images captured across all channels containing complex data from all 4 polarimetric channels.
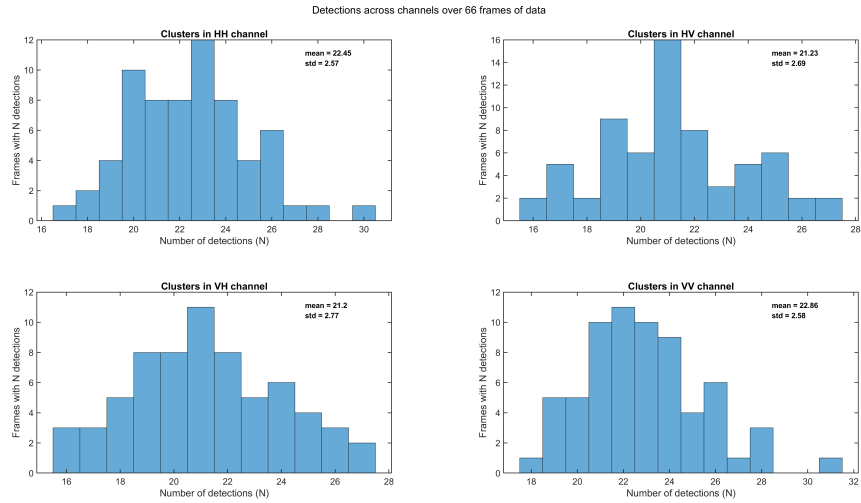
Figure 3.35: Histograms depicting targets clusters across channels collected over 66 frames of data, it is observed that Co-polar channels and Cross-polar channels have a variation as expected
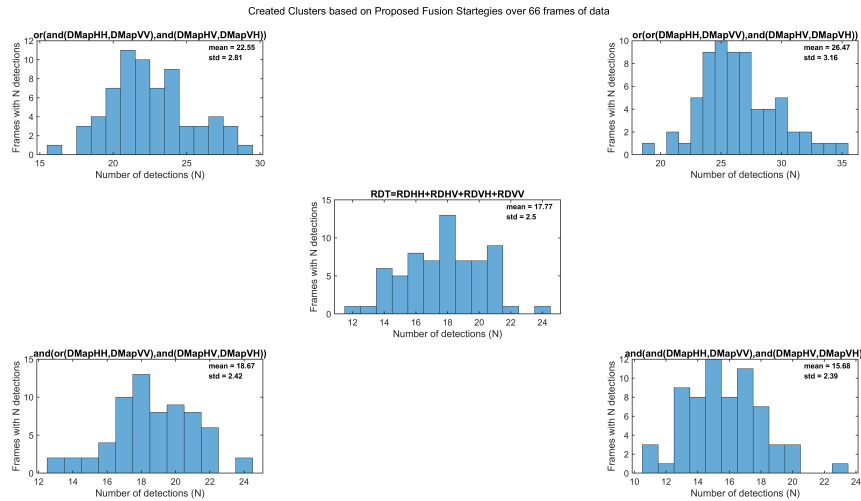
Figure 3.36: Histograms depicting targets clusters created by fusion algorithms it is observed that Fusion algorithm A out performs the other proposed methods and best fits the detections across channels

3.4.1. Detection Database

Using the Multi-Channel Data Extraction Algorithm (MCDA), a database consisting of targets detected across all 4 channels for a given frame is created. The structure of the created database is as shown in figure3.42-3.43

The Detections data base created is free from inter channel data association problems.
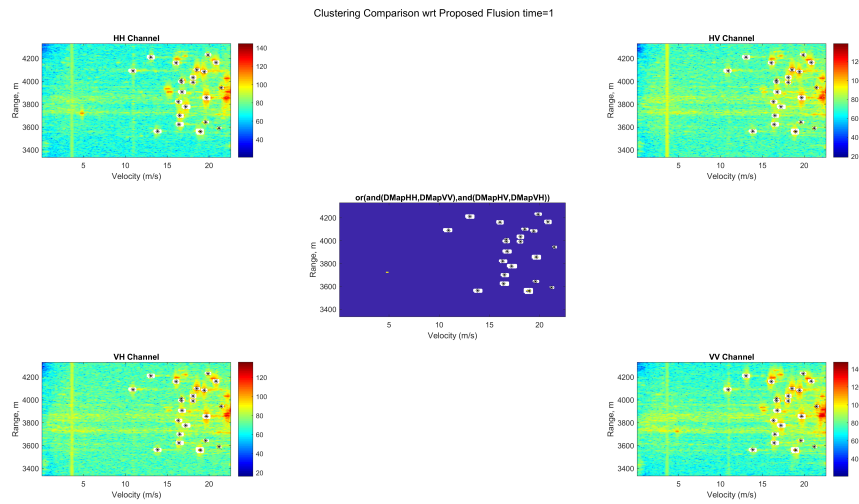
Figure 3.37: Logical Fusion A for targets in all Range Doppler maps
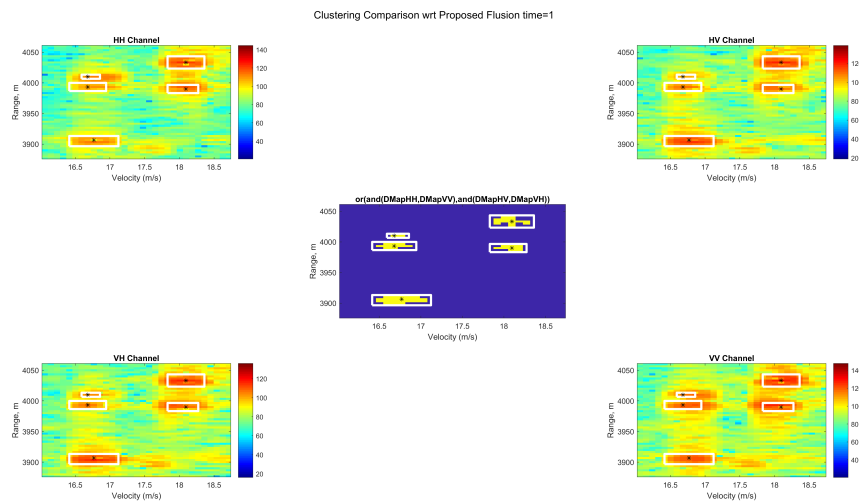
Figure 3.38: Logical Fusion A for targets in all Range Doppler maps close up, it is observed that the targets from each channel are bound perfectly

3.5. Conclusion

- The fundamentals of radar polarimetry have been introduced along with the importance of polarimetry features in differentiating the various types of target based on physical properties.

- A novel Multi Channel Data fusion algorithm for effective clustering and efficient data extraction has been proposed.

- The robustness of the algorithm against different inter channel data association issues have been presented, the resulting frame wise database consisting of target data and detections across multiple frames of measurements has been created.

However as this study deals with extracting information from multiple moving targets, the need to analyse the evolution of the target statistics over multiple frames of data is
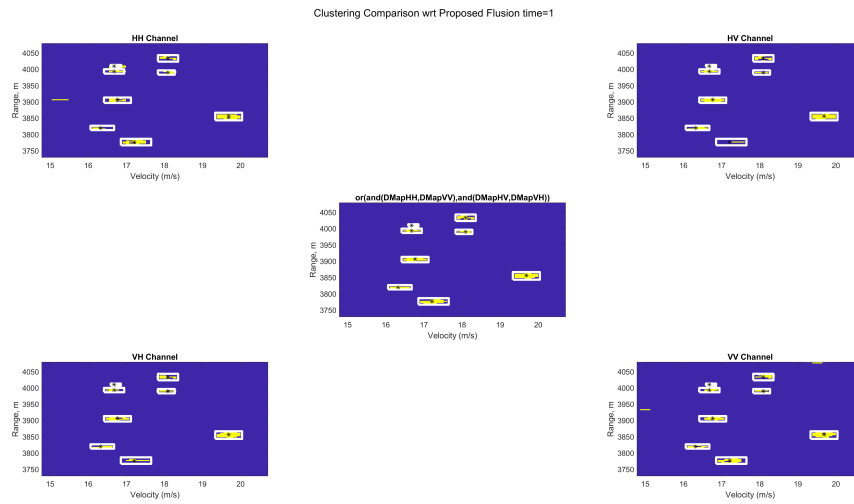
Figure 3.39: Logical Fusion A for targets in all detection maps close up, it is observed that the targets from each channel are bound perfectly
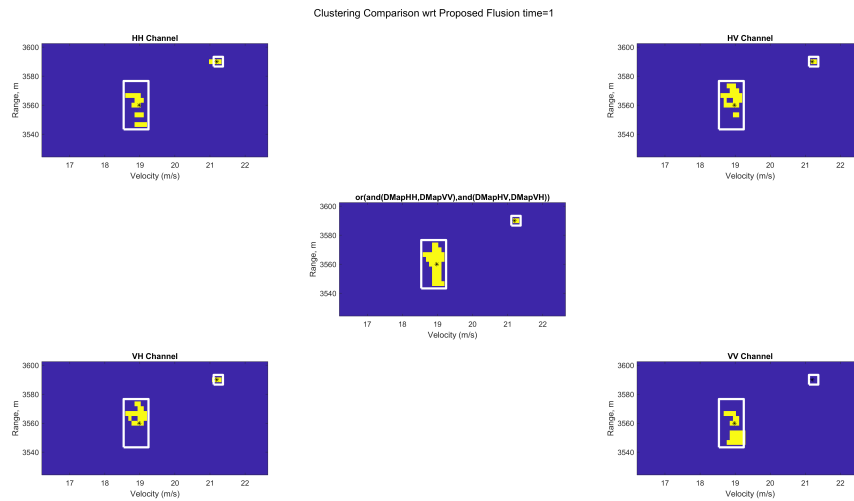
Figure 3.40: Bounding region for targets

mandatory, hence it is required to track the targets, by means of Multi Target Tracking (MTT) algorithm. The details of the MTT chosen for the study will be discussed in 4.
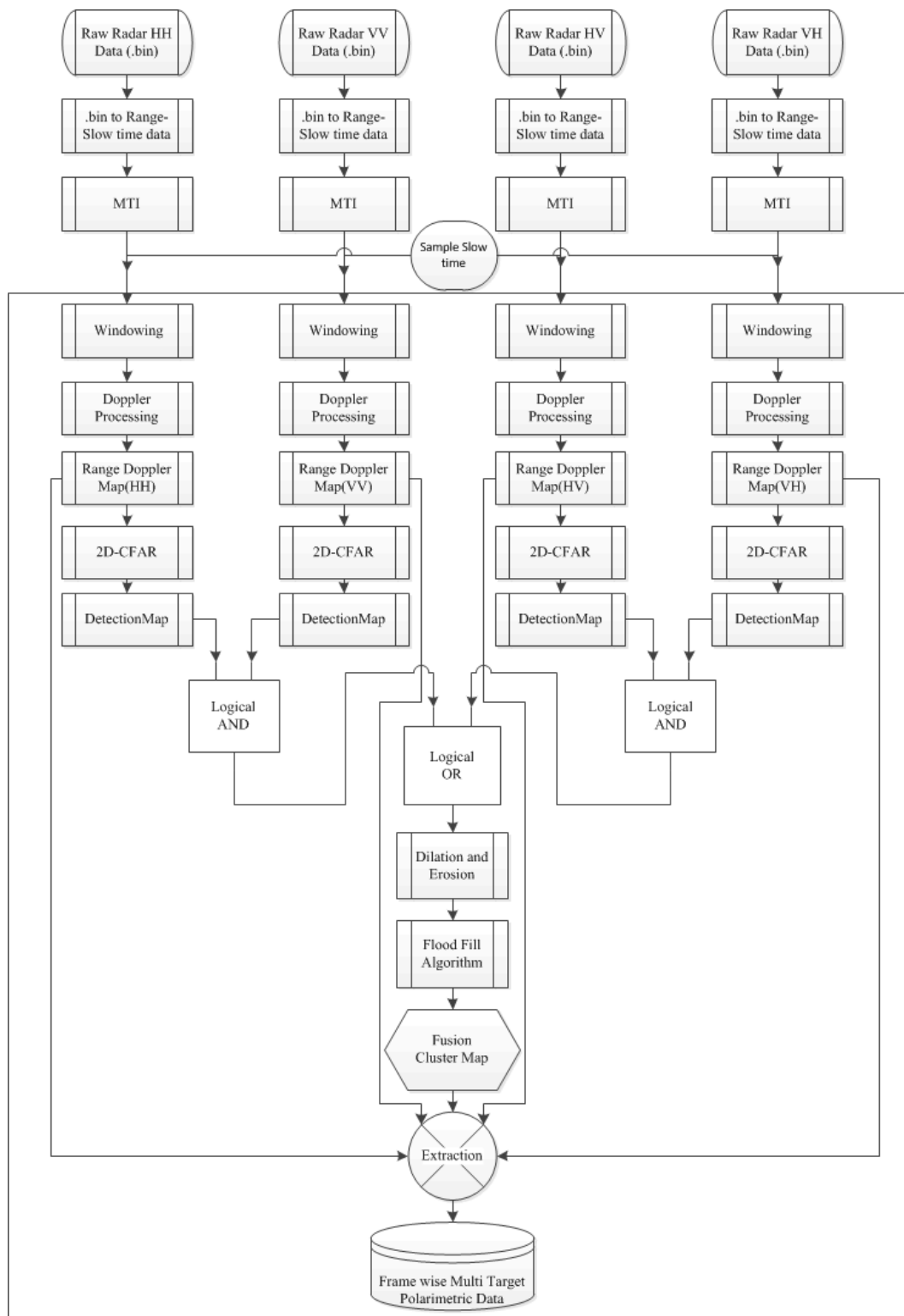
Figure 3.41: Multi Channel Data Extraction Algorithm
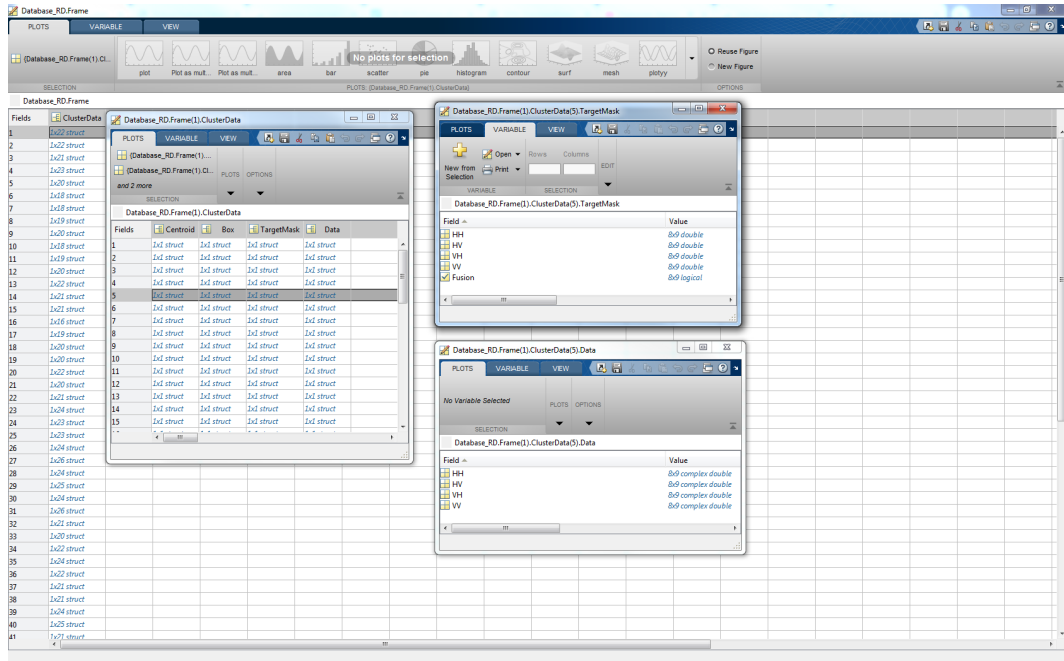
Figure 3.42: Frame wise Targets Detections Database- Structure
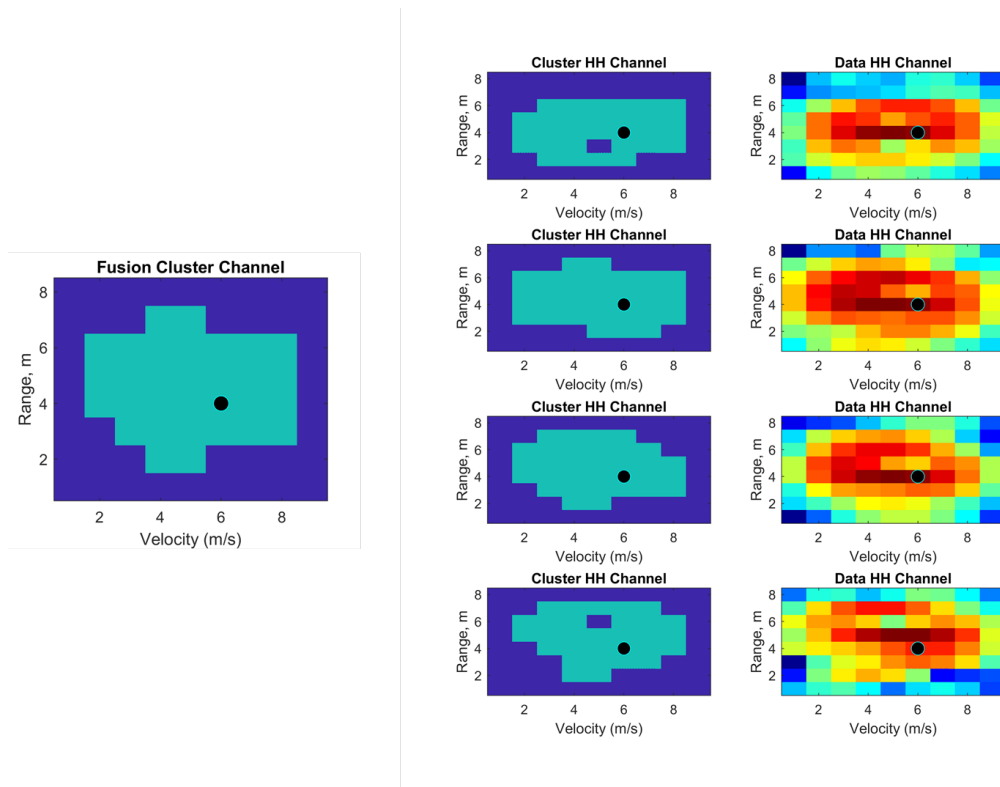
Figure 3.43: Example of Frame wise Targets Data extracted, the figure shows the fusion cluster and geometric centre crated, which is perfect sync across all channel clusters and data

4

Inter-frame Data Association mitigation using Multi Object Tracking

All real world scenarios consist of random occurrences of events, hence when considering the case of extracting information/data related to a target in motion in real world, there arises a need to confirm if the object of interest detected on two individual sequential events are the same, if the later proved false it would not be possible to confirm if the data extracted in the current observation frame was due to a target or a false alarm, to address this point of concern, the science of target tracking is investigated. When considering tracking problems with a one point target, the approach is more or less direct, but when considering multiple targets present within the same frame of observation, the tracking algorithms have to be modified to account for possible data association problems. In this chapter a study related tracking algorithms and Data Association problems are discussed, a simple Nearest Neighbour (NN) Multi Object/Target Tracking (MTT) algorithm is investigated for tracking multiple objects on a range velocity map. The NN filter is modified to accommodate the functionality of creating a list of correlated measurements in addition to tracking is proposed and implemented. As the scope of the thesis concentrates more on extracting data from automobiles in non manoeuvring scenarios, the study is limited to linear models and focuses primarily on data extraction.

4.1. Data Association Scenarios

The general meaning of data association translates to matching of data or information of an individual object of interest over two or more frames of measurements in the presence of other similar/different objects of interest. The matching of information can be based on the characteristics, trajectories or labels as identities of the object. [15]

In this study three levels of data association have been identified and steps to mitigate the same have been discussed.

4.1.1. Level 1 Inter Channel Data Association

For given instant of time 'k', if there are 'N' objects of interest and 'S' sensors with NXS measurements, than associating each measurement from each sensor to its individual object of interest is considered as the first level of data association , in the case of

this study the 4 Polarimetric channels capturing data from multiple moving targets, is considered as the $4XN$ measurements. In the previous chapter ??, details of different scenarios of Inter-channel data association and steps mitigate the same using the novel, "Multi Channel Fusion Cluster" have been discussed. Inter channel data association is limited to only the considered frame/ 'kth' instant of measurement.

4.1.2. Level 2 Inter Frame Data Association

Problems related to data association arises under the conditions when the number of existing objects (N) in a frame say 'k' are different from the new objects(M) in the next frame say 'k+1'or when number of existing objects (N) and the new objects(M) are the same but have to be assigned appropriately. Data association in this study is based on the trajectory of the target characterised on a collection of Range Doppler/Velocity maps to form a Range Velocity movie. $\hat{x}_{k+1|k}$ predictions are aimed at being associated with $z_{k+1|k+1}$ measurements. The different data association cases are as explained below:

1. Number of existing objects (N) more than number of new detections(M)ie.. N>M, the following are

   - False Alarm in Frame 'k'

   - Target Undetected in Frame 'k+1'

   - Measurements for target is no longer available-exit measurement space.

   A pictorial depiction of the same can be seen in figure 4.1
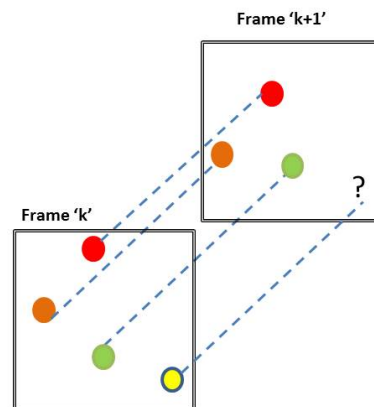
Figure 4.1: N>M

2. Number of existing objects (N) less than number of new detections (M). $N \leq M$

   - False Alarm in Frame 'k+1'

   - New Target in Frame 'k+1'

   A pictorial depiction of the same can be seen in figure 4.2

3. Number of existing objects (N) is equal to number of new detections (M); (N=M)

   - No anomalies in both frames, target count remains the same
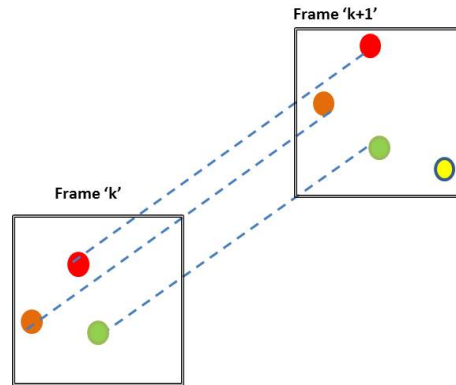
Figure 4.2: N>M

- Exit of a target in frame 'k' and simultaneous entry of target or possible false alarm in frame 'k+1'.

A pictorial depiction of the same can be seen in figure 4.3
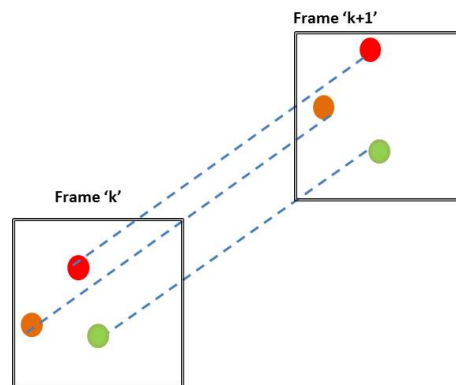
Figure 4.3: N=M

Problems related to false alarms and miss detections can be evaluated to provide a figure of metric of a considered data based on designed parameters of the CA-CFAR detector such as probability of false alarm P_{Fa} and probability of miss detection $P_M = 1 - P_D$ and concerns regarding the fluctuating target measurements and simultaneous entry-exit of targets in measurement space can be handled by the use of tracking algorithms, which will be discussed in the next section.

4.1.3. Level 3: Merging and Splitting Measurements

Merging and Splitting measurements occurs as a result two closely space objects following a similar trajectory over multiple frame of measurements, causing a cross over in tracks, as a result the measurements of the targets tend to combine in one frame to result in larger object and break off as two individual objects in the next frame, in these cases it is no longer possible to individually associate a measurement to its respective target, there are various computationally expensive methods to mitigate the same [3][15][54][55], which in itself is an extensive study. However the objective of this study does not require to mitigate the issue but to merely evaluated the occurrence of Level 3 situations for providing a quality metric for the list of correlated measurements for every tracked

object. Details regarding the same will be discussed in the next section.

4.2. Tracking Algorithm

Target tracking can be considered as a two stage process:

1. Track Filtering

2. Measurement-to-track Data Association.

Track Filtering deals with the estimation of the possible trajectory of a target ie.. position, velocity or acceleration by considering information from a measurement space, the uncertainty related to estimation of the dynamics concerning the movement of a target are characterised by the covariance of the estimate.

Measurement-to-track Data Association deals with assigning measurements to an existing target track record, post a validation stage.The validation of a measurement to an existing track is considered by calculating the difference between the predicted measurement and the detected measurement for a considered motion model, when difference is within validation bounds the predicted measurement is used updated the estimated position and velocity. In the case of a failed validation to an existing track the measurement is considered either as a new detection or false alarm and a new track is initiated.In the case of tracks that no longer have a measurement may either indicate a miss detection or end of target trajectory[5].

In most literature related to tracking problems a coordinate transformation stage is required, as the target tracking space would be handled in a Cartesian coordinate while radar measurements would be obtained from polar or spherical coordinates, hence requiring are two models for every tracking algorithm, which is the Kinematic motion model which contains the kinematic states of a target in a dimensional Cartesian space and a measurement model which transforms the measurements from polar or spherical space to Cartesian space and acts as the linear observation of the kinematic states[5].

"Let X_k be the 1D kinematic state vector at time instant t_k and the measurement at the same instant be denoted by Z_k. When considering the estimation of a state at instant "k" based on measurement, from another instant say "j" is given by $\hat{X}_{k|j}$, throughout this thesis the following convention related to state estimation is to be followed. a single subscript denotes an actual detection or modelled value, if the variable has a double subscript, it represents an estimate. $\hat{X}_{k|k}$ is referred to as a filtered state estimate, $\hat{X}_{k|k-1}$ is considered a one step prediction of the state vector and $\hat{X}_{k|k+1}$ is a smoothing of the estimate"[5].

In this study however we consider the tracking space and the measurement space to be the same, hence the step for a co-ordinate transform is eliminated. Since the aim of the thesis is to "extract data" meaning to say, to form a track of observed measurements related to a target, the measurement to track association is slightly modified, rather than considering the validated measurement to just update the track record it is also simultaneously correlated with previous detection to form a time series data. The details of the time series data would be considered in the next chapter ??.

As the track filtering stage for this study requires a stochastic state estimation, the Kalman filter and its respective kinematic motion model and measurement model are

derived in the following sections.

4.2.1. Kinematic Motion Model

Kinematic Motion model provides the dynamical equations representing the motion of a target relative to its platform [5], since the measurement space and tracking space are the same for the case of this study, the kinematic model is used for estimating the next possible measurement of the target, hence the state space equation of the predicted measurement for target with linear motion in case of Gaussian noise is given by 4.1:

$$X_{k+1} = F_k X_k + w_k \tag{4.1}$$

where, X_k represents the states of the target given by 4.2

$$X_k = \begin{bmatrix} r_k \\ v_k \end{bmatrix} \tag{4.2}$$

with r_k is range estimate of target at k and v_k is velocity estimate of the target at k,

F_k represents the relation between states of the target to characterise its motion given by 4.3

$$F = \begin{bmatrix} 1 & \Delta T \\ 0 & 1 \end{bmatrix} \tag{4.3}$$

with ΔT is the update interval which is constant.

w_k represents the processes noise is given by equation4.4

$$w_k = \sigma_{qk}^2 \begin{bmatrix} \frac{\Delta T^4}{4} & \frac{\Delta T^3}{2} \\ \frac{\Delta T^3}{2} & \Delta T^2 \end{bmatrix} \tag{4.4}$$

with w_k related to errors in the estimated state vector of the target at time t_k with $N(0, \sigma_{qk})$
σ_{qk} is variance of the process noise.

In addition to proposed state space equation 4.1 a slight modification is considered in case of velocity estimation, in order to account for possible accelerations occurring at a few random instances , a three stage prediction is considered as given by equation 4.5

$$v_{k+1} = v_k + (v_k - v_{k-1}) \tag{4.5}$$

4.2.2. Measurement Model

The measurement considered in this study is the Range Velocity video discussed in chapter 2, the measurement space as mentioned earlier is the same as tracking space hence will consists of the same states, the measurement model is given by 4.6:

$$Z_k = HX_k + n_k \tag{4.6}$$

where H is state observation matrix given by 4.7 and n_k is the measurement noise at instant k given by

$$H = \begin{bmatrix} 1 & 0 \\ 0 & 1 \end{bmatrix} \tag{4.7}$$

$$n_k = \begin{bmatrix} \sigma r_k \\ \sigma v_k \end{bmatrix} \tag{4.8}$$

where, σr_k and σv_k are measurement uncertainties in range and velocity respectively.

The Measurement and Kinematic models are made use in recursive linear state estimation filter - Kalman filter for predicting the states of target over multiple instances of measurement.

4.2.3. Kalman Filter

The Kalman filter computes the MMSE and minimum variance estimate for the considered stochastic state X_k, since the random process associated with the state estimation is additive Gaussian and state estimate relationship is linear in nature, the state estimate error of the Kalman filter will also be linear Gaussian. Hence only a mean and covariance are needed to fully characterise the state estimation error. The Kalman filter in general is a predictor corrector algorithm which accounts for both changes in time / updates and measurement processing[5]. Hence the two stages of the algorithm are as shown below:

- Prediction of state and covariance given by 4.9-4.10:

$$\hat{X_{k|k-1}} = F_{k-1} \hat{X_{k-1|k-1}} \tag{4.9}$$

$$\hat{P_{k|k-1}} = F_{k-1} P_{k-1|k-1} F_{k-1} + w_k \tag{4.10}$$

- Update of state estimate and covariance with measurement are given by equations 4.11-4.14

$$\hat{X_{k|k}} = \hat{X_{k|k-1}} + K_k[Z_k - H\hat{X_{k|k-1}}] \tag{4.11}$$

$$\hat{P_{k|k}} = [I - K_k H]\hat{P_{k|k-1}} \tag{4.12}$$

$$K_k = \hat{P_{k|k-1}} H^T S_k^{-1} \tag{4.13}$$

$$S_k = H\hat{P_{k|k-1}} H^T + R_k \tag{4.14}$$

where, $\hat{X_{k|k-1}}$ is the predicated states of target in our case the next possible measurement, $\hat{P_{k|k-1}}$ is the predicted uncertainty in estimated measurement, F_k is the system dynamics matrix as per equation 4.3, K_k is considered the Kalman filtering gain, S_k is the covariance measurement residual, $Z_k - H\hat{X_{k|k-1}}$ is the innovation measurement calculated based on the model 4.6, I is the identity matrix.

The above given steps are considered for a general Kalman filter capable of tracking the states of a single target, however as this study requires handling more than one target of interest per frame , the since of multi target tracking (MTT) is exploited.

4.2.4. Multi Target Tracking

Multi target tracking algorithms are recursive state estimation filters capable of mitigating the association ambiguities , due to multiple observation from multiple targets presents between two or more successive frames of measurements. In general MTT algorithms are widely classified as shown in figure 4.4
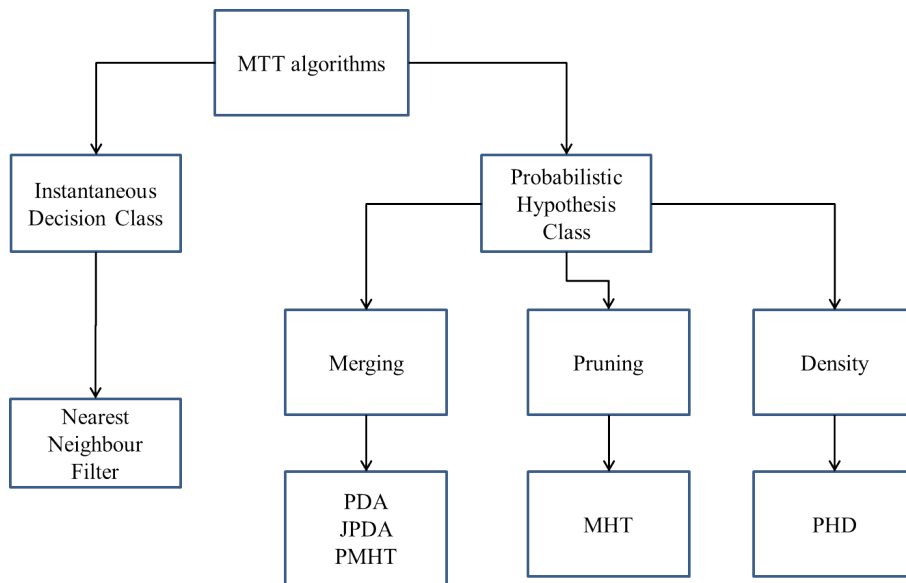
Figure 4.4: Various Multi Target Tracking algorithms

MTT algorithms are designed based its accuracy or efficiency in "tracking multiple targets" simultaneously, the details of the studies are elaborated in [3] [15] [55] [56]. However as the focus of this thesis is not tracking as mentioned earlier, we consider the most simplest of the MTT algorithms, which is Nearest Neighbours (NN) filter.

There are 4 stages to all MTT algorithms:

1. Prediction

2. Gating

3. Data Association

4. Update

The prediction and update stages are similar to the a single target tracking Kalman filter as discussed in the previous section, however the effectiveness of an MTT is based on the gating and data association stages,hence more the same are explained more detail.

Gating region

For a considered case of N tracks in frame 'k' and M observations in frame 'k+1', where $N \neq M$ as shown in figure 4.1-4.3, finding the right candidate measurement for a specific task is mandatory, the gating step is used to set up a validation region around the predicted trajectory of a target, targets falling within this validation region are considered are suitable candidates to be considered of data association. There are various studies on how gating region can be determined [13][14], the most general methods are as given below:

- Constant Geometric gating: Rectangular Gating , Circular Gating

- Three frame Velocity gating

- Ellipsoidal gating

A target is validated as present within a gating region when, the distance between the measurement and prediction is less than fixed/ predetermined gating threshold. In the case of this study a rectangular gating region based on Elucidean distance is considered and is given by equation 4.15

$$|Z_k - H\hat{x}_{k|k-1}|^T |Z_k - H\hat{x}_{k|k-1}| \leq G \tag{4.15}$$

where, z_k is the measurement at k, $x_{k|k-1}\hat{}$ is the estimated measurement/ state based on measurement at 'k-1'. G is the gating threshold.

Data Association

The gating region determines the possible set of candidates which are closest to the predicted measurement. In order to choose the best measurement to solve the gating level data association, the likelihood of associating a measurement to a target is calculated, the likelihood score is given by equation 4.16:

$$A_{score} = exp(-(|z_k - H\hat{x}_{k|k-1}|^T |z_k - H\hat{x}_{k|k-1}|)^2) \tag{4.16}$$

Amongst the all the validated measurement the measurement with the highest score is chosen as best match to be associated to the track.

Nearest Neighbours Filter

The stages of the NN filter, based on discussion are considered as in equation 4.28-4.26

- PREDICTION
    - Predicted state

$$\hat{X}_{k|k-1} = F_k \hat{X}_{k-1|k-1} \tag{4.17}$$

    - Predicted Covariance

$$P_{k|k-1} = F_k P_{k-1|k-1} F_k^T + Q_k \tag{4.18}$$

    - Predicted Measurement

$$\hat{Z}_{k|k-1} = H_k \hat{X}_{k|k-1} \tag{4.19}$$

- Gating
    - Euclidean Distance Gating

$$[\hat{Z}_{k|k-1} - Z_k]^T [\hat{Z}_{k|k-1} - Z_k] \leq \begin{bmatrix} R_g \\ V_g \end{bmatrix} \tag{4.20}$$

$$Z_k{}^i \subset Z_k \tag{4.21}$$

where
$Z^i{}_k$ is a vector of validated measurements for the ith target at instant k

    – Data Association

        ⋄ Association Score

$$A_{score} = exp(-(|Z_{k|\hat{k}-1} - Z^i{}_k||Z_{k|\hat{k}-1} - Z^i{}_k|^T)) \qquad (4.22)$$

        ⋄ Measurement residual

$$\tilde{y}_k = Z^i{}_k(A_{score(max)}) - H_k\hat{x}_{k|k-1} \qquad (4.23)$$

    $Z^i{}_k(A_{score(max)})$ is the measurement with highest association scores.

    – Update

    – Kalman gain

$$K_k = P_{k|k-1}H_k^T H_k P_{k|k-1} H_k^T + R_k{}^{-1} \qquad (4.24)$$

    – Update State Estimate:

$$\hat{x}_{k|k} = \hat{x}_{k|k-1} + K_k\tilde{y}_k \qquad (4.25)$$

    – Update Estimate Covariance

$$P_{k|k} = (I - K_k H_k)P_{k|k-1} \qquad (4.26)$$

As mentioned earlier, the focus of this thesis is not tracking the true trajectory of the targets but forming a list correlated measurements for a target moving on the range velocity space. Hence the tracking filter is used as figure of merit to validate the uniqueness of each measurement list for a given target. In the next section the discussed NN filter is modified for data extraction.

4.3. Multi Target Data Association filter (MTDF)

In section 3 the Multi-Channel Data Fusion algorithm (MCDA) and the resultant Detection database free from Level 1 data association scenarios was introduced, using the geometric centres for the extended target clusters for tracking the movement of the targets on range doppler space, level 2 data association is solved using a modified NN Kalman filter to perform a measurement to measurement correlation step for data extraction, in addition to the measurement to track association step.

The measurement to measurement associator uses the same steps as the general NN filter but differs in the update step, instead considering the calculated Kalman gain to predict a the best estimate of the targets trajectory the validated measurement itself is considered as the update for the next stage of recursion. Hence the update stage as per equation 4.25 post gating for measurement correlator is given by 4.27

$$\hat{x}_{k|k} = Z^i{}_k(A_{score(max)}) \qquad (4.27)$$

where, $x\hat{}_{k|k}$ is the estimated state update, Z_k^i are the measurements validated measurements post gating, $A_{score(max)}$ is the association score for measurement with highest

likelihood.

A block diagram of the Multi Target Data Association filter is as shown in figure 4.5
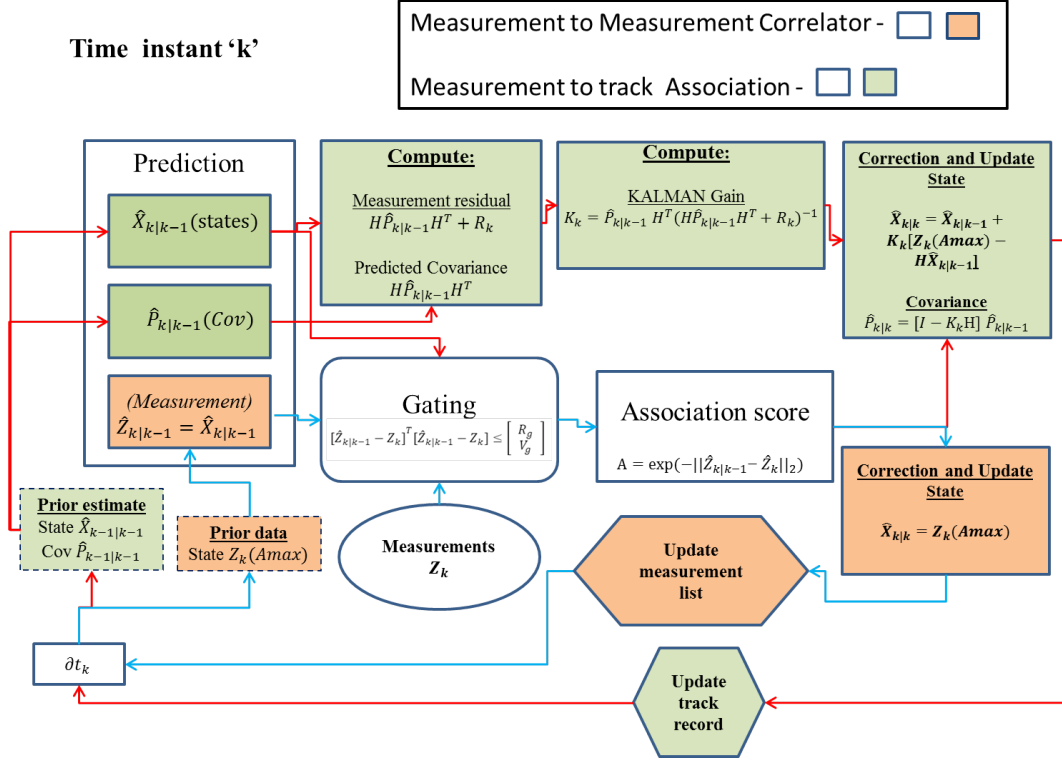
Figure 4.5: Multi Target Data Association filter block diagram

As seen in figure 4.5 the stages of the general NN filter and the proposed measurement correlator only slightly differ from each other. The blocks in orange represent sections of measurement to measurement correlator connected by cyan arrows, the blocks in green represent section of the tracking filter connected by red arrows, the white boxes are common sections used by both sections.

4.3.1. Performance Metric

The purpose of the Multi Target Data Association filter (MTDF) is to solve level 2 data associations and extract data for an individual target by creating a list of measurements characterising its trajectory on the range velocity map.

In order to evaluate the quality of data extracted for a given target, the following metrics are investigated [58]:

- number of wrong assignments due to crossing trajectories.

- number of track breakages due to non validated gating regions.

- number of measurements for given targets free from any corruption.

It is to be noted that there is limited literature for evaluating performance metric for data association, which in general are specific to each application or case scenario, hence,

the performance metrics presented are derived and adapted for data association based on literature for performance metric of MTT algorithms[58][59][60].

An efficient way of evaluate these metrics is by considering a cost matrix with number of rows 'n' equal to number of valid tracks up to the 'k^{th}' instant and number of columns 'm' be the measurement at the 'k+1' instant. For every row i.e. for every target track a gating step to find the suitable candidates for association and association score for each validated candidate as discussed in the previous sections is calculated [57], hence the cost matrix is given by:

$$A_{ij} = \begin{bmatrix} a_{1,1} & a_{1,2} & \dots & a_{1,m} \\ a_{2,1} & a_{2,2} & \dots & a_{2,m} \\ . & . & \dots & . \\ a_{n,1} & a_{n,2} & \dots & a_{n,m} \end{bmatrix} \tag{4.28}$$

where, A_{ij} is the association cost matrix, a_{ij} is the association score for i^{th} row and j^{th} column

For a formulated cost matrix following are possible entries [57]:

1. If a_{ij} is empty indicates no measurement due to un-gated/ non validated measurement in the gated region.

2. If a_{ij} consists of more than one value it indicates a merge into measurements due to cross trajectory.

3. If increase in the number of rows indicates new tracks.

4. If the number columns at 'k+1' is $\leq$ number of columns at 'k' it indicates loss in measurements.

5. In case of step 1 is repeated for than 'l' instances it indicates exit of target and the respective row can be eliminated from the cost matrix.

6. In case repeated events of step 2, indicates repeated merging and splitting tracks.

7. If the cost matrix has full rank with elements only on the principle diagonal elements, it indicates a perfect association no miss detections and track breakages detected as an ideal case.

Hence using the cost matrix proposed the three following metric are evaluated:

- ASSOCIATION ERROR-(AE):
  Association error measures the error for associations in range and velocity of a consider target with respect to all other associations in the current measurement instant. Given N number of targets with m measurement each, the list of correlated measurements must be unique for each target,hence the association of range and velocity measurements for a target 'i' is evaluated by equation 4.29 for range and 4.30 for velocity.

$$iE_R(t) = \sqrt{(mR_i(t) - (NmR(t)))^2} \tag{4.29}$$

$$iE_V(t) = \sqrt{(mV_i(t) - (NmV(t)))^2} \tag{4.30}$$

where, i represents the index for a considered target, mR_i is the correlated list of range measurements for the target 'i', mV_i is the correlated list of velocity measurements for the target 'i', t is the index of track value, N is total number of data extracted and associated lists, $NmR(t)$ is is total number of range trajectories, $NmV(t)$ is total number of velocity trajectories, E_R is the error for range, E_V is the error for velocity

As the trajectory of target is represented by range and velocity together, the number of range and velocity measurements for an object are always the same. Hence for a considered i^{th} target, only one list of associated measurements from the total N_m associated measurements must have an error in range and velocity equal (/ converging) to zero.

Hence the error of measurement to measurement association for a single target is given by equation 4.31:

$$AE_i = \frac{Num(E_{tr})}{T_F} \tag{4.31}$$

where, $Num(E_{tr})$ is the number of instances with more than 1 target with track Error close to zero, T_F is total frames of measurement of the target, AA_i is the Association accuracy of the ith target
.

The Track accuracy for a data set is calculated using the average track error over all tracked objects given by equation4.32

$$AE_{total} = \frac{1}{N} \sum_{i=1}^{N} AE_i \tag{4.32}$$

where, N is total number of targets.

- TRACK CROSSING - (TCross):

Track Crossing evaluates the number of crossing trajectories of target, causing merging and splitting measurements, subsequently intersecting / overlapping list of target measurements. Track crossing for a data set can be accessed by means of the cost matrix, at any instant 't' if 2 or more rows in the cost matrix has the same association score in more than one column, it indicates a case of merging or splitting measurements shared by a common target. The number of occurrences of the event for a target 'i' is given by equation 4.33-4.35

$$A_{ij}(t) = \begin{bmatrix} a_{1,1}(t) & a_{1,2}(t) & ... & a_{1,m}(t) \\ a_{2,1}(t) & a_{2,2}(t) & ... & a_{2,m}(t) \\ . & . & ... & . \\ a_{n,1}(t) & a_{n,2}(t) & ... & a_{n,m}(t) \end{bmatrix}$$

$$\hat{A_{iM}}(t) = \sum_{j=1}^{M} aij(t)$$

$$\hat{A_{iM}}(t) = [a1M(t), a2M(t), ..., anM(t)]^{T}$$
$$S.T : a1M(t) = a11(t) + a12(t) + a13(t) + ... + a1m(t)$$

(4.33)

where, t is the instant of measurement, $A_{ij}(t)$ represents the cost matrix at the measurement instant 't', $a_{ij}(t)$ are elements with values between 0 and 1 for an ith track and j^{th} measurements with 1 indicating perfect match and 0 indicating no match at the instant 't', $\hat{A_{iM}}(t)$ represents a vector containing the sum of total association for a target 'i' at instant 't', the value of association lies below two for ideal cases.

From Equation 4.33 we arrive at :

$$TCross_i(t) = num(A_{iM}(t) > 2)$$

(4.34)

where
$num(A_{iM}(t) > 2)$ gives number of instances when the column sum is greater than 2, for the ith target at an instant t

The total number of cross events for a considered data-set is given 4.35

$$TCross_{total} = \frac{1}{2 * N * T_F} \sum_{i=1}^{N} TCross_i$$

(4.35)

where, $TCross_i$ represents the total number of crossing events for the ith target, $TCross_{total}$ is the total crossing events for 'N' targets over T_F frames recorded in the data-set. The factor 2 is considered as a minimum of 2 targets are involved in a crossing

- ASSOCIATION LOSS (AL): Association loss measures the number of instances without validated measurements for association. In ideal cases given a stable target with number of detections equal to total frames of data without any false alarms, for every prediction made by the MTDF filter a measurement to be associated will be found. As real target situations consists of miss detections and false alarms, the chances of a measurement not available for association occurs, in these cases the estimate by the Kalman filter is considered to be associated in the list of measurements. As this value is not a true value it is considered as a "Loss in data association".

The association loss (AL) can be identified for a given target using the cost matrix. If the given row for a target is empty meaning not value between 0 to 1 is present it indicates, no measurement was gated and the value associated in the target's measurement list is a Kalman estimate. The association loss (AL) is thus calculated using equation 4.33 and 4.36, for a consider cost matrix:

$$AL_i(t) = num(A_{iM}(t) == \emptyset) \tag{4.36}$$

where, $num(A_{iM}(t) == \emptyset)$ gives number of instances when the ith target gating region is empty.

The total number of Association Losses for a considered data-set is given by equation 4.37

$$AL_{total} = \frac{1}{N * T_F} \sum_{i=1}^{N} AL_i \tag{4.37}$$

where, AL_i represents the total number of association losses for an ith target, AL_{total} is the total number of Association losses for a considered data set, N is total number of targets and T_F is total frames of measurements.

4.3.2. Simulation results

In order to evaluate the proposed Multi Target Data Association filter, a simulated data set containing 7 targets moving at different velocities and possible variations in velocities characterised as accelerations is considered. The data set is evaluated for correctness in associating data for each target in presence of false alarms,random Gaussian noise and access possible level 3 data association conditions of crossing trajectories. It is to be noted that the simulations focuses on association of measurements and NOT tracking the trajectory of the objects.

The considered ground truth of the targets is as shown in figure 4.6
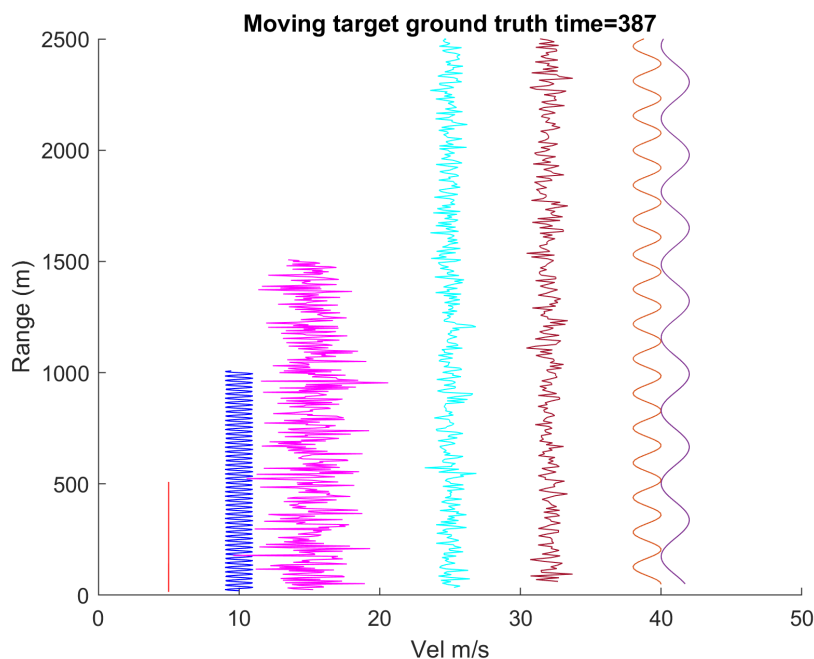
Figure 4.6: The figures represents the ground truth for 7 individual moving targets on range velocity space , each colour represents an individual target

Starting from left to right; Targets 1, 2, 4, 5, are considered as targets with nearly constant velocities where as Targets 3, 6 and 7 are considered as targets with variations in velocity characterised as accelerations.

The simulated measurement environment for the targets trajectory in presence of false alarms and random Gaussian noise can be visualised as seen in figure 4.7
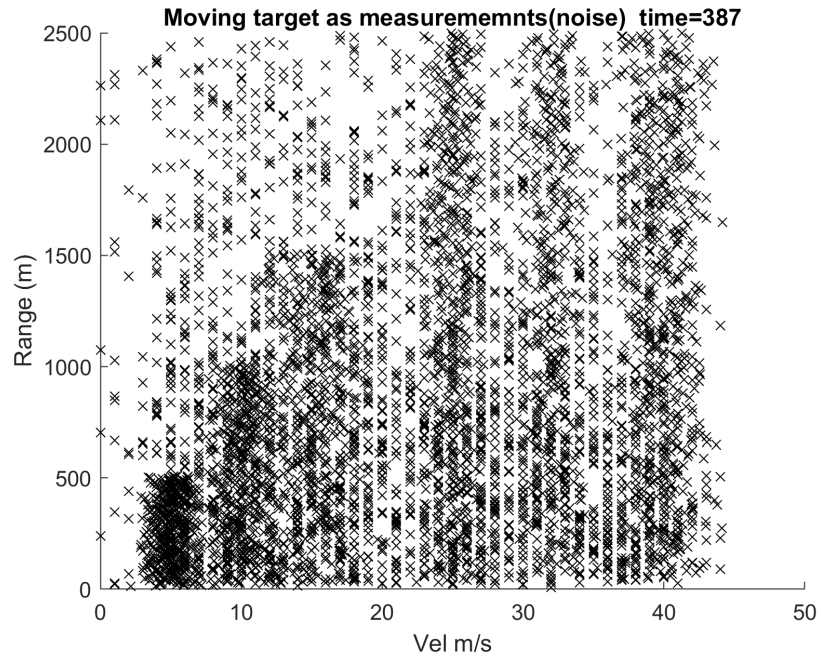
Figure 4.7: Noisy Measurements detected by the radar in presence of false alarms, as measurements have not yet been associated to a specific target, hence it is considered as cloud of detections. Every 'x' presents a detection in presence of noise and false alarm.

As discussed the object of the MTDF algorithm is to associate measurement of an individual target and produce a list of correlated measurements for each target. The output of the measurement to measurement associator block of the proposed Multi Target Data Association filter is as shown in figure 4.8.
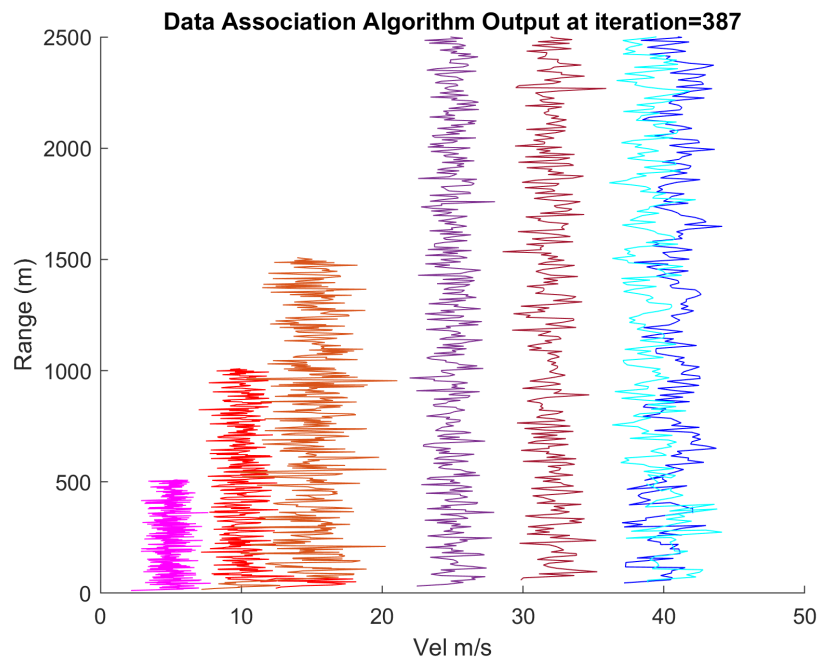
Figure 4.8: Trajectory of targets formed as a list of correlated measurements based on associating the radar detections, uniquely for each target

It can be noticed that the colour coding followed on figure 4.6 is not the same as in figure 4.8, but the trajectory formed for an individual target consists of only a single colour, this shows that, based on the cloud of detections in figure 4.7 formed by the radar, a list of uniquely associated measurements has been formed, as there no prior knowledge related to ground truth of the targets for a radar, the list of measurements formed are assigned a colour in a sequential order, but as each list is required to associate detections of an only one target, the measurement list formed has the same colour assigned from the start to end.

As the Multi Target Data Association filter has a secondary functionality of estimating the targets true trajectory based on the NN filter output, the results of the measurement to track associator and measurement to measurement associator are compared against the simulated noisy measurements as seen figure 4.9, 4.10a and 4.10b
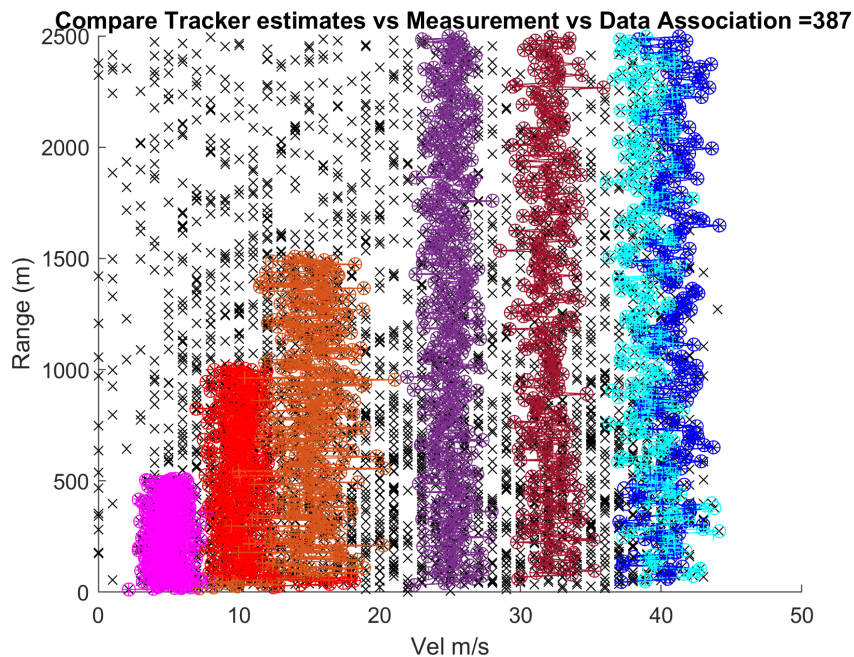
Figure 4.9: Comparison of trajectory of target formed by *NN* filter output based on Kalman estimation and trajectory of target based on correlated measurements

(a) 1a   (b) 1b
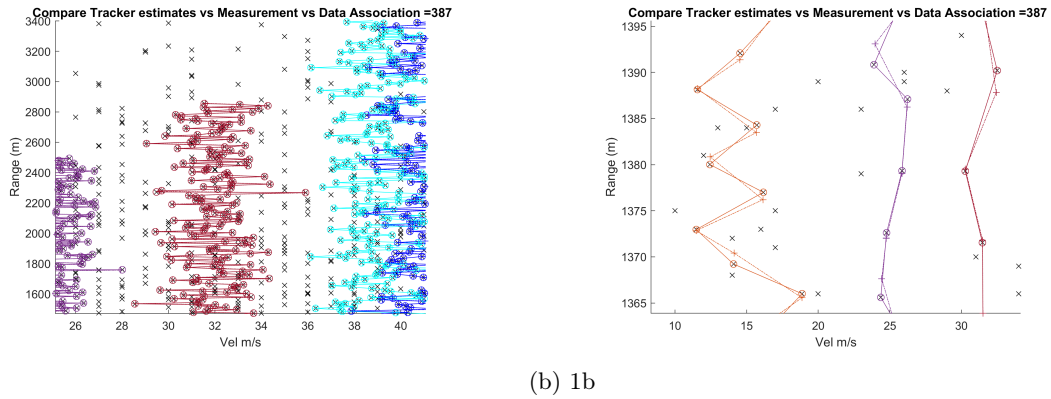
Figure 4.10: As shown it is clear that for every target its individual measurement is found and thus the tracks by the MTDF filter intersects a detection by the radar at every instant, this is confirmed by the $\otimes$ where $\odot$ represents the trajectory and x represents the detection, where the '+' represents the NN filter estimates.

The performance of the MTDF is calculated using the performance metric discussed in section 4.3.1. Parameters such as Track crossing 4.35 and Association Loss 4.37 for the data set over the frames of measurement are as shown in figure 4.11
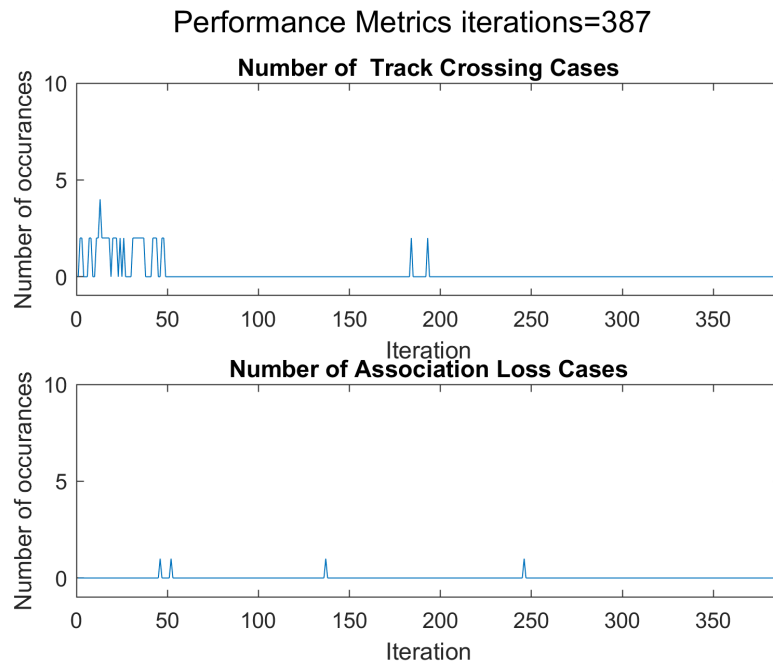
Figure 4.11: Figure shows the total number of crossing events and total number missed measurements for the data-set

For the given data set it is observed that the first 50 frames have 4 targets with crossing trajectories, hence the spikes in the "Number of Track Crossing" plot , the same is seen in iterations between 160 to 200.

In lower section of the image it is observed that the number of un-gated events leading to Association loss is zero through the data set except in 4 individual instances indicating , 4 targets missed a measurement at 4 different instances or 1 target missed a measurement at 4 different instances.

In order to evaluate the accuracy of association of each target, the Performance metric

Association Accuracy as per equation 4.31 and 4.32 is calculated. The results are as shown in figure 4.12.

The following points have to be considered when referring to figure 4.12:

- For the association error calculated in range or velocity, only one target can have a value close to zero, if two targets have a near to zero value it indicates a level 3 data association of merging tracks due to closely spaced measurement or targets.

- The association error of all other targets will diverge.

- Association error of range and velocity will always complement each other as for each target a detection is characterised by a range and velocity measurement.

- In cases when there is no target with a association error equal to zero, we can concur that either the list of measurements are invalid or there is no longer data available from the target, as it has left the field of view.

The following can be concluded from figure 4.12:

- Targets 2 and 4 have nearly 50 frames of crossing, hence the data associated in these frames belongs both the targets hence is to be discarded.

- Targets 1, 3, 5, 6 and 7 each have 1 instant of miss association.

- Target 7 has no value for mmse until iteration 45, indicating the target was detected at instant 45

- During the start of simulation all target are initialised with zero mmse.
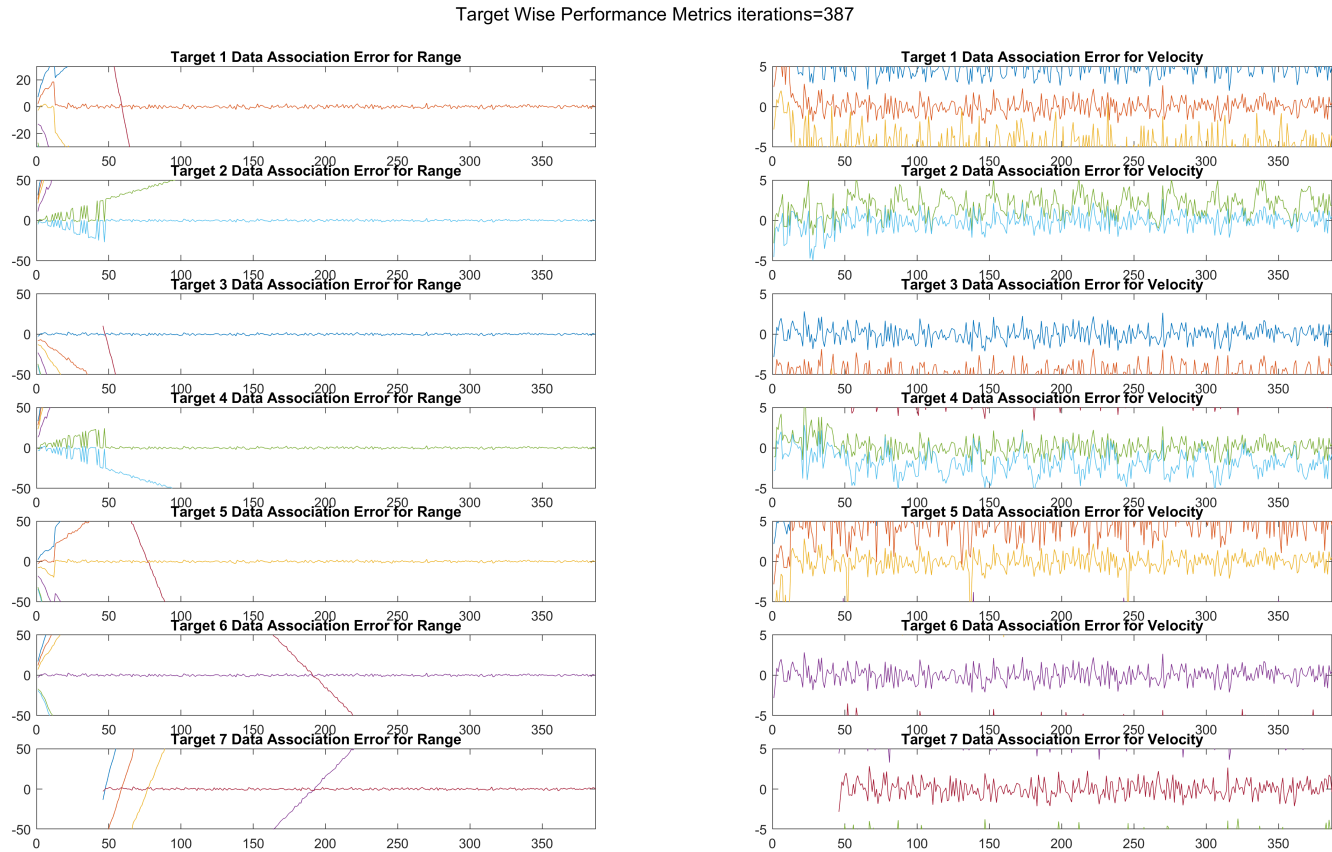
Figure 4.12: Association Accuracy for each target

The consolidated metric evaluating the quality of data extracted in the simulated situation is tabulated as shown below in table 4.1, Target number is followed wrt figure 4.12:

Target Index	Association Accuracy	Track Crossing Events	Association Loss
1	97.16%	11	0
2	86.56%	50	0
3	99.17%	1	1
4	86.26%	50	1
5	96.90%	9	0
6	99.17%	1	1
7	98.54%	5	1
Mean	94.82%	4.76%	0.15%

Table 4.1: Data Association Quality metric

Based on the defined performance of metrics for the algorithm, the quality of data extraction is evaluated. Based on values from table 4.1, it can be concluded that 94.52% of the data has been perfectly associated , 4.56% of data is corrupted due to level 3 data association issues such as merging and splitting measurements in case of closely moving targets with crossing trajectories, loss of data is recorded as 0.15%.

Using the data metrics for each target, the total number of use-able frames of data per target is calculated.

4.3.3. Target Database

The extracted and associated data sets for each target are stored as a target specific database. As shown in figure 4.13.
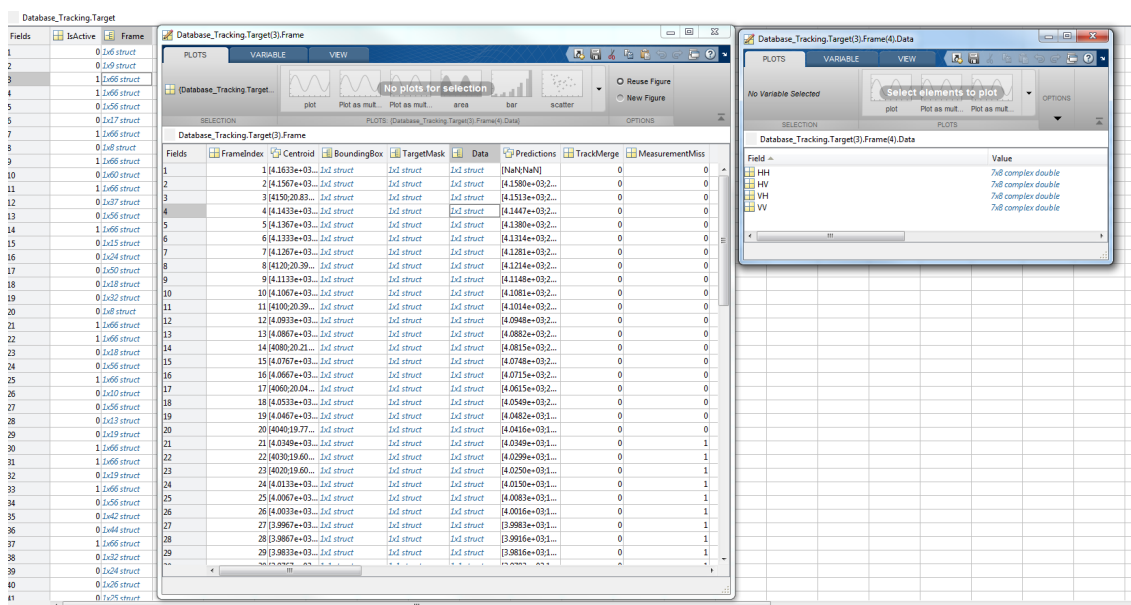
Figure 4.13: Target Specific database- consisting of time series data of moving targets on range velocity space

The target database consists of a time series data explaining the evolution of the target measurements as a function the target motion on a range velocity map.

4.4. Conclusion

- An assessment of the different levels of data association when concerning handling data in a multi channel multi target scenario have been discussed.

- The fundamentals of tracking filters for a single target and Multi target scenarios have been analysed.

- In order to associate the detections between successive frames of measurement and mitigate Inter frame data association situations a Multi Target Data Association filter (MTDF) based on a nearest neighbours (NN) filter has been designed.

- Three performance metric to evaluate the performance of the algorithm and assess the quality of the data association have been developed.4.3.1

- The proposed MTDF filter is evaluated on a synthesised data set contain 7 moving targets in the presence on noise and false alarms.

- The extracted data set is evaluated based on the defined performance metric and the results are tabulated as in table 4.1.

- A database consisting of uniquely associated measurements characterising a time series data for every target detected on the measurement space has been created.

The Target database is used for analysis of stable features in moving targets, which can be used to categorise the targets into sub-classes. The details of feature analysis to be considered from the extracted time series data will be discussed in the next chapter ??

5

Feature Analysis for Extended Moving Targets using time series data

Conventional radar target signatures used for identifying and characterising stationary targets may not be useful in the case of moving targets, as they now are a function of motion of the target, thus augmented by variations due to Doppler effect and changing incident wave vectors as a result of the targets velocity or acceleration[21]. An interesting way to understand the variation of a considered radar signature for a moving target, would be to present it as a time series data. By detecting, tracking and associating measurements of moving targets over a specified duration, a time series data can be obtained, using which stable features amongst the moving targets can be identified.

Theoretically speaking, given a diverse data-set of different types of targets, the possibilities to find similarities or dissimilarities to group or differentiate the targets into sub-classes is most likely possible using the identified stable features.

In the previous sections we discussed techniques to effectively detect, extract and associate measurements from multiple moving targets over multiple frames of range velocity movie (collection of range velocity maps), to form the Target Database, in this section, the extracted measurements are firstly processed by compensating for possible variations/effects common amongst all targets, the compensated measurements are than presented as a time series data to investigate possible stable/ close to stable parameters, which can represent the target or a class of targets over the measurement frames. Such parameters are identified as "Features" for a target and in-case of similarities or dissimilarities among more than one target, identified as features for a class of targets. thus creating a feature data base, which can be used for categorising the studied targets into sub-classes using possible "Data Clustering" methods[61].

5.1. Target Feature Analysis

When considering features related to radar objects, the type of scattering mechanism plays a vital role in determining the same, it is important to take into account the dependencies on the size of the scattering body say 'L' to that of wavelength 'λ' of the incident field.

With respect to extracted data set the target consists of cars moving on a highway

captured by a radar operating at wavelength of $\approx$ 9cm, the typical size of a target varies from 1.5m (from small city car) to a maximum of 15m (Heavy mover) [4], hence the size of the target is very large compared to the wavelength, ie.. $L >> \lambda$, as a result the target is treated as a collection of independent scatters, hence the geometry of the target becomes a major contributor to the scattering process, thus the extracted back-scattered returns from a target is the complex phasor sum of all individual scattering centres.[5].

The general scattering mechanisms from various literature[5][22][27] [31][34][29] for high frequency scattering (optical regime $L >> \lambda$) are summarised below:

1. Specular scattering : Considering the assumption $\lambda \to 0$, with angle of reflection equal to angle of incidence, scattering effect similar to those of true optics (mirror reflections) , hence responsible for sharp spike like scatterings.

2. End-region Scattering: Scattering effects at corners of flat surfaces, causing side lobes in directions away from the spikes from specular scattering .

3. Diffraction : Scattering from corners in the same direction as the incident beam due to edge induced currents.

4. Multiple Bounce: Scattering effect observed due to the interaction of a incident wave with multiple bodies, where the reflections from one body are incident on another body, before being reflected back to the observer, typical effect at corners.

Given stationary conditions the above mentioned information can be used to identify possible features in shapes/ structures in automobiles to differentiate between one another. However when, considering the case of moving targets the situation is far more unstable. In the following section, with respect to the extracted data, possible candidates to characterise an extended moving target are investigated.

5.1.1. Radar Cross Section

When there is a relative motion between a radar and a target, the relative path length between the radar and the various scattering centres characterising the target will change, in addition when considering real life scenarios with taking into account the effects of the moving parts and vibrations from surface of the target, it is observed the amplitude of a target returns will fluctuate between different coherent processing intervals, causing amplitude to spread around the target's respective doppler shift, there by constituting an extent in doppler in addition to extent in range, an comparison of amplitude of non fluctuating target and that of a fluctuating target as described in literature is as shown in figure 5.1[5][34]. Hence conventional methods to classify targets based RCS calculation may not be useful.

The fluctuating target as in real radar measurements is as shown in figure 5.2

However,it is expected that the total energy of the moving target inclusive of its parts is contained within the extent of the fluctuating target, though the energy may vary from between each CPI, it is expected to be consistent with the PDF of the target and its correlation properties of the target amplitude. Thus, we can expect targets of the similar extent to have the similar distributions of energy, hence can be considered as a feature for categorisation.
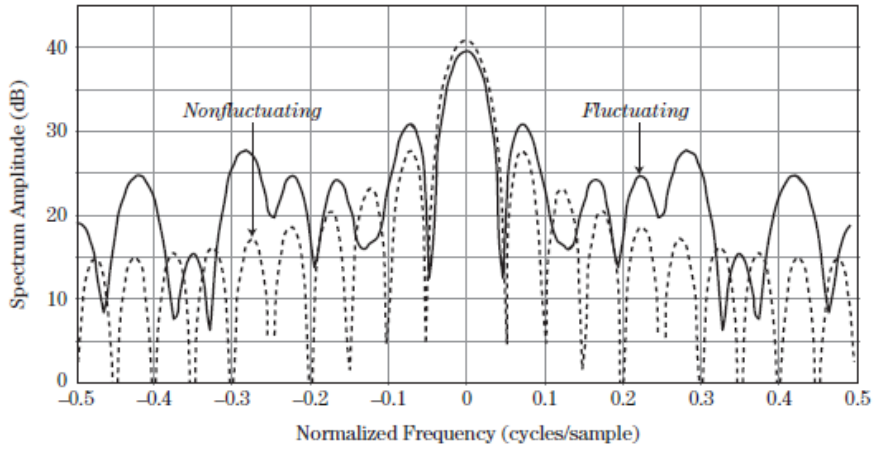
Figure 5.1: Comparison of amplitude spectrum of fluctuating and non fluctuating target[5]
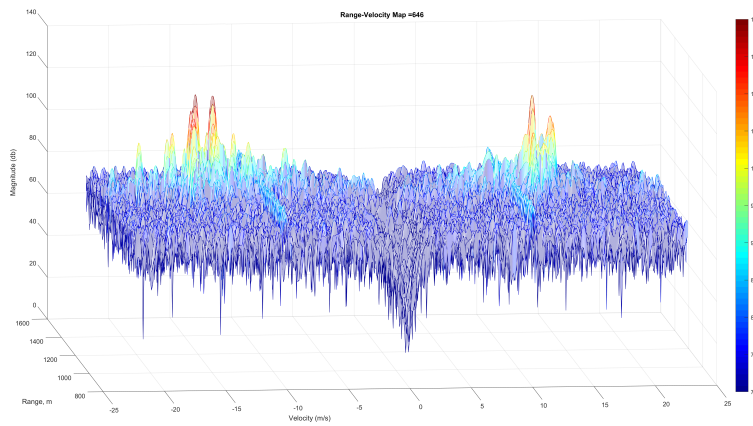
Figure 5.2: The figure shows the 3 extended targets on the range doppler map, the significantly high side-lobes, due to other moving parts of the target are clearly visible

Consider the Polarimetric Scattering Matrix (PSM) is described in chapter 3 equation 3.6 by taking into account the extent of the target in range and velocity, the total range compensated amplitude for a single target in single frame in the co-polar and cross polar channels is given by equation 5.1

$$TS_{XY} = \sum_{i=1}^{R} \sum_{j=1}^{V} S_{XY}(r_i, v_j) \frac{R_i{}^4}{r_{ref}} \tag{5.1}$$

where, XY represent the channels of measurement, if X=Y, the it is consider Co-polar channel if $X \neq Y$, it is consider as cross-polar channel, TS_{XY} is the total range compensated amplitude of the respective channel, S_{XY} are amplitudes from the scattering matrix, r_i is range bin at index 'i', v_j is velocity bin at index 'j', R_i/r_{ref} is the range compensation with respect to a reference range.

The mean of the total amplitude over the time series data $TS_{XY}(t)$ is considered as a possible feature to represent the target.

Another important which can be considered, is the max amplitude of the fluctuating

target across all channels, the strongest reflection from the target would be from the main body of the target, which is represented by the main lobe of the target amplitude spectrum as seen in figure 5.1, hence would is the least effected due to the fluctuations, the maximum amplitude across channels is given by equation 5.2

$$MS_{XY} = max(S_{XY}(r_i, v_j)) \tag{5.2}$$

where, XY represent the channels of measurement, if X=Y, the it is consider Co-polar channel if $X \neq Y$, it is consider as cross-polar channel. M_{XY} represents the maximum value of the respective channels.

The mean of the maximum amplitude over the time series data is also consider as a possible feature to represent the target.

The variation of the range compensated Total amplitude TS_{XY} and Max amplitude MS_{XY}, for a moving target as a time series data is as shown in figure 5.3
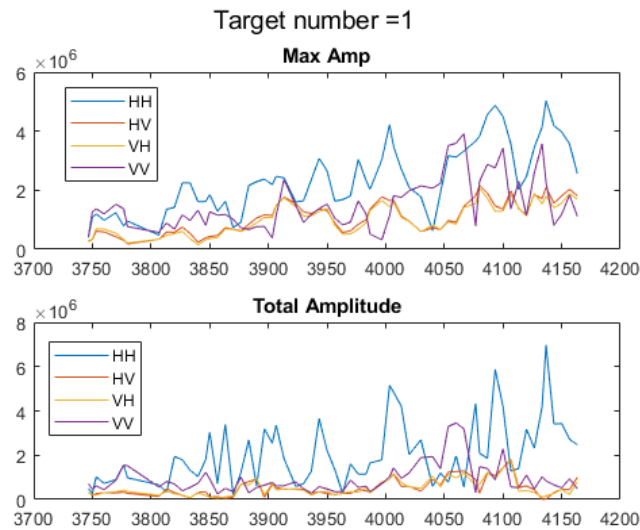
Figure 5.3: Time series data of Max amplitude and total amplitude of a moving target

The probability distribution of Total amplitude TS_{XY} and Max amplitude MS_{XY}, detected over multiple frames of measurement is as shown in figure 5.4 and 5.5 respectively.
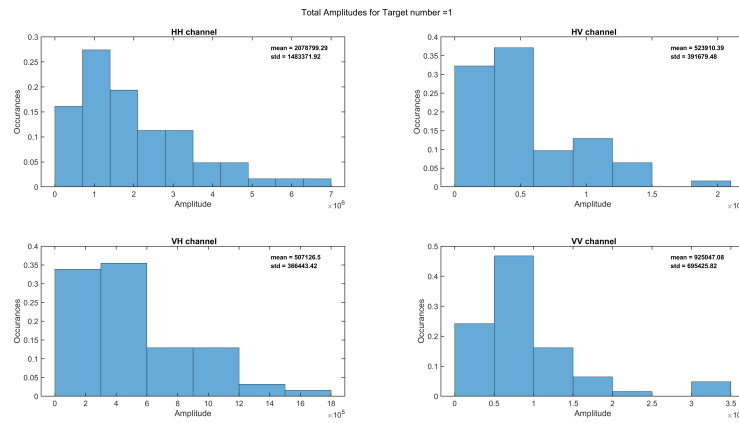
Figure 5.4: Histogram representing Total amplitude detected on all 4 channels
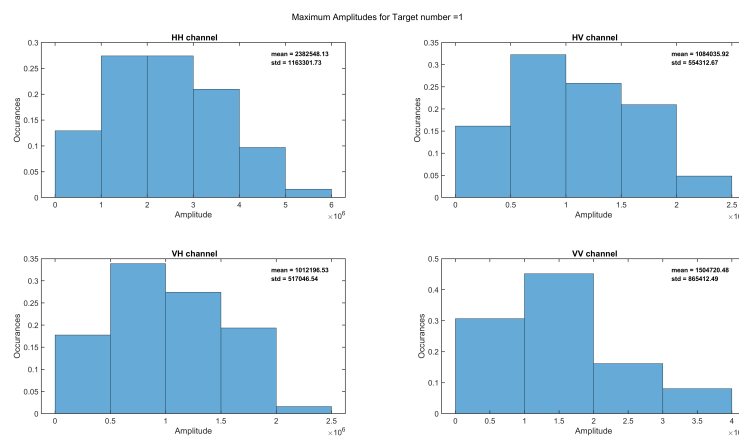
Figure 5.5: Histogram representing Max amplitude detected on all 4 channels

5.1.2. Range Extent

The extent of the target in this study are contributed by two parameters, the physical size of the target and an effect of doppler processing to characterise the velocity of the target. Th extent target fusion cluster created is based on the extents in range and velocity across all channels, as seen in figure 5.6

As seen in the figure, as the extent is range is consistent across channels, the number of range bins occupied by the target is considered , the variation of the range over the frames is investigated as time series data, and the average value is chosen to represent the target.

Th extent in doppler is ignore as it does not represent the physical aspects of the targets but rather its variation in velocity, which can be the same for targets of any size.

The distribution of the range extent, for a moving target is as shown in figure 5.7

5.1.3. Polarimetric Features

When considering features related to polarisation scattering matrix it can be observed that the scattering amplitudes extracted from the extended moving targets are time
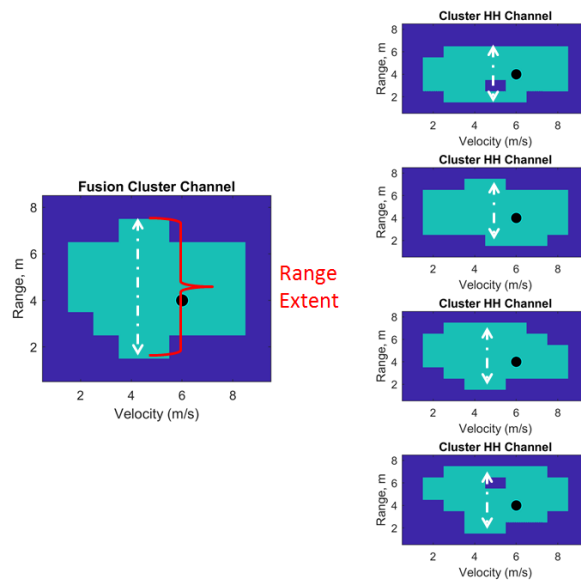
Figure 5.6: Range Extent based on range extent in each channel
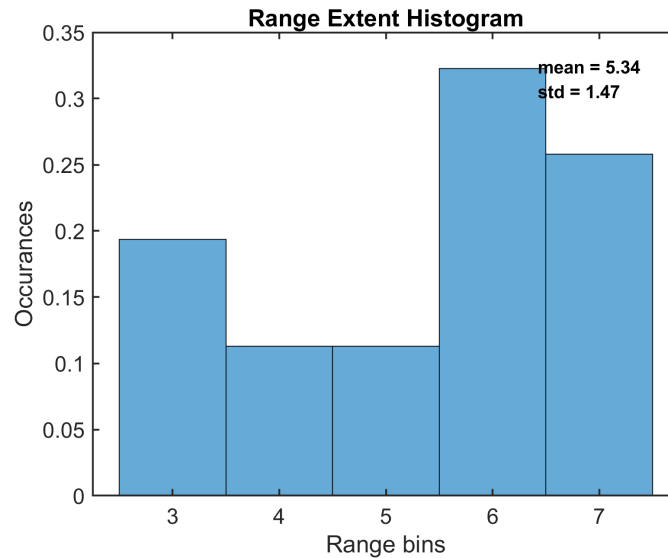
Figure 5.7: Distribution of range Extent over frames of measurement

varying stochastic processes due to the fluctuations from one CPI to another, much similar to the case of scattering due to partially polarised waves [31][62], hence a target can be described by considering, it as the second order harmonics of the fluctuations. The polarimetric coherency or covariance matrices can be used to extract these second order moments of the fluctuations, based on linear combinations arising, respectively, from the Pauli or the Lexicographic matrices [31] using the scattering matrix described in equation 3.6 in chapter 3. Ideally speaking, for a monostatic configuration the value in the cross polar channels are similar, however since the study is carried out using real radar measurements, there is difference in amplitudes of the cross polar channels, hence

all 4 elements of the scattering matrix (similar to a bi-static configuration) are considered. Since the coherency matrix and covariance matrix both give the same information we consider the covariance matrix for further study.

Covariance Matrix

The Covariance matrix is calculated based on the "4-D Lexicographic feature vector" or as known as "4D- Ω target vector" [31][62] given by equation 5.3

$$\Omega = \begin{bmatrix} S_{HH} & S_{HV} & S_{VH} & S_{VV} \end{bmatrix}^T \tag{5.3}$$

The scattering matrix S thus related to a polarimetric scattering target vector considered is given by equation 5.4

$$S = \begin{bmatrix} S_{HH} & S_{HV} \\ S_{VH} & S_{VV} \end{bmatrix} = \begin{bmatrix} \Omega_1 & \Omega_2 \\ \Omega_3 & \Omega_4 \end{bmatrix} \tag{5.4}$$

The 4x4 Lexicographic covariance (C_4) is generated from the outer product of the 4k target vector and its conjugate given by equation 5.6

$$C_4 = \langle \Omega \Omega^{*T} \rangle \tag{5.5}$$

where, "$\langle ... \rangle$ indicates temporal or spatial ensemble averaging, assuming homogeneity of the random medium"[31][62].

The obtained 4x4 Covariance matrix C_4 is given by equation 5.6

$$C_4 = \begin{vmatrix} \langle |S_{HH}|^2 \rangle & \langle (S_{HH}S^*_{HV}) \rangle & \langle (S_{HH}S^*_{VH}) \rangle & \langle S_{HH}S^*_{VV} \rangle \\ \langle (S_{HH}S^*_{HV}) \rangle & \langle |S_{HV}|^2 \rangle & \langle S_{HV}S^*_{VH} \rangle & \langle S_{HV}S^*_{VV} \rangle \\ \langle (S_{VH}S^*_{HH}) \rangle & \langle S_{VH}S^*_{HV} \rangle & \langle |S_{VH}|^2 \rangle & \langle S_{VH}S^*_{VV} \rangle \\ \langle S_{VV}S^*_{HH} \rangle & \langle S_{VV}S^*_{HV} \rangle & \langle S_{VV}S^*_{VH} \rangle & \langle |S_{VV}|^2 \rangle \end{vmatrix} \tag{5.6}$$

In this study as only amplitude of the scattering matrix are considered, the C4 matrix is symmetric along the principle diagonal elements. Hence only the upper diagonal elements are considered as features of the target.

The covariance matrix can be calculated based on two values :

1. Maximum amplitude

2. Total amplitude

As both values have significance of their own, a covariance matrices $C_4(Tot)$ and $C_4(Max)$ is calculated based on the total amplitude and maximum amplitude as described by equations 5.1 and 5.2

5.1.4. Correlation Co-efficient

In addition to the Covariance matrix discussed in the previous section, an additional feature could be the correlation co-efficient of the targets detected across different channels over multiple frames of measurements. As discussed in 3, when concerning backscattering from polarised EM waves, targets of same category (such as composition or shape) are most likely to have the same effect across channels, in addition when considering the effect over a time series data, the parameter would provide more insight on behaviour of similar physical characteristics which are not dependent on motion of the target (considered angular change in measurement area is minimal), thereby making it possible to better categorise the targets. Though covariance and correlation matrices both provide the degree of agreement between two values, when considering over a time series data as in this study, the values of the are expected to provide significant contributions, provided the data is wide-sense stationary (Stationary in the Mean).

The correlation coefficient is calculated using the equation5.7

$$Corr(X,Y) = \frac{\sum_{i=1}^{N} (X_i - \hat{X})(Y_i - \hat{Y})}{\sqrt{\sum_{i=1}^{N} (X_i - \hat{X})^2 (Y_i - \hat{Y})^2}} \qquad (5.7)$$

where, X and Y in this case can be the channels of measurement.

The correlation coefficient calculated across Co-polar channels and cross polar channels for the Max amplitudes extracted and total amplitude extracted are as shown in figure 5.8 and 5.9 respectively.
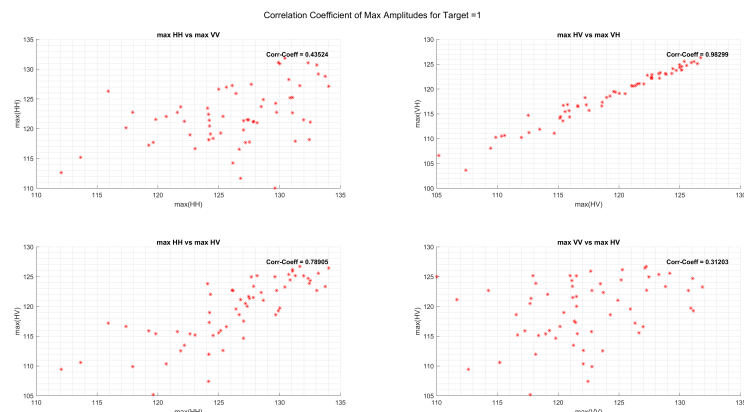
Figure 5.8: The figure shows the correlation coefficient calculated for extracted time series data for target, the values in cross polar channels are in good agreement as expected for a monostatic case,it is seen that for the consider target, Maximum amplitude from copolar channels agree weakly with each other, where as agree strongly with Maximum amplitude from cross polar channels.
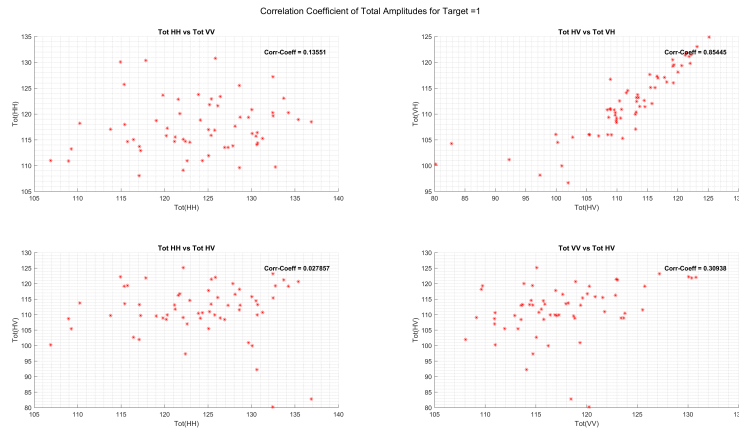
Figure 5.9: The figure shows the correlation coefficient calculated for extracted time series data for target, the values in cross polar channels are in good agreement as expected for a monostatic case,it is seen that for the consider target, total amplitude from copolar channels agree weakly with each other and with those of cross polar channels.

5.2. Feature Database

Based on the features discussed in the previous sections a feature data base characterising the moving extended target on the range velocity maps has been created. The structure of the database is as shown in figure 5.10

The final extracted features are summarised as below:

- Range Extent

- Maximum Amplitude extracted from all 4 channels.

- Total amplitude of the extended target cluster from all 4 channels

- Upper Triangular of Target Covariance matrix

- Upper Diagonal elements of Target Correlation matrix
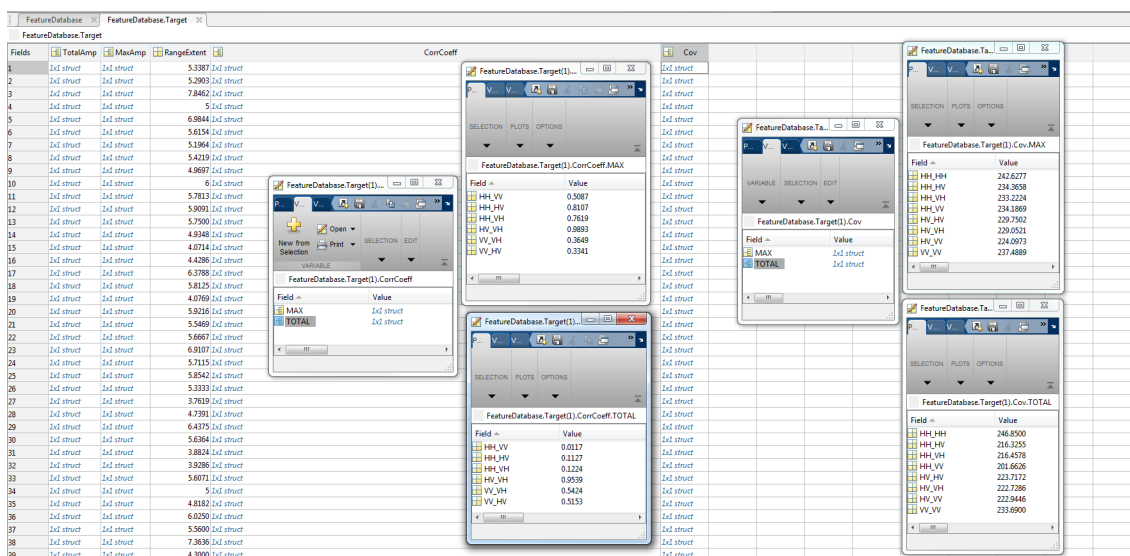
Figure 5.10: Feature database structure

5.3. Data Clustering

Data clustering a useful tool for effective categorisation of an unlabelled data, clustering algorithm must be capable of identifying structures within the same by organising the data into homogeneous groups, such that an index for the measure of similarity is minimised and the index of dissimilarity between groups is maximised. A data set is considered static if the data and all its features do-not change wrt time, where as a time series data set consists of parameters with change wrt to time, in many cases unlabelled time series data are more preferred as they determine the groups with similarities in fluctuations , in the considered study as the reflections from a target change from one CPI to the next, the data is considered as a time series data.

Three major components are required in case performing time series clustering [61]:

1. Choice of approach - Clustering Algorithm

2. Data distance measurement - distance metric

3. Performance evaluation criterion - accuracy , speed ,etc..

Based on the above components time series clustering can be categorised into 3 types as shown in figure 5.11
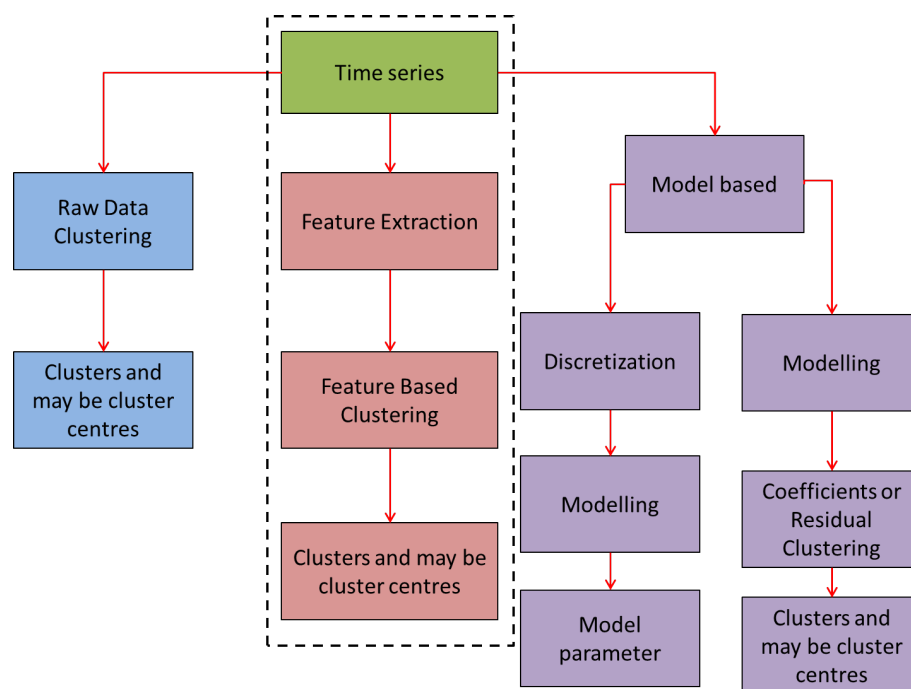
Figure 5.11: Time series approaches, raw data based, feature based and model based

In scope of this study, the raw polarimetric data from 4 polarimetric channels of the radar have been extracted, processed, associated and decomposed into possible features that can characterise a moving target. Hence a feature based clustering technique is most suitable for this study, however, prior to the feature database two other databases, the "Detection database" created using the (MCDA) Multi-Channel Data Extraction Algorithm, and "Target Database" created using (MTDF) Multi-Target Data Association Filter consists of raw data collected from each frame of measurement and from each

individual target respectively, these databases can be used for possible approaches in raw data based clustering.

The choice of clustering algorithm most suitable for the extracted data set and analysis of the created clusters, is a research topic by itself and is not contained within the scope of this study and can be considered as the further scope of this research.

However, as an additional topic, to provide a proof of concept that clustering of data is possible from the data set, the most fundamental feature based clustering approach 'k-means' clustering is investigated using examples from literature[61][63][64][65].

5.3.1. k-means Clustering

"k-means" clustering algorithm partitions a given dataset into " k mutually exclusive clusters" by considering each data sample as an object in space with its own coordinates. Given a distance metric and number of clusters , the algorithm find partitions such that, the distance with in a cluster is minimised and distance between clusters is maximised. For each cluster a centroid is calculated based on the point where sum of distances from all objects in that cluster is minimum. The centroid is dependent on the distance metric chosen.

An example of a clustering study conducted over randomly generated data sample is as shown in figures 5.12-5.13, using the following parameters:

- Distance : Squared Euclidean $Dist(x,c) = (x-c)(x-c)'$

- Number of clusters

- Number of realisations - chooses the best out estimate over defined realisations.
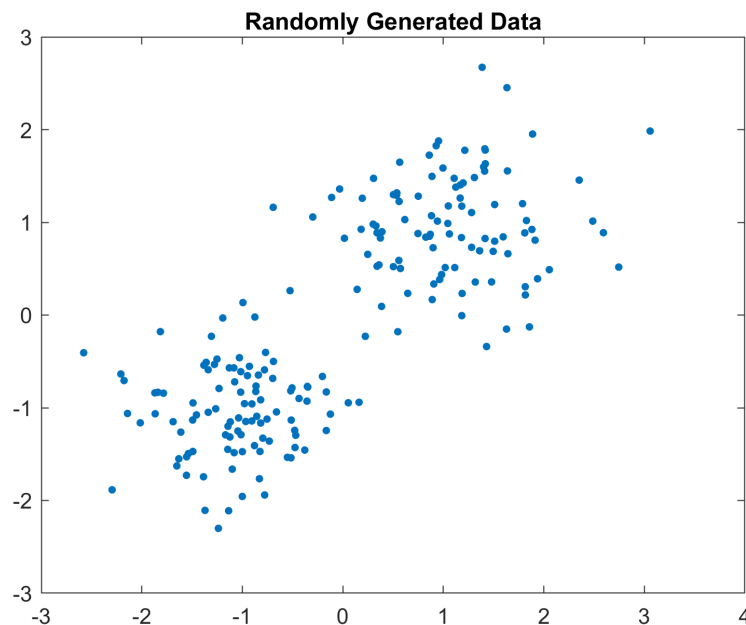
Figure 5.12: Randomly generated data

As the number of data-sets used to create the random data-set was known, it was possible to obtain the perfectly separated clusters. However, in case of this study, the objective
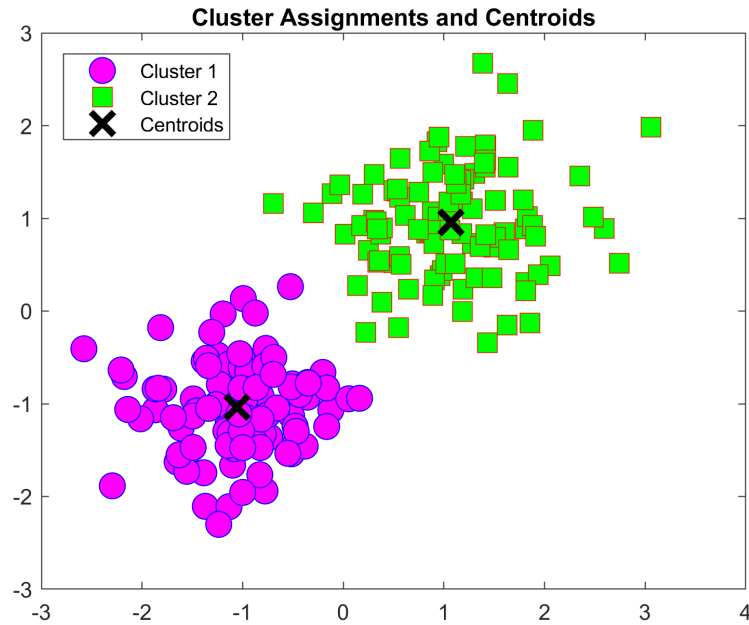
Figure 5.13: Output of k-means algorithm showing the two clusters identified within the randomly generated data

is to find the number of clusters, hence this number of clusters will be chosen based on different iterations. The results of clustering of the data-set are present in the next chapter.

5.4. Conclusion

In this chapter the basic concepts related to a time series data was introduced. The "Target database" created using algorithms from the previous sections, was investigated to find suitable features that could be used to categorise the extracted unlabelled data for moving extended targets into possible sub-classes.

Concepts related to range extent, extended target amplitude fluctuations, strategies to calculate RCS, target covariance matrix and correlation effect between channels were explained.

A Target feature database which can be used for further studies related to "Unlabelled Clustering" [61] was created and the basics of label-less classification was explained using a simple example.

In the next section the strategies explained from chapter 2 to chapter 5 are used on a dataset collected from a dense target location and the result relative to each section are presented.

6

Measurements and Results

In the previous sections, 3 stages/ sub modules of the proposed Multi Target Feature Extraction algorithm were discussed, the overall consolidated block diagram of the algorithm, describing the various stages discussed is as shown in figure 6.1.
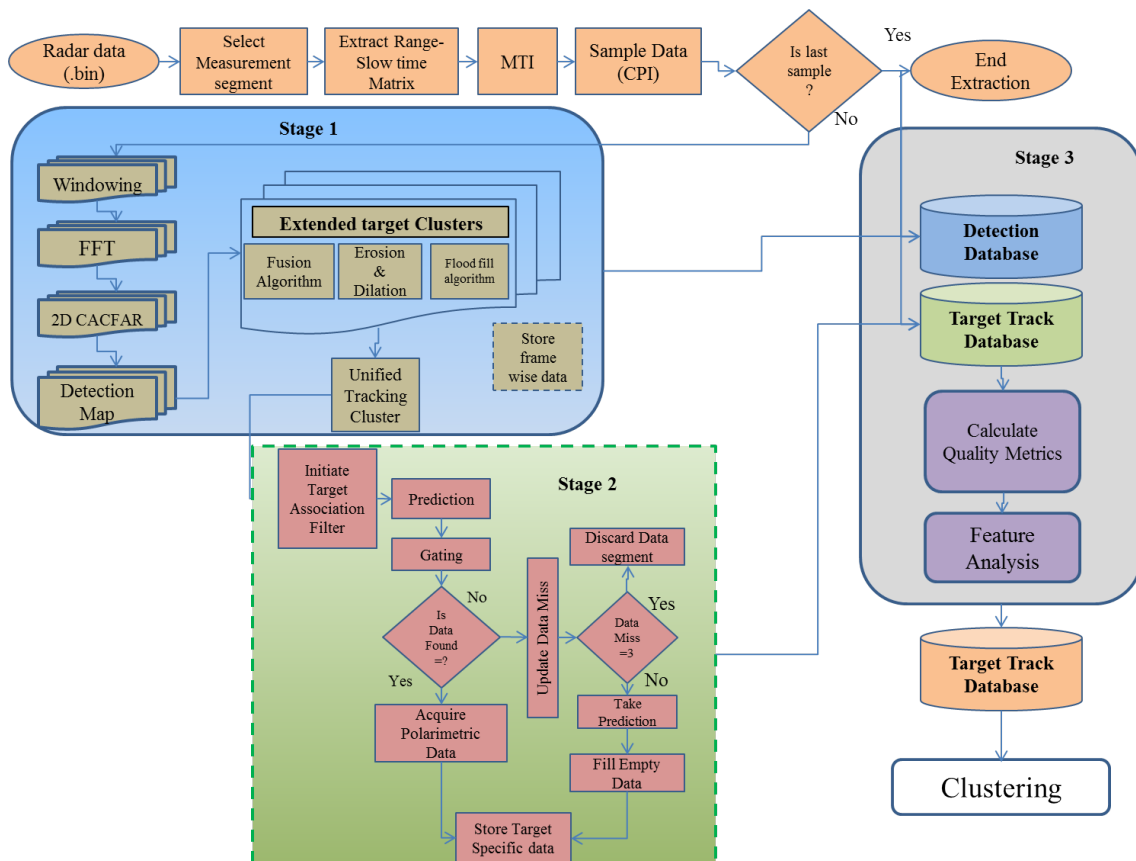
Figure 6.1: Multi-Target Feature Extraction Algorithm, the figure shows the 3 stages of the algorithm, each sub-module of the algorithm and its respective databases are represented by a different colour

The proposed algorithm is used to extract features from moving targets on range doppler space created based on measurements from a High Target Density location - A13 Highway (3.4kms from radar).

The measurement location is as shown in figure 6.2
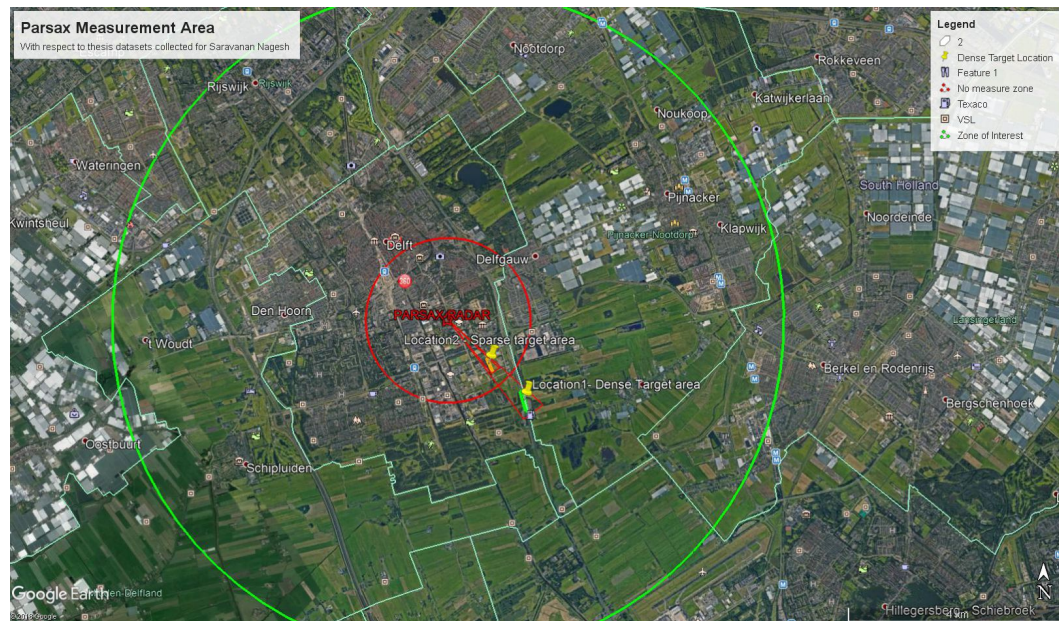
Figure 6.2: Measurement setup and location

The extracted data from location is evaluated on based the performance metrics described in chapter 3 the results for each data set is tabulated . For the sake of simplicity, the only positive velocity targets are considered, to reduce computational load.

6.1. Location 1: A13 Highway

Targets on a highway are dense target situations, well suited for extracting rich statistics from different types of targets over a short measurement interval. The details of the radar parameters during the measurement session are as follows:

- Azimuth: 137
- Range 3.3Km from Radar
- Elevation: -4.9

The measurement location is as shown in figure 6.3

Figure 6.3: Measurement Location 1-A13 Highway

6.1.1. Stage 1 - Multi Channel Data Extraction

The data collected over all 4 channels of the radar are characterised as the range velocity movie described in chapter 2. On an average over 50 extended targets are detected per frame of measurement for each individual receiver channel. The targets are inclusive of approaching and receding vehicles wrt to the measurement setup. As mentioned only targets with positive velocity are considered for reduction of computational load.

A distribution of the number of targets detected over 66 frames of data over 4 different channels is as shown in figure 6.4
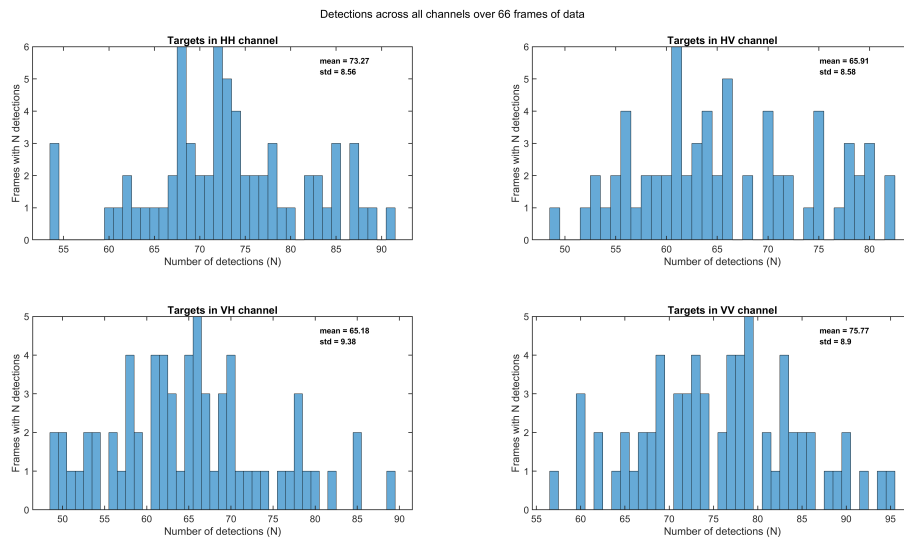
Figure 6.4: Distribution of number targets detected over 66 frames of data with positive velocity

It can be observed that as the targets are now closed space unconnected/ non clustered detections across multiple frames, the number of targets in not uniform across channels, this mainly because of the behaviour of the targets wrt the effect of polarisation.

Hence the proposed Multi Channel Data extraction algorithm is required, which clusters closed spaced detections to form larger target clusters for simultaneous data extraction from all 4 channels over multiple frames of measurements, the distribution for number of targets from the MCDA algorithm is as shown in figure 6.5
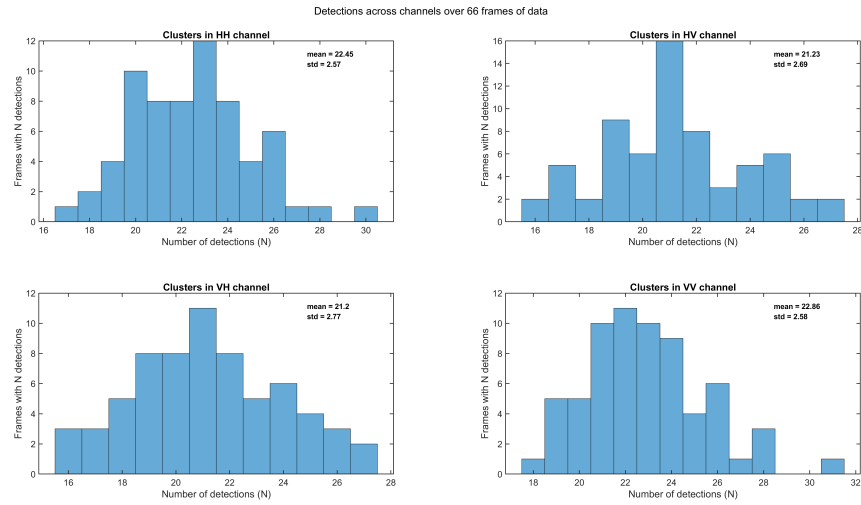
Figure 6.5: Distribution for created clusters using proposed MCDA over 66 frames of data

In order to evaluate the same the Flood Fill algorithm based clustering approach is applied on each individual channel and compared against the number of clusters created using the Fusion Algorithm as shown in figure 6.6
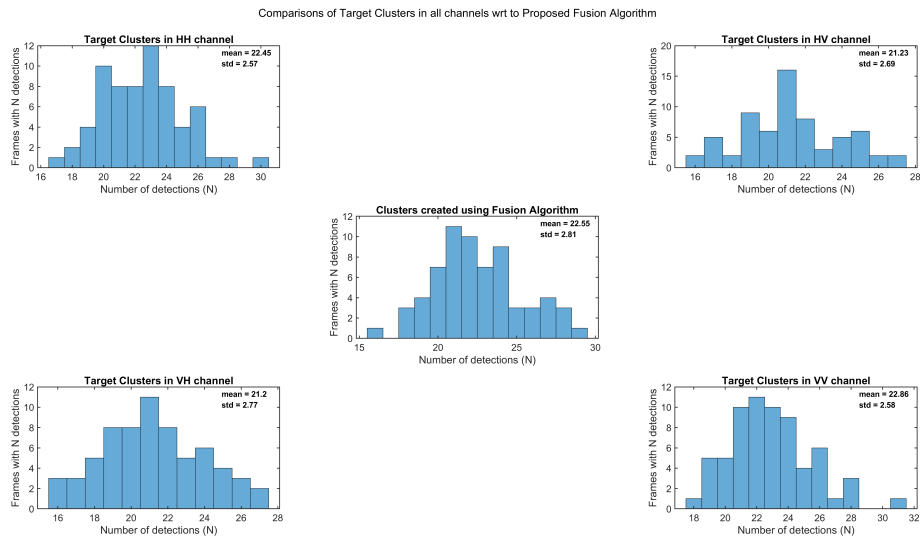
Figure 6.6: Comparing the number of Clusters created in each channel against the number of clusters by the proposed algorithm

It is seen that the number of clusters in each channel and the number of cluster by the proposed extraction are excellent agreement.

To additionally validate the same, the correlation coefficient for number of clusters in channel for each frame of measurement is calculated against the number of clusters by

the proposed algorithm. The results is as shown in figure 6.7
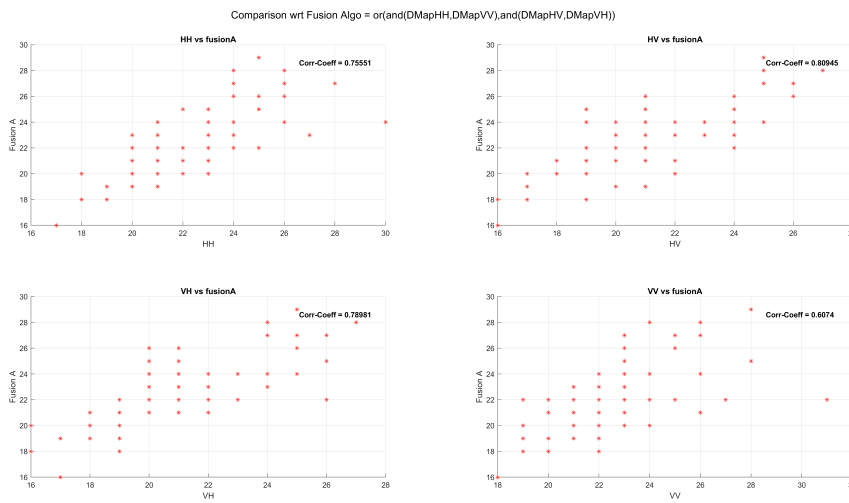
Figure 6.7: Correlation between Clusters in each channel wrt Cluster by algorithm

Thus from the first stage a detection database consisting of nearly 25 targets per frame from 66 frames of data has been extracted, for each target following parameters are accessible.

1. Choice of Geometric centroid or Weighted centroid for each target.

2. A bounding region around every cluster isolating from other targets.

3. Target Data from each individual channel

4. Target Mask specifying values above noise floor for every channel.

A visual depiction of the same as presented in chapter 3 is as seen in figure 6.8
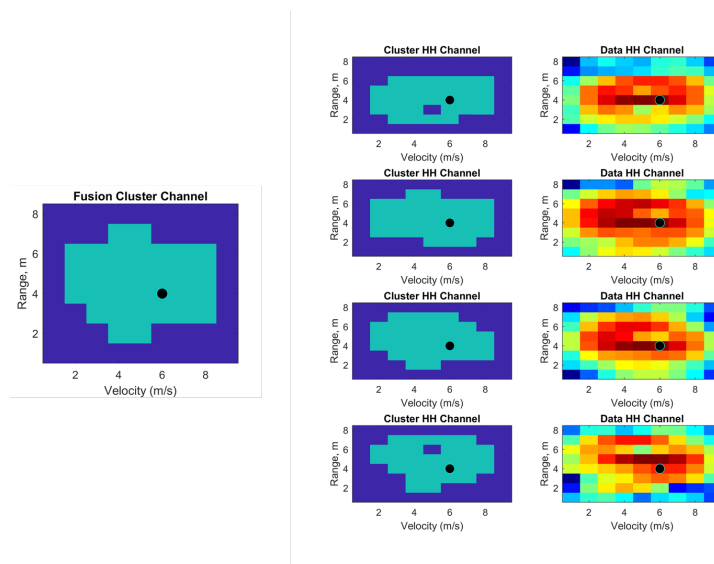
Figure 6.8: Extracted data

6.1.2. Section 2- Multi Target Data Association

As described in the previous section, a database consisting of a total 1452 unassociated target clusters, detected over 66 frames of measurements has been extracted. A depiction of all unassociated cluster centres detected on the range velocity space is as shown in figure 6.9
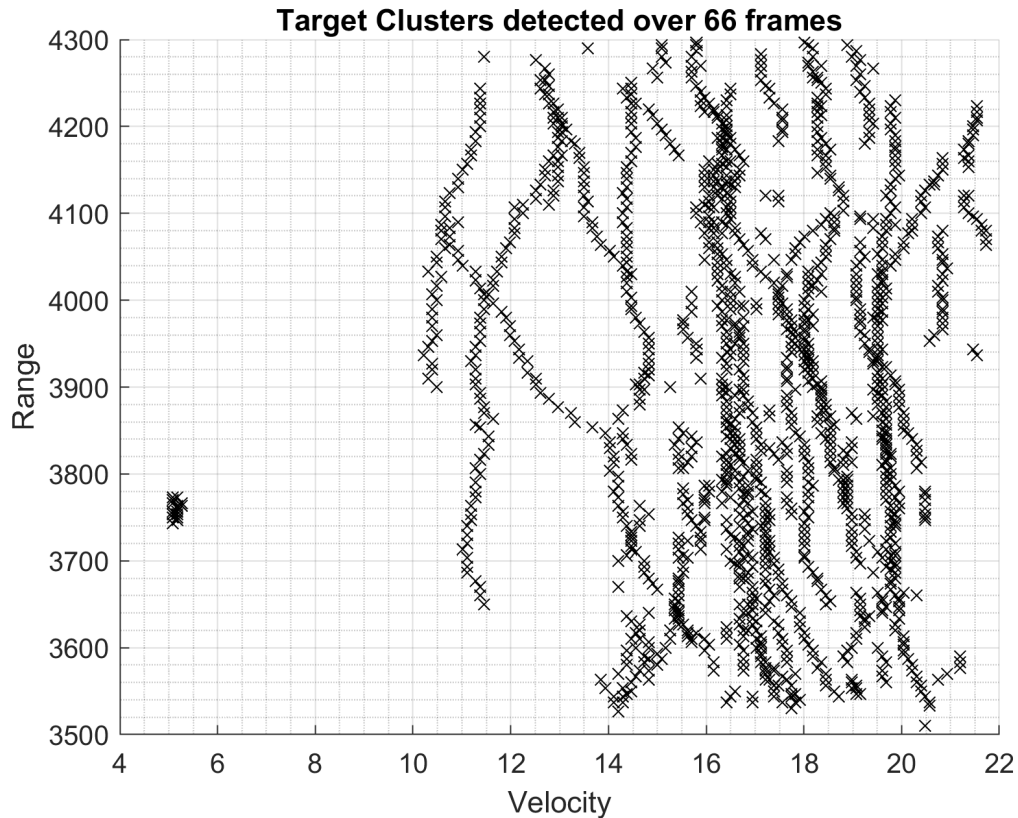
Figure 6.9: Extended target Centres detected over 66 frames

In order to do the feature analysis of moving targets, the evolution of the target's statistics over the frames measurement is required. This can be obtained by finding trajectories of each individual target over the multiple frames of measurement on which "the target was detected".

To create the target trajectories, as tracks of correlated measurements for each target, the proposed Multi Target Data Association filter is used .

The following points are considered as ground truth for the data set:

- The data set consists of targets following a linear trajectory but at different velocities and accelerations.

- Multiples targets may have the same velocity "OR" same range but not both for a full track duration.

- If say two or more tracks are detected with identical trajectories, the case is considered as duplicate track of a common target. In this case the minimum mean square error for range and velocity for the duplicates tracks will be a perfect match.

- If the trajectories are close to identical tracks but are slightly varied ie.. mmse is not a perfect match, it can be considered as a case of closely moving targets with level 3 data-association as explained in chapter ?? section 1.

- As we are considering real data situations, the targets detected at the entry point of the measurement area and exit point. Targets detected at initial frames (frame 1-6) near to exit point and targets detected at the entry point during the last frames (60-66) are expected to have a short track duration.

Considering the mentioned points, the tracks created for 16 different targets are as seen figure 6.10
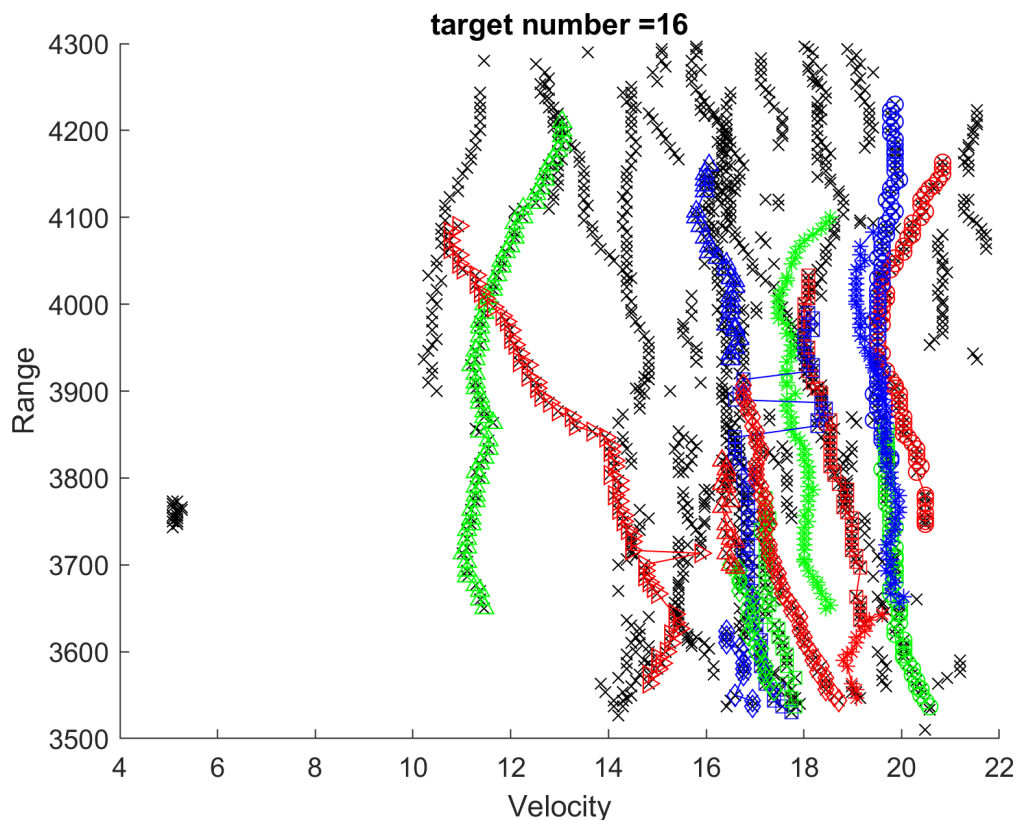
Figure 6.10: Tracks of correlated measurements for 16 targets

The output of the Multi Target Data Association filter produces a of 118 associated track trajectories, the tracks are evaluated for the 3 performance metric discussed in chapter ?? section:4.3.1. As it is not practical to show the evaluations metrics for all 118 targets, only a few cases are considered in the report, however the total performance metric for the data set are presented as graphs and the individual track quality details are tabulated in table 6.1

TRACK CROSSING

Measures the number of instants trajectories of target cross each other caused due to merging and splitting measurements, or overlapping trajectories. Is calculated based on equation 4.34 and 4.35 given by:

$$TCross_{total} = \frac{1}{2 * N * T_F} \sum_{i=1}^{N} \text{TCross}_i \tag{6.1}$$

where, $TCross_i$ represents the total number of crossing events for the ith target, $TCross_{total}$ is the total crossing events for 'N' targets over T_F frames recorded in the data-set,The factor 2 is considered as a minimum of 2 targets are involved in a crossing

The Track crossing metric evaluated for the data set is as shown in figure 6.12
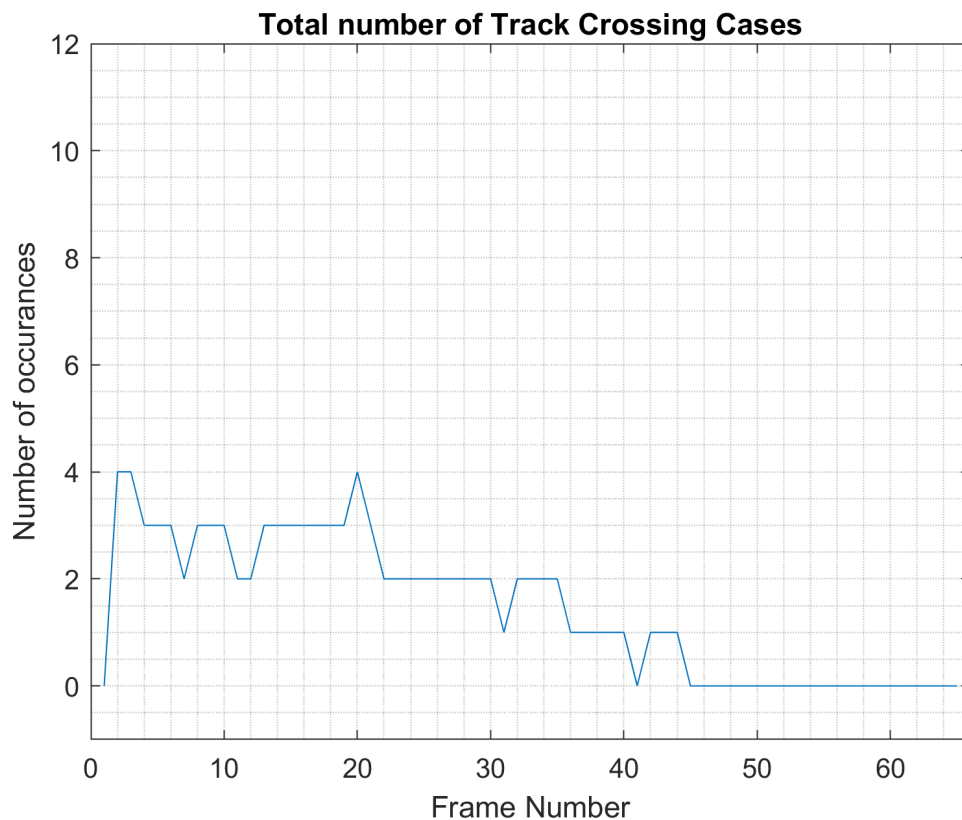
Figure 6.11: Number of Cross events recorded for all targets over 66 frames

Track Association Loss

Measures the number of instance a prediction for a target did not find a suitable measurement to associate, is calculated based on equation 4.36 and 4.37 given by:

$$AL_{total} = \frac{1}{N * T_F} \sum_{i=1}^{N} \text{AL}_i \tag{6.2}$$

where,AL_i represents the total number of association losses for an ith target,AL_{total} is the total number of Association losses for a considered data set,N is total number of targets and T_F is total frames of measurements.

The track association loss metric evaluated for the data set is as shown in figure 6.13
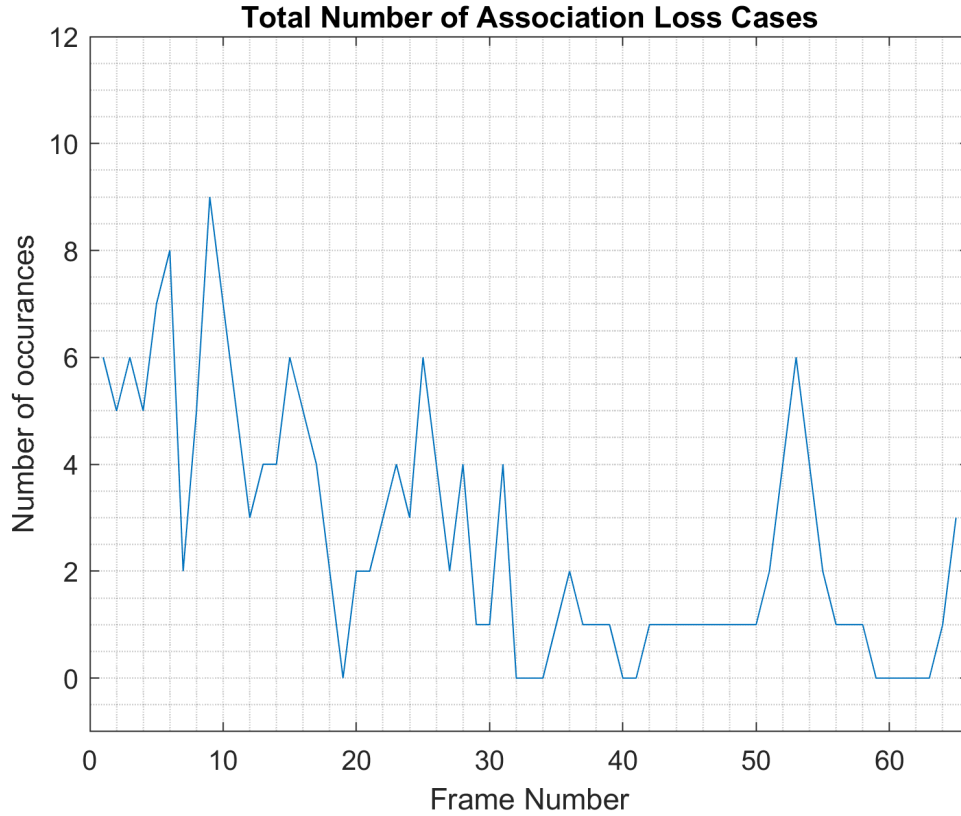
Figure 6.12: Number of Association losses for the dataset, it is observed that the association loss is relatively high during the first few frames due to number of target exiting the measurement area, it is observed the value gradually stabilises

Association Error in range and velocity

Figure of merit to identify duplicate tracks, at a given instant of evaluation over all tracks of associated measurements, only one target track must have a value equal to zeros, calculated based on equation 6.4-4.32 an given by:

$$iE_R(t) = \sqrt{(mR_i(t) - (NmR(t)))^2} \tag{6.3}$$

$$iE_V(t) = \sqrt{(mV_i(t) - (NmV(t)))^2} \tag{6.4}$$

The performance metric has been for 4 randomly chosen tracks as seen in figure 6.13

In order to consider a time series data for the feature analysis, a minimum 10 frames of associated measurements for each target is required, hence the targets with less than ten frames of measurements are removed from the database, this eliminates the following:

- False Tracks- All detected are tracked to a minimum of 4 consecutive frames before confirmed as a track of target, however detections due to random events may some sometimes lead to detections , which also are tracked for 4 successive iterations, random events are inconsistent the probability such an event appears on on 4 successive frame is rare, hence false tracks consisting of only predictions but no associations are eliminated.
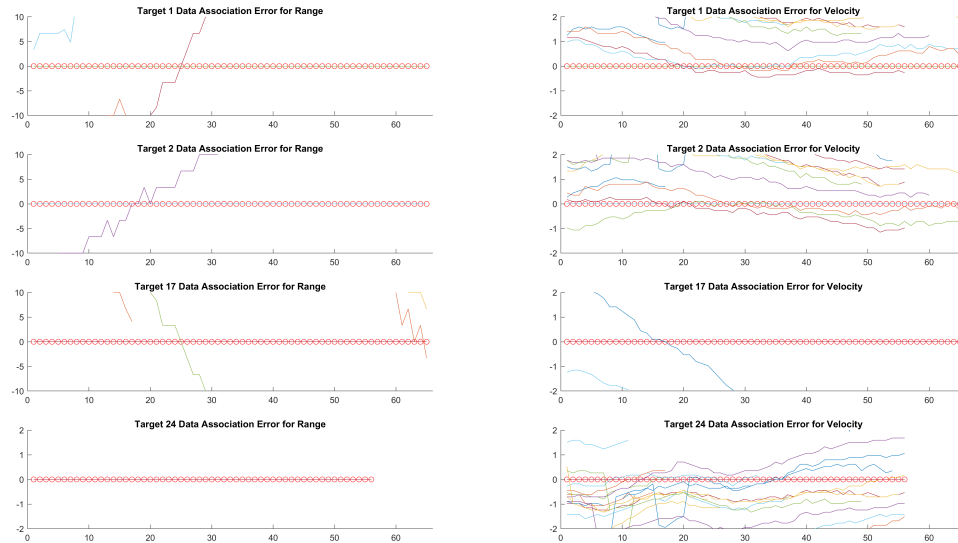
Figure 6.13: Association Error in range and velocity calculated for tracks created for 4 target, the circles highlight the trajectory of target considered is zero, hence showing that the associated measurements belong to only 1 target, in case of presence of crossing at range errors for targets 1 ,2 and 4 is result of a another track which had a crossing trajectory leading to the same measurement shared by two targets, the point of intersection indicates the exact instant of the event, in case of the velocity error, as many targets can have the same velocity on a highway situation it is seen that many trajectories appear close to zero but only those of crossing trajectories have an intersection as seen in difference between target 2 and 17

- Short Tracks- As mentioned earlier, targets detected at initial frames (frame 1-6) near to exit point and targets detected at the entry point during the last frames (60-66) are expected to have a short track duration. Though, there are successful detections and association for the target, the minimum number of samples required for the time series analysis is insufficient, hence need to eliminated.

Based on the above criteria from the total 118 targets tracks formed 68 targets with reliable trajectories are extracted. The quality metric for each target is tabulated in table 6.1.

The Targets with an associating accuracy less than 50% are discarded , thus the final created Target Track Database consists of 62 Targets tracks. Based on the metrics calculated in table 6.1, it can be concluded that from the provided Detection Database, 87.15% of detections has been perfectly associated, 2.4265% of the track data are corrupted by level 3 data association issues such as merging and splitting measurements from the radar, 2.12% loss due to unsuccessful gating due to fluctuating target centre has been recorded.

6.1.3. Features Analysis

The output of the Multi Target Data Association filter is a target database consisting of a time series for the raw data extracted from 4 polarimetric channels for 62 moving targets. Based on the topics discussed in chapter ?? , the identified features are extracted from the Target database to create a Target Feature Database. In the following sections the extracted features from 2 randomly chosen targets are presented .

Target Number	Total Detected Frames	Number of Track Crossing Events	Number of Association Loss	Association error (%)	Number of usable frames
1	66	1	4	3.03	61
2	66	2	4	13.64	54
3	56	0	4	21.21	42
4	17	0	4	4.55	13
5	66	0	2	30.30	45
6	66	0	1	16.67	55
7	60	0	4	68.18	18
8	66	14	2	90.91	6
9	37	0	2	0.00	36
10	56	14	4	33.33	35
11	66	14	2	90.91	6
12	15	0	4	7.58	11
13	24	0	4	4.55	20
14	50	0	4	69.70	14
15	18	0	2	0.00	17
16	32	0	2	0.00	31
17	66	2	0	7.58	61
18	66	1	2	10.61	58
19	17	0	4	7.58	13
20	55	14	4	9.09	47
21	64	1	0	13.64	55
22	49	9	4	12.12	40
23	11	0	4	1.52	8
24	56	2	0	10.61	50
25	54	13	2	40.91	31
26	50	11	2	13.64	42
27	40	4	2	0.00	39
28	25	0	4	16.67	18
29	27	0	4	7.58	22
30	48	1	0	27.27	35
31	13	0	4	1.52	10
32	13	3	4	1.52	10
33	45	7	1	9.09	41
34	21	0	4	4.55	17
35	13	0	4	4.55	10
36	18	0	4	6.06	14
37	32	1	4	1.52	29
38	35	0	4	13.64	28
39	15	1	4	1.52	12
40	12	0	4	3.03	9
41	40	22	0	9.09	36
42	29	0	4	6.06	24
43	26	0	2	0.00	25
44	32	0	2	31.82	21
45	32	7	1	1.52	32
46	11	0	4	1.52	8
47	17	0	4	13.64	12
48	19	0	4	16.67	13
49	28	0	0	22.73	22
50	27	0	1	10.61	24
51	16	0	4	6.06	12
52	25	2	0	9.09	23
53	24	22	0	7.58	22
54	21	0	0	4.55	20
55	19	0	4	1.52	16
56	20	0	0	1.52	20
57	20	0	2	6.06	18
58	18	0	0	9.09	16
59	18	0	1	1.52	18
60	18	0	3	4.55	15
61	18	0	0	1.52	18
62	15	0	4	1.52	12
63	15	0	0	4.55	14
64	14	0	0	4.55	13
65	14	0	1	4.55	13
66	13	0	0	6.06	12
67	12	0	0	4.55	11
68	11	0	0	10.61	10

Table 6.1: Quality Metric For Tracks of associated measurements, provides information about number of tracks from a target that are usable, the final value has been rounded off to the nearest whole number

Range Extent

Range extent is described as the number of range bins spanned by the consolidated extended target fusion cluster representing a target on all 4 channels. A depiction of the same is as shown in figure 6.14

Figure 6.14: Target Extent in range

The distribution representing the variation of range extent for the targets wrt its trajectory on the range velocity map is as shown in figure 6.16

(a) 1a   (b) 1b

Figure 6.15: Range Extent for 2 different moving Targets

Maximum Amplitude

The strongest reflection from an extended target is usually obtained from the main body of the target, hence contains properties of the strongest reflector from a target. The maximum amplitude of an extended target is as shown in figure 6.16
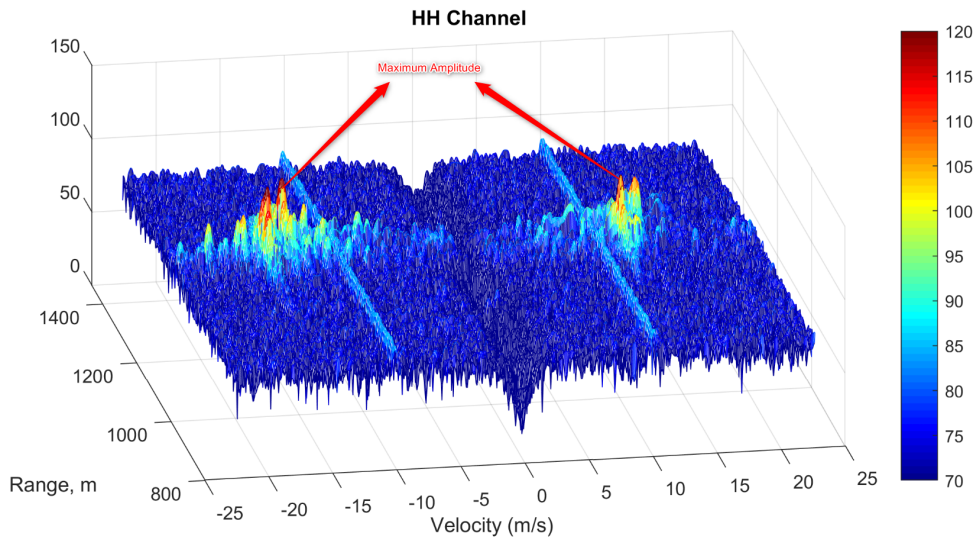
Figure 6.16: Maximum amplitude from peaks of the main lobe of two different extended targets

The distribution representing the variation of maximum amplitude on 4 polarimetric channels for the targets wrt its trajectory on the range velocity map is as shown in figure 6.17- 6.18
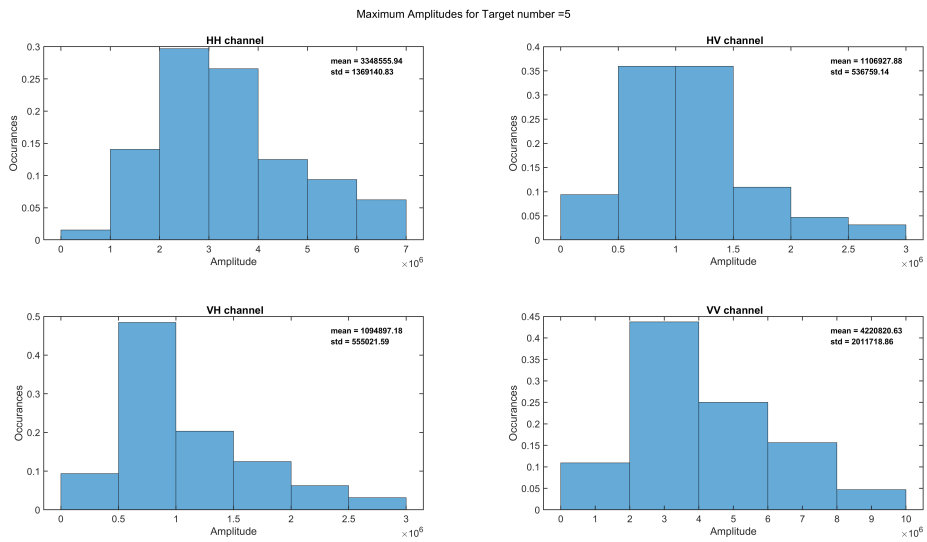
Figure 6.17: Histogram for the Value of maximum Amplitude for a moving target wrt 4 polarimetric channels-example 1

Total Amplitude

Reflection from a extended moving target fluctuate from one CPI to another, its total amplitude is inclusive of its moving parts and vibrations from surface of the target, thus
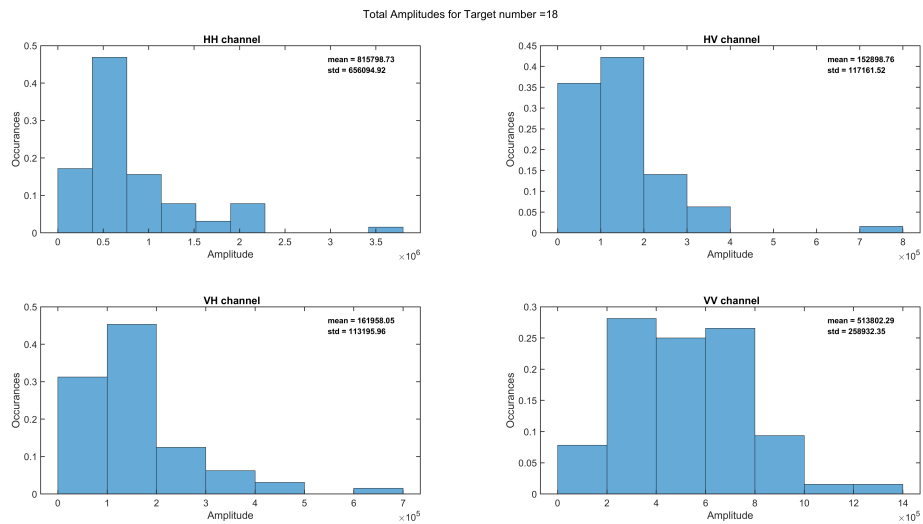
Figure 6.18: Histogram for the Value of Maximum Amplitude for a moving target wrt 4 polarimetric channels-example 2

the total energy of the moving target inclusive of its parts is contained within the extent and considered to be consistent with the PDF of the target and its correlation properties of the target amplitude.

The total energy from an extended moving target is as shown in figure 6.19
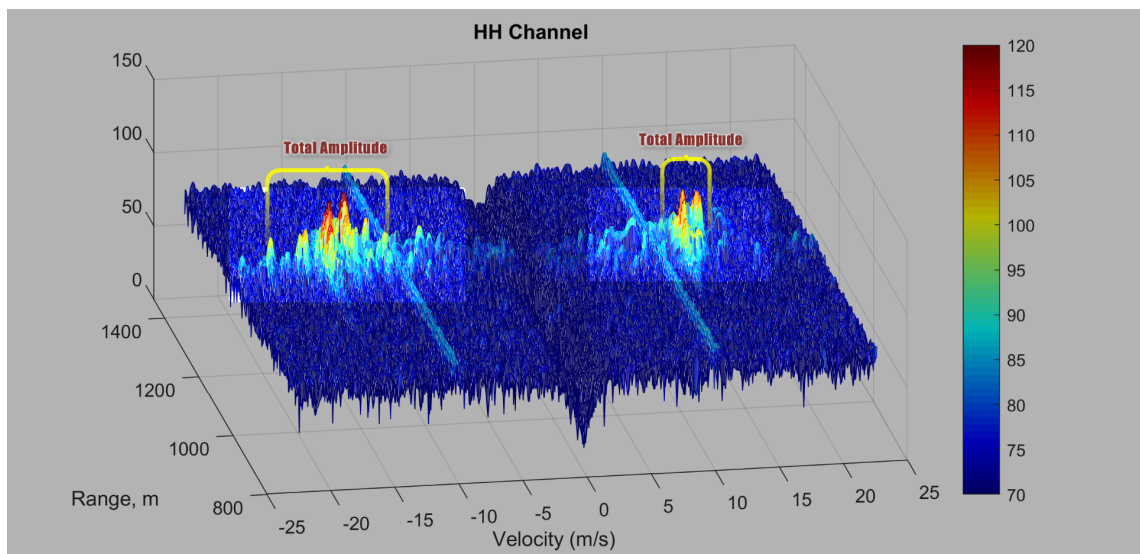
Figure 6.19: Total amplitude for two different extended moving targets

The distribution representing the variation of total amplitude for the targets wrt its trajectory on the range velocity map is as shown in figure 6.20- 6.21

Correlation Co-efficient

Targets of similar nature would provide similar interactions with signals received in the Copolar and Cross polar channels of the radar, the Correlation Co-efficient calculated between co-polar channels (HH and VV), cross-polar channels (HV-VH) and also between
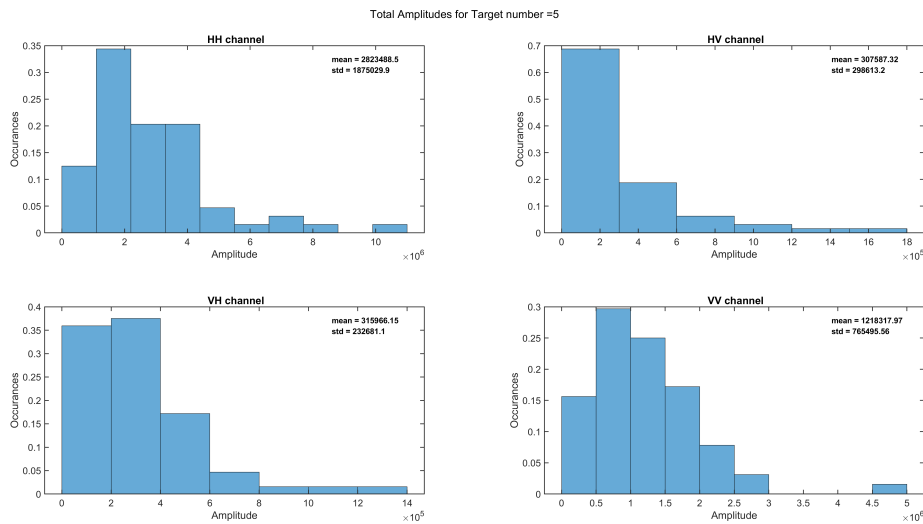
Figure 6.20: Histograms for the Value of Total Amplitude for a moving target wrt 4 polarimetric channels-example 1
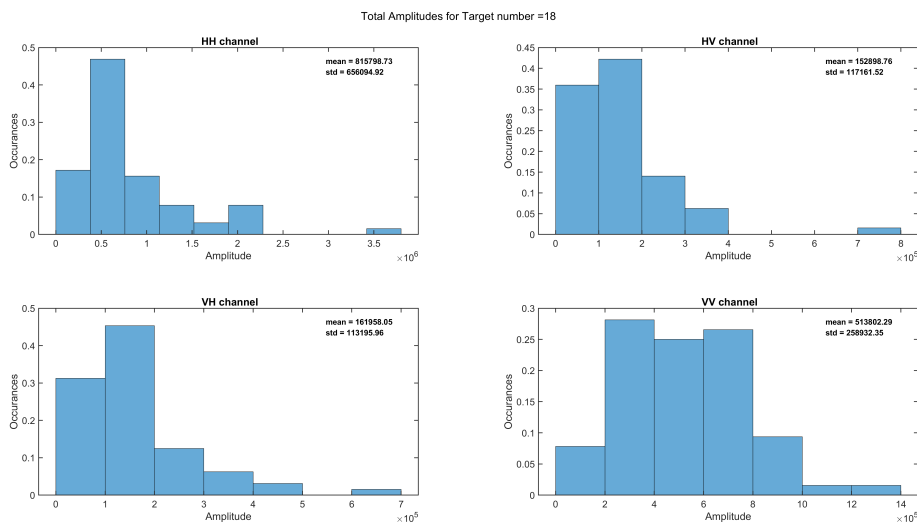
Figure 6.21: Histograms for the Value of Total Amplitude for a moving target wrt 4 polarimetric channels-example 2

Copolar and Cross polar (HH-HV . VV-HV) calculated for interactions of possible 3 target of different nature are as shown in figure 6.22- 6.24.

Covariance Matrix

Covariance matrix similar to correlation coefficient measures the degree of agreement of the effects considered with respect to considered channels by also considering the magnitude from each channel,

As discussed in chapter ?? when dealing with a time series data, the effects are expected to be different from those of the correlation effects. The Covariance effect between co-polar channels (HH and VV), cross-polar channels (HV-VH) and also between Copolar and Cross polar (HH-HV . VV-HV) calculated for interactions of possible 3 target of different nature are as shown in figure 6.25- 6.27.
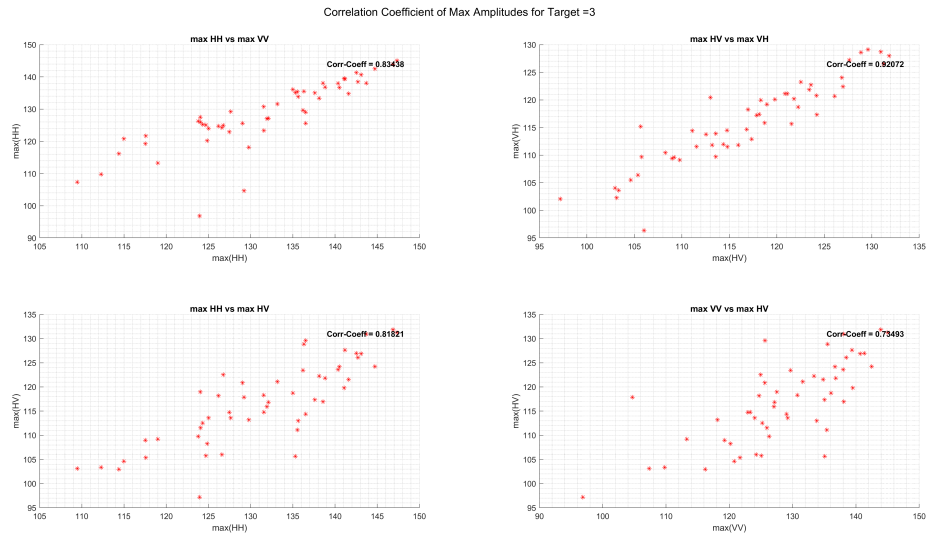
Figure 6.22: Target with good correlation effects on all channels
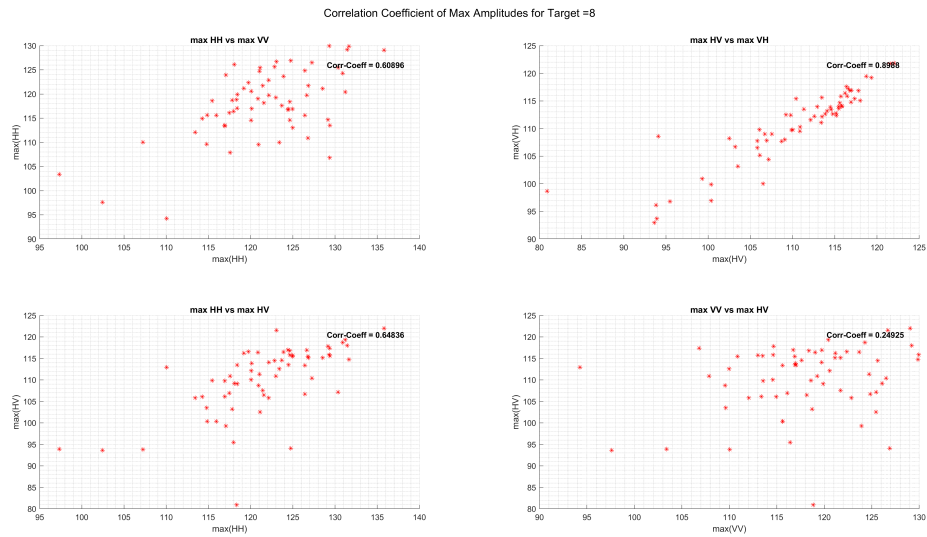
Figure 6.23: Target with good correlation in Copolar channels(HH vs VV) and Cross Polar Channels(HV vs VH) , but bad correlation with Copolar to Cross polar interactions (HH vs VH) (VV vs VH)

6.1.4. Clustering Validation

As discussed in chapter ?? section 5.3.1 the k-means clustering algorithm is tested on the extracted feature database on the following values;

1. Correlation Coefficient
    - CorrCoeff(VVHH) vs CorrCoeff(HVHH)
    - CorrCoeff(VHHV) vs CorrCoeff(VVHV)

2. Covariance Matrix
    - Cov(VVHH) vs Cov(HVHH)
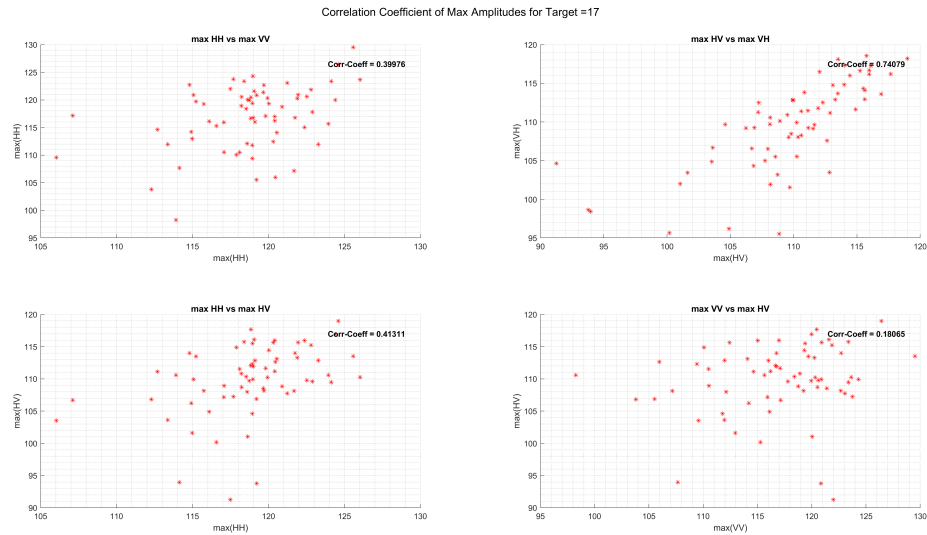
Figure 6.24: Target with Bad correlation on all channels
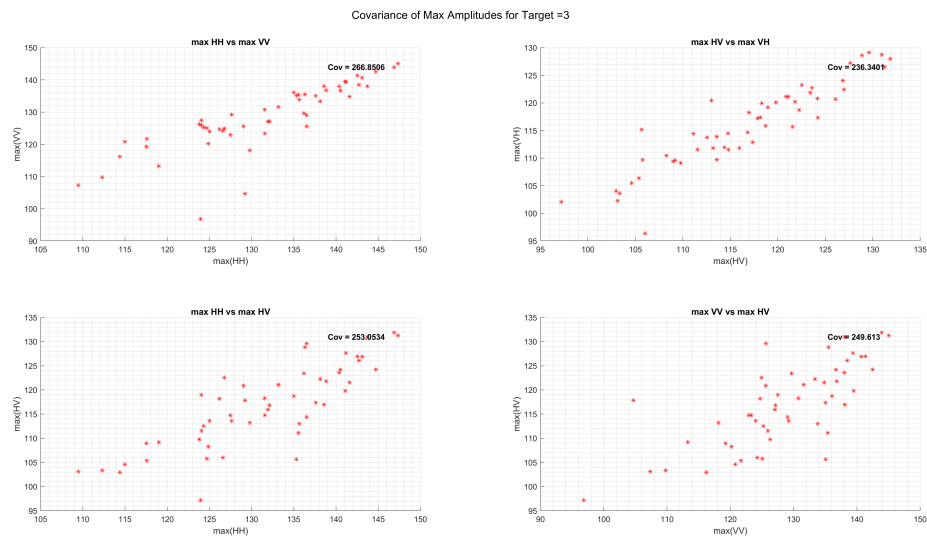
Figure 6.25: Target with differing covariance across all channel combinations

- Cov(VHHV) vs Cov(HVHH)

The following parameters are configured:

- Distance : Square Euclidean

- Number of Cluster : 3 (calculated based of best centroid separation)

- Number of realisations : 100

The obtained results are as shown in figure 6.28 for correlation coefficient based clusters and figure 6.29 for covariance based clusters.

From the presented results it is clear that the formulated research direction can be used as a means for target categorisation, which can be considered as an open research topic
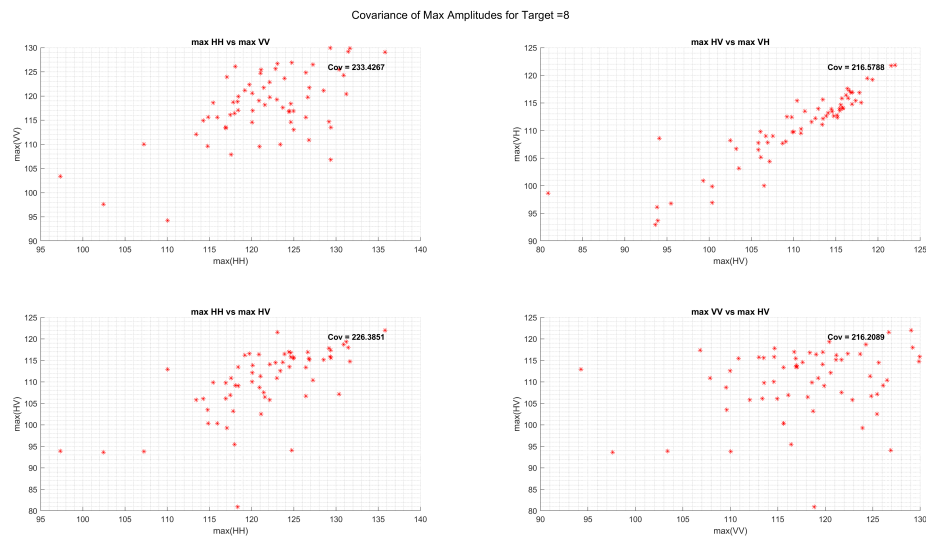
Figure 6.26: Target with matching values for VV vs HV (Copolar to cross polar for VV only) and HV vs VH (Croos polar)
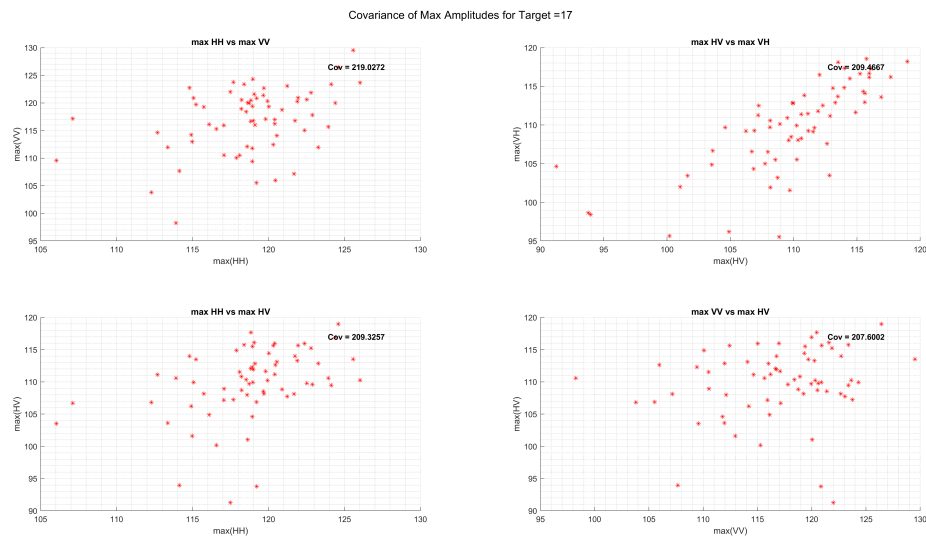
Figure 6.27: Target with similar values for VV vs HV , HH vs HV, and HV vs VH, (copolar to cross polar and (cross polar to cross polar), but differing for copolar to coplar.(HH vs VV)

and future scope of this study.

6.2. Conclusion

Using the raw .bin files collected from the radar, the Robust Multi Target Feature extraction algorithm is used to extract statistics of the moving targets.

The extracted - associated data is evaluated for performance metrics to validate the robustness of the algorithm.

The created time series data is analysed for features and identified features are extracted
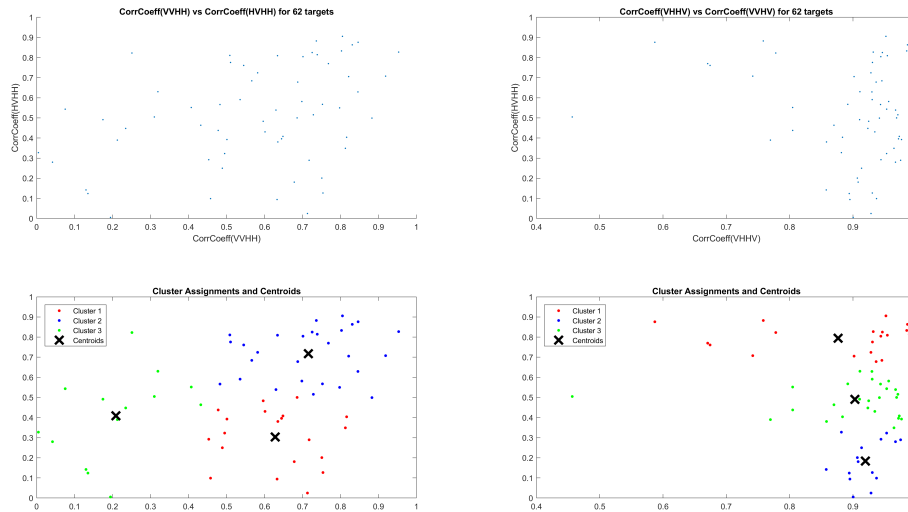
Figure 6.28: It can be seen that 3 well separated clusters are obtained for the two combinations - in the figure to the left we can see that information of correlation effects of targets detected in VVHH against HVHH , it is observed that the dataset contains targets with weak, medium and strong correlation in both Copolar channels and Copolar -Cross Polar combinations. Where as in figure to the right, we can see the database consists of targets with strong correlation effects VHHV channel but significant variation in HVHH channels
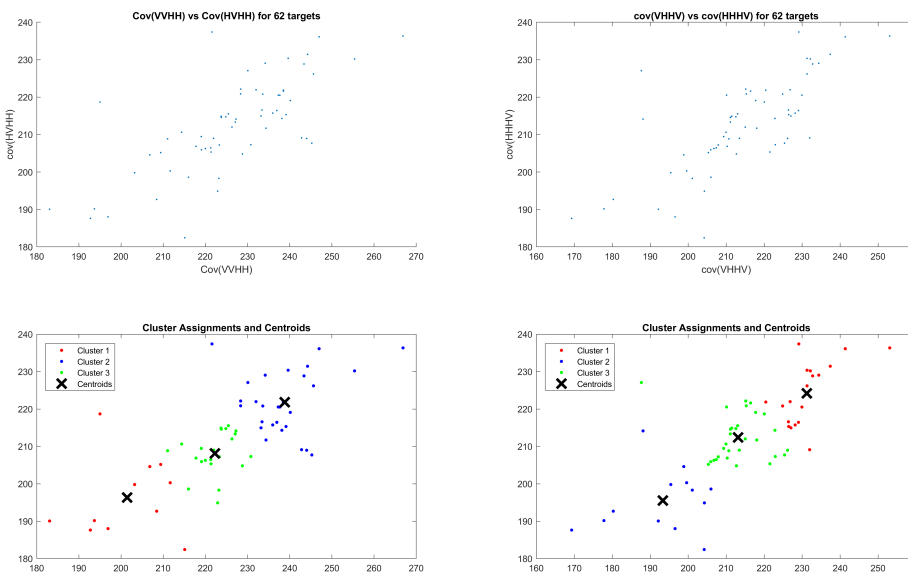
Figure 6.29: It can be seen that 3 separated clusters have been obtained , wrt to figure 6.28 describing only the relation of effects, it is seen that covariance is different, an interesting aspect to note is the clusters numbering in both channels occupy different positions, for the same targets

and formulated as a feature database.

The possibility of clustering the time series data using the extracted features has been successfully presented.

7

Conclusion and Future Work

In this thesis we have investigated, analysed and implemented concepts from radar doppler processing, radar polarimetry, sensor fusion and multi target tracking for the successful extraction of features from moving extended targets, through the mitigation of the data association bottle necks when dealing with multiple targets over multiple frames of measurement obtained from channels of different polarimetry (diverse behaviour).

The thesis provides a proof of concept, for the use of radar polarimetry in studies related to target categorisation and opens up possibilities for radar target classification based on polarimetric data.

The thesis has been divided into 3 sub-parts explaining the different stages of the proposed approach and dependencies on each stage . Mathematical formulation of the algorithm and supporting validation, based on synthesised and real radar data cases have been presented for each sub-part.

In the following sections the final outputs of the study have been summarised as conclusions. The limitations concerning the scope of study has been explained and possible open research topics encountered during the study have been presented as a part of the future scope.

7.1. Conclusions

As a result of this study, 3 standalone algorithms which can be used independently or in combinations have been formulated. The output of each stage of the algorithm provides a database which can be used for future studies. The following are the outcomes of this research:

- A measurement and tracking space termed the "Range Velocity Cube", free from stationary targets and clutter spread at zero doppler, is created for the extraction of polarimetric data from moving extended targets.

- A Novel Multi-Channel Data Fusion algorithm (MCDA), based on the flood fill algorithm is proposed, for effective clustering of detections from extended targets and efficient extraction of polarimetric data simultaneously from all 4 channels of the radar. The algorithm mitigates Level 1 data association issue related to multi

channel data. The MCDA provides a detection database consisting of raw data segments of the targets detected over multiple frames.

- A Robust Multi Target Data Association filter (MTDF), based on a nearest neighbours algorithm is proposed, for effective and precise association of raw data segments of a target that was extracted over multiple frames of measurement from 4 polarimetric channels.

  The MTDF mitigates Level 2 and level 3 data association problems related to varying number of targets detected over multiple frames of data. The Robustness of the algorithm is evaluated based on the performance metric which emphasises on track continuity, association accuracy and evaluation of track crossing events. The output of the MTDF stage is a Target track database which consists of a time series data, of associated measurements of raw polarimetric data for maximum number of targets detected during the measurement.

- A feature analysis is conducted on the extracted time series of raw data for every target recorded, in the target track database. The result of the analysis is a time series feature database consisting of 25 features for every target, present for a minimum of 10 frames of measurements.

- The proposed algorithm is evaluated on real radar data collected from a high density target space - the A13 highway, by an in house Doppler Polarimetric Radar - PARSAX.

  Three databases consisting of real polarimetric data for 62 targets collected over 66 frames is successfully extracted.

- The features extracted are used in an off the shelf 'k means', clustering algorithm, and as a result 6 sub-classes based on covariance and correlation properties of the targets wrt to the channel of measurements has been identified.

7.2. Limitations

The measurement and tracking space considered in this study is range velocity map formed by a pixels limited to the range and doppler resolutions of the radar data, as a result when estimating a target position during the tracking stage high association error is recorded in terms of velocity bins, though targets following a constant velocity model or nearly constant acceleration model fair well, the algorithm fairs poorly when a high accelerating target is detected.

In addition as any measurement above the CA-CFAR threshold, is considered a possible target candidate detected on the range velocity map , random events occurring due to real data conditions creates multiple false target tracks, at certain issues the a series of random events may create a false track.

The algorithm fairly poorly against ambiguities, the measurement space is divided into two sub-spaces individually for positive and negative velocities, as the tracker filter is designed works on each sub-space independent of the other, presence of opposite direction tracks causes faulty associations , loss of tracks and decrease in quality of dataset.
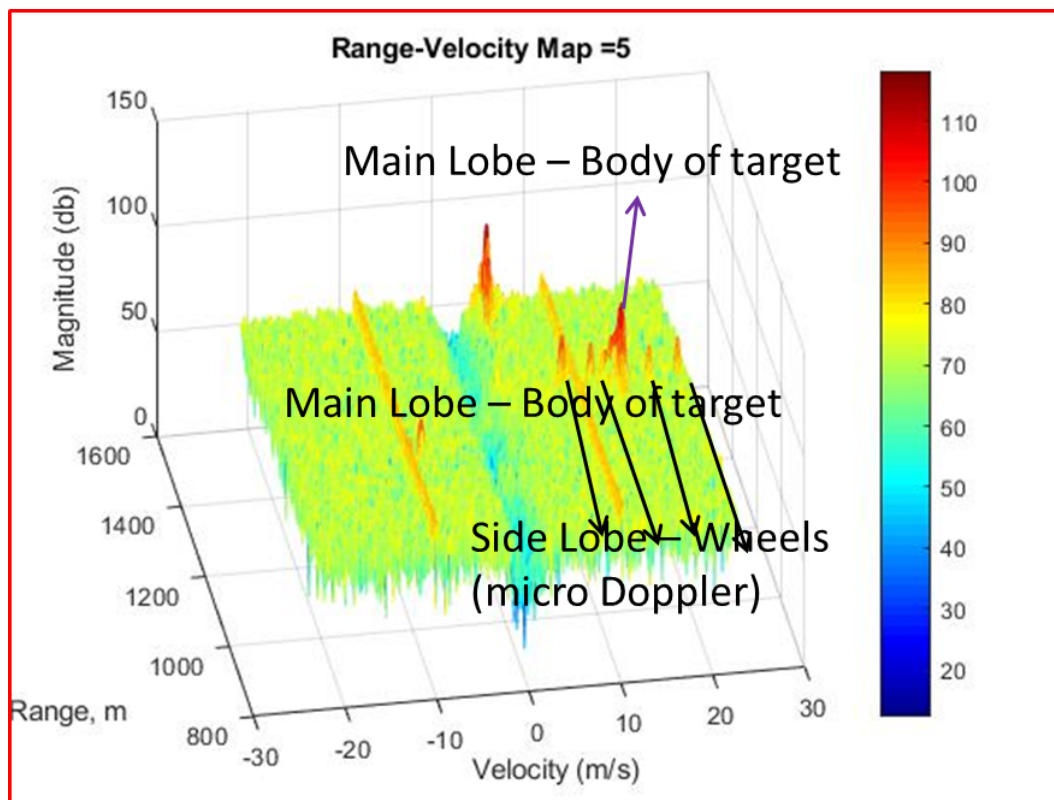
Figure 7.1: Doppler spectrum of a complex target

7.3. Open topics and Future Scope

The following topics have been identified as possible research directions, thesis topics and future scope of this study:

7.3.1. Polarimetric data fusion

The polarimetric data fusion strategies discussed in chapter 3, are limited to using only the detection map stage of the CA-CFAR across channels, future study towards adaptive detectors [66][?] and possible polarimetric fusion studies [51] can be investigated for the improvement of this study.

7.3.2. Use of Micro Doppler Features

"The Doppler spectrum of a complex target may also include discrete features due to moving parts on a target. Peaks in its Doppler spectrum corresponding not only to the radial velocity of the target as a whole but also to the velocity of the moving parts viewed from the radar."[5] In this study there interesting examples of such micro-doppler patters for cars as seen figure 7.1

"Doppler components from the rotational speed of the wheels of the vehicle can be useful for target classification or identification, hence can be considered for future scopes."[5]

Figure 7.2: Round About on N470 highway, targets moving will provide returns at different angles, due to the turns around the round about

7.3.3. Data Extraction for different angular values

The carried out measurements in this study consist of data extracted from targets at fixed angle, hence the results obtained are specific to the considered azimuth value, in order to acquire the data of targets different angles it is required that either have a radar which can be rotated around a target or a target rotated at different angles.

It is possible to exploit the case of extracting data from different angles by considering the measurement location shown in figure 7.2

By modifying the tracking stage of the algorithm proposed in the study to, accommodate non linear trajectories around the round about, we can extract data from the moving target at different angles when a vehicle drives around the round about.

Bibliography

[1] E. P. Blasen and S. A. Israel, "Situation/threat context assessment," 2015 18th International Conference on Information Fusion (Fusion), Washington, DC, 2015, pp. 1168-1175.

[2] S. Haykin, "Cognitive radar: a way of the future," in IEEE Signal Processing Magazine, vol. 23, no. 1, pp. 30-40, Jan. 2006 .doi: 10.1109/MSP.2006.1593335

[3] M. Beard, S. Reuter, K. Granström, B. Vo, B. Vo and A. Scheel, "Multiple Extended Target Tracking With Labeled Random Finite Sets," in IEEE Transactions on Signal Processing, vol. 64, no. 7, pp. 1638-1653, April 1, 2016. doi: 10.1109/TSP.2015.2505683

[4] L. Yang, P. Luo, C. C. Loy and X. Tang, "A large-scale car dataset for fine-grained categorization and verification," 2015 IEEE Conference on Computer Vision and Pattern Recognition (CVPR), Boston, MA, 2015, pp. 3973-3981. doi: 10.1109/CVPR.2015.7299023

[5] M. A. Richards, J. A. Scheer, and W. A. Holm, "Principles of Modern Radar: Basic Principles" Raleigh, NC: SciTech Publishing, 2010

[6] Acosta, Gerardo Gabriel and Sebastián A. Villar. Accumulated CACFAR Process in 2-D for Online Object Detection From Sidescan Sonar Data. IEEE Journal of Oceanic Engineering 40 (2015): 558-569.

[7] R. Khudeev, "A new flood-fill algorithm for closed contour," 2005 Siberian Conference on Control and Communications, Tomsk, Russia, 2005, pp. 172-176. doi: 10.1109/SIBCON.2005.1611214

[8] Niemeijer, R.J. "Doppler-polarimetric radar signal processing.", 1996 Institutional Repository, doctoral thesis, ISBN 90-407-1332-4

[9] V. Santalla, Member, IEEE, Yahia M. M. Antar, Senior Member, IEEE, and A. G. Pino, Member, IEEE "Polarimetric Radar Covariance Matrix Algorithms and Applications to Meteorological Radar Data", IEEE TRANSACTIONS ON GEOSCIENCE AND REMOTE SENSING, VOL. 37, NO. 2, MARCH 1999

[10] O. A. Krasnov, L. P. Ligthart, Z. Li, G. Babur, Z. Wang and F. van der Zwan, "PARSAX: High-resolution Doppler-polarimetric FMCW radar with dual-orthogonal signals," 18th INTERNATIONAL CONFERENCE ON MICROWAVES, RADAR AND WIRELESS COMMUNICATIONS, Vilnius, 2010, pp. 1-5.

[11] Karl Granstríom, Marcus Baum, and Stephan Reuter, "Extended Object Tracking: Introduction, Overview and Applications", Journal of Advances in Information Fusion, Volume 12, Number 2, Pages 139-174, December 2016, ISSN 1557-6418

[12] Lyudmila Mihaylova , Avishy Y. Carmi , François Septier , Amadou Gning , Sze Kim Pang , Simon Godsill "Overview of Bayesian sequential Monte Carlo methods for group and extended object tracking" Digital Signal Processing 25 (4 December 2013) 116, https://doi.org/10.1016/j.dsp.2013.11.006

[13] V. D. Nguyen and T. Claussen, "Reducing computational complexity of gating procedures using sorting algorithms," Proceedings of the 16th International Conference on Information Fusion, Istanbul, 2013, pp. 1707-1713.

[14] Robert Collins CSE598C Vision-Based Tracking CSE Department, Penn State University, 2012

[15] S. S. Blackman, "Multiple hypothesis tracking for multiple target tracking," in IEEE Aerospace and Electronic Systems Magazine, vol. 19, no. 1, pp. 5-18, Jan. 2004. doi: 10.1109/MAES.2004.1263228

[16] James Munkres   "Algorithms for the Assignment and Transportation Problems", in Journal of the Society for Industrial and Applied Mathematics,P 32-38,10.1137/0105003.

[17] Harold W. Kuhn, "The Hungarian Method for the assignment problem", Naval Research Logistics Quarterly, 2: 8397, 1955. Kuhn's original publication.

[18] R. Viswanathan and V. Aalo, "On counting rules in distributed detection," in IEEE Transactions on Acoustics, Speech, and Signal Processing, vol. 37, no. 5, pp. 772-775, May 1989. doi: 10.1109/29.17574

[19] Y. Norouzi, M. S. Greco and M. M. Nayebi, "Performance evaluation of k out of n detector," 2006 14th European Signal Processing Conference, Florence, 2006, pp. 1-5.

[20] Elmenreich, W., An Introduction to Sensor Fusion. Institut für Technische Informatik Vienna University of Technology, Austria wil@vmars.tuwien.ac.at. Research Report 47/2001.

[21] Sabihi, Ahmad. On the radar cross section (RCS) prediction of vehicles moving on the ground. United States: N. p., 2014. Web. doi:10.1063/1.4904666.

[22] A. G. Stove, "Modern FMCW radar - techniques and applications," First European Radar Conference, 2004. EURAD., Amsterdam, The Netherlands, 2004, pp. 149-152.

[23] Bassem R. Mahafza. Radar Systems Analysis and Design Using MATLAB. CRC Press, Inc., Boca Raton, FL, USA, 2000

[24] F. Le Chevalier, O. Krasnov, F. Deudon and S. Bidon, "Clutter suppression for moving targets detection with wideband radar," 2011 19th European Signal Processing Conference, Barcelona, 2011, pp. 427-430.

[25] B. Barboy, A. Lomes and E. Perkalski,
 "Cell-averaging CFAR for multiple-target situations," in IEE Proceedings F - Communications, Radar and Signal Processing, vol. 133, no. 2, pp. 176-186, April 1986. doi: 10.1049/ip-f-1.1986.0028

[26] El Mashade, Mohamed Target Multiplicity Performance Analysis of Radar CFAR Detection Techniques for Partially Correlated Chi-Square Targets. Aeu-international Journal of Electronics and Communications - AEU-INT J ELECTRON COMMUN. 56. 84-98. 10.1078/1434-8411-54100077.

[27] Alexander Yarovoy, Scattering from extended targets, ET4169 - Microwaves, Radar and Remote Sensing, 2017-2018, lecture series, EEMCS ,TU Delft.

[28] Nikita Petrov; Migrating Target Detection in Wideband Radars PhD thesis, Delft University of Technology, June 2019. DOI: 10.4233/uuid:08556a7c-ef90-43f7-998b-f103ceea6267

[29] D. Barton, S. Leonov Radar technology encyclopedia, 1997

[30] He, Y., Aubry, P., Le Chevalier, F., et al. Self-similarity matrix based slow-time feature extraction for human target in high-resolution radar, Int. J. Microw. Wirel. Technol., 2014, 6, Special Issue 34, pp. 423434

[31] Lee, Jong-Sen and Pottier, Eric. Polarimetric Radar Imaging : From basics to applications..(2009). 10.1201/9781420054989.

[32] Raynal, Ann and Bickel, Douglas and Denton, Michael and Bow, Wallace and Doerry, Armin. Radar Cross Section Statistics of Ground Vehicles at Ku-band.(2011). 10.1117/12.882875.

[33] Duy H. Nguyen, John H. Kay, Bradley J. Orchard, and Robert H. Whiting Classification and Tracking of Moving Ground Vehicles, Volume 13, number 2, 2002 Lincoln Laboratory Journal pg 275-308

[34] Merrill Skolnik Radar Handbook, 2nd Ed. Chapter 11, McGraw-Hill, 1990

[35] Boerner, W.-M. et al. (Eds.),
Inverse methods in electromagnetic imaging, Proceedings of the NATO-Advanced Research Workshop, (Sept. 1824, 1983, Bad Windsheim, FR Germany), Parts 1and2, NATO-ASI C-143, D. Reidel Publ. Co., Jan. 1985.

[36] Boerner, W.-M. et al. (Eds.), Direct and inverse methods in radar polarimetry, Proccedings of the NATO-Advanced Research Workshop, Sept. 1824, 1988, Chief Editor, 19871991, NATO-ASI Series C: Math and Phys. Sciences, vol. C-350, Parts 1and2, D. Reidel Publ. Co., Kluwer Academic Publ., Dordrecht, NL, 1992.

[37] Boerner, W.-M., Mott, H., Lüneburg, E., Livingston, C., Brisco, B., Brown, R.J., and Paterson, J.S., with contributions by Cloude, S.R., Krogager, E., Lee, J.S., Schuler, D.L.,van Zyl, J.J., Randall, D., Budkewitsch, P., and Pottier, E.,
Polarimetry in radar remote sensing: Basic and applied concepts, Chapter 5 in F.M. Henderson and A.J. Lewis, Eds., Principles and Applications of Imaging Radar, Vol. 2 of Manual of Remote Sensing, (R.A. Reyerson, Ed.), 3rd ed., John Wiley and Sons, New York, 1998.

[38] Boerner, W.M.,
Introduction to radar polarimetry with assessments of the historical development and of the current state-of-the-art, Proceedings of International Workshop on Radar Polarimetry, JIPR-90, March 2022, 1990, Nantes, France.

[39] Kostinski, A.B. and Boerner, W.M.,
On foundations of radar polarimetry, IEEE Transaction on Antennas and Propagation, 34, 1986, pp. 13951404.

[40] F. Belfiori, O. Krasnov and A. Yarovoy,
"Polarimetric channels exploitation for improved target detection: Preliminary experiments with the PARSAX radar system," 2014 15th International Radar Symposium (IRS), Gdansk, 2014, pp. 1-4. doi: 10.1109/IRS.2014.6869255

[41] D. Giuli, M. Fossi and L. Facheris, "Radar target scattering matrix measurement through orthogonal signals," in IEE Proceedings F - Radar and Signal Processing, vol. 140, no. 4, pp. 233-242, Aug. 1993. doi: 10.1049/ip-f-2.1993.0033

[42] D. Giuli, L. Facheris, M. Fossi, and A. Rossettini,
Simultaneous scattering matrix measurement through signal coding, in Radar Conference,1990., Record of the IEEE 1990 International, May 1990, pp. 258262.

[43] BASIC RADAR CONCEPTS,
http://electriciantraining.tpub.com/14190/css/Basic-Radar-Concepts-14.htm

[44] Everitt, Brian   Cluster analysis. Chichester, West Sussex, U.K: Wiley. ISBN 9780470749913.(2011).

[45] Ester M. Density-based Clustering. In: LIU L., ÖZSU M.T. (eds) Encyclopedia of Database Systems. Springer, Boston, MA (2009)

[46] El Bahi, Hassan and Zatni, Abdelkarim. (2018).
Document text detection in video frames acquired by a smartphone based on line segment detector and DBSCAN clustering. Journal of Engineering Science and Technology. 13.

[47] P. M. Chu, S. Cho, Y. W. Park and K. Cho,
"Fast point cloud segmentation based on flood-fill algorithm," 2017 IEEE International Conference on Multisensor Fusion and Integration for Intelligent Systems (MFI), Daegu, 2017, pp. 656-659. doi: 10.1109/MFI.2017.8170397

[48] Rafael C. Gonzalez and Richard E. Woods. 2006. Digital Image Processing (3rd Edition). Prentice-Hall, Inc., Upper Saddle River, NJ, USA.

[49] No machine-readable author provided. Wereon assumed (based on copyright claims).   https://commons.wikimedia.org/wiki/File:Two-pass-connected-component-labeling.svg CC BY-SA 4.0,https://creativecommons.org/licenses/by-sa/4.0

[50] Baruzzi, Aurora and Martorella, Marco. (2015). Multi-sensor multi-target tracking based on range-Doppler measurement. International Journal of Microwave and Wireless Technologies. 8. 10.1017/S175907871500046X.

[51] M. Novey and T. Adali, "Using complex-valued ICA to efficiently combine radar polarimetric data for target detection," 2009 IEEE International Conference on Acoustics, Speech and Signal Processing, Taipei, 2009, pp. 1673-1676. doi: 10.1109/I-CASSP.2009.4959923

[52] Venkatachalaperumal, Shenbaga Rajan. (2016).
Fusion of dual frequency fully polarimetric SAR data and hyperspectral data for enhanced land cover classification. 10.13140/RG.2.1.5154.8563. , pg-15-22

[53] L. Sheugh and S. H. Alizadeh, "A note on pearson correlation coefficient as a metric of similarity in recommender system," 2015 AI and Robotics (IRANOPEN), Qazvin, 2015, pp. 1-6. doi: 10.1109/RIOS.2015.7270736

[54] Johnson, D.
 "Minimum Mean Squared Error Estimators". Connexions. Archived from Minimum Mean Squared Error Estimators the original Check |url= value (help) on 25 July 2008. Retrieved 8 January 2013.

[55] SAMUEL S. BLACKMAN Abstracts of previous tutorials in this series: Multiple hypothesis tracking for multiple target tracking

[56] S. P. Coraluppi and C. A. Carthel, "Multiple-Hypothesis Tracking for Targets Producing Multiple Measurements," in IEEE Transactions on Aerospace and Electronic Systems, vol. 54, no. 3, pp. 1485-1498, June 2018. doi: 10.1109/TAES.2018.2796478

[57] Miller, Matt L., Harold S. Stone, and Ingemar J. Cox, Optimizing Murty's Ranked Assignment Method, IEEE Transactions on Aerospace and Electronic Systems, 33(3), 1997.

[58] A. A. Gorji, R. Tharmarasa and T. Kirubarajan,
 "Performance measures for multiple target tracking problems," 14th International Conference on Information Fusion, Chicago, IL, 2011, pp. 1-8.

[59] S. J. Symons, J. A. H. Miles and J. R. Moon,
 "A practical method for specifying radar track extraction performance," IEE Colloquium on Specifying and Measuring Performance of Modern Radar Systems (Ref. No. 1998/221), London, UK, 1998, pp. 8/1-8/7. doi: 10.1049/ic:19980150

[60] X. Shi, F. Yang, F. Tong and H. Lian,
 "A comprehensive performance metric for evaluation of multi-target tracking algorithms," 2017 3rd International Conference on Information Management (ICIM), Chengdu, 2017, pp. 373-377. doi: 10.1109/INFOMAN.2017.7950411

[61] T. Warren Liao,   Clustering of time series dataa survey, Pattern Recognition,   Volume 38,   Issue 11,2005,Pages 1857-1874,ISSN 0031-3203, https://doi.org/10.1016/j.patcog.2005.01.025.

[62] Wolfgang-Martin BOERNER BASIC CONCEPTS IN RADAR POLARIMETRY, POLSARPRO V3.0 LECTURE NOTES, UIC-ECE Communications, Sensing and Navigation Laboratory 900 W. Taylor St., SEL (607) W-4210, M/C 154, CHICAGO IL/USA-60607-7018

[63] JOAKIM STRANDBERG
 Time series classification for identification of radar targets,Master Thesis,Department of Signals and Systems CHALMERS UNIVERSITY OF TECHNOLOGY

[64] Dr. Guy Kouemou EADS Deutschland GmbH, Germany Radar Target Classification Technologies

[65] MATLAB Version: 9.3.0.713579 (R2017b) MATLAB License Number: 329139 KMEANS K-means clustering, Copyright 1993-2014 The MathWorks, Inc.

[66] F. Robey, D. Fuhrmann, E. Kelly, R. Nitzberg,
 A CFAR adaptive matched filter detector, IEEE Trans. Aerospace and Electronic Systems, vol. AES-28, no 1, pp 208-216,, 1992

[67] E.J. Kelly, An Adaptive detection Algorithm, IEEE Trans. Aerospace and Electronic Systems, vol. AES-22, no 3, pp 115-123, 1986.

[68] Pavlo O Molchanov, Jaakko T Astola, Karen O Egiazarian and Alexander V Tot-
sky Classification of ground moving targets using bicepstrum-based features extracted
from Micro-Doppler radar signatures.EURASIP Journal on Advances in Signal Pro-
cessing , December 2013, 2013:61

[69] O. H. Y. Lam, R. Kulke, M. Hagelen and G. Möllenbeck,
"Classification of moving targets using mirco-Doppler radar," 2016 17th International
Radar Symposium (IRS), Krakow, 2016, pp. 1-6. doi: 10.1109/IRS.2016.7497317

[70] Schipper, Tom and Fortuny-Guasch, J. and Tarchi, D. and Reichardt, Lars and
Zwick, Thomas. (2011).
RCS measurement results for automotive related objects at 23-27 GHz. Proceedings
of the 5th European Conference on Antennas and Propagation, EUCAP 2011. 683 -
686.

[71] Cheng, Qiang and Chen, Li and Zhang, Yaolin. (2019). Classification of RCS se-
quences based on KL divergence. The Journal of Engineering. 10.1049/joe.2019.0358.

[72] Maio, A. and Farina, A. and Foglia, G.. (2004). Target fluctuation models and
their application to radar performance prediction. Radar, Sonar and Navigation, IEE
Proceedings -. 151. 261 - 269. 10.1049/ip-rsn:20040842.

[73] Krasnov, O.A. and Yarovoy, A.G. "Residual Video Phases in Polarimetric FMCW
Radars with Dual-Orthogonal LFM Signals". EuCAP 2016 - 10th European Confer-
ence on Antennas and Propagation, Davos, Switzerland, 10-15 April 2016.

Appendices